UNIVERSITY OF TRENTO

Department of Industrial Engineering

Doctoral School in Materials, Mechatronics and Systems Engineering

XXXVIII *Cycle*

Stabilization and avoidance for unmanned vehicles via hybrid control architectures

Supervisors:
Prof. Luca Zaccarian
Prof. Philipp Braun

Ph.D. Candidate:
Riccardo Ballaben

Academic Year 2024/2025

CONTENTS

LIST OF ABBREVIATIONS

US	Uniformly Stable
UGS	Uniformly Globally Stable
UGB	Uniform Global Boundedness
(p)AS	(pre-)Asymptotically Stable
U(p)AS	Uniformly (pre-)Asymptotically Stable
UG(p)AS	Uniformly Globally (pre-)Asymptotically Stable
R(p)AS	Robustly (pre)-Asymptotically Stable
RU(p)AS	Robustly Uniformly (pre)-Asymptotically Stable
RUG(p)AS	Robustly Uniformly Globally (pre)-Asymptotically Stable

LIST OF FIGURES

NOTATION

Throughout this work, we use the following notation:

- $\mathbb{N}$ for the set of natural numbers;
- $\mathbb{Z}$ for the set of integers;
- $\mathbb{R}$ $(\mathbb{R}_{>0}, \mathbb{R}_{\geq 0})$ for the set of (positive, non-negative) real numbers;
- $\mathbb{R}^n$ for the n-dimensional Euclidean space;
- $\mathbb{R}^{m\times n}$ for the set of $m \times n$ real matrices, for $n, m \in \mathbb{N}$;
- $\{0\}$ for the origin in $\mathbb{R}^n$;
- $\mathbb{N}_\beta \coloneqq \{1, \ldots, \beta\}$ and $\mathbb{Z}_\beta \coloneqq \{-\beta, \ldots, 0, \ldots, \beta\}$ with $\beta \in \mathbb{N}$;
- $|x| = \sqrt{x^\top x}$ denotes the Euclidean norm in $\mathbb{R}^n$;
- $||A||$ for the matrix norm induced by the vector norm $|\cdot|$ for a matrix $A \in \mathbb{R}^{m\times n}$;
- $|x|_y \coloneqq |x - y|$ for all $x, y \in \mathbb{R}^n$;
- I for the identity matrix in $\mathbb{R}^{n\times n}$;
- $\mathbb{B} \coloneqq \{x \in \mathbb{R}^n : |x| \leq 1\}$ for the closed unit-ball in $\mathbb{R}^n$;
- $\eta\mathbb{B} \coloneqq \{x \in \mathbb{R}^n : |x| \leq \eta\}$ for the closed ball of radius $\eta \in \mathbb{R}_{\geq 0}$, for any $\eta \in \mathbb{R}_{\geq 0}$, in $\mathbb{R}^n$;
- $\eta\mathbb{B}(y) \coloneqq \{x \in \mathbb{R}^n : |x|_y \leq \eta\}$ for the closed ball of radius η centered at $y \in \mathbb{R}^n$;
- $\mathcal{C} + \mathcal{D} = \{c + d : c \in \mathcal{C}, d \in \mathcal{D}\}$ for the Minkowski sum, given $\mathcal{C} \subset \mathbb{R}^n$, $\mathcal{D} \subset \mathbb{R}^n$;
- int $\mathcal{C}$, $\overline{\mathcal{C}}$, $\partial\mathcal{C}$, and $\overline{\text{con}}\mathcal{C}$ for, respectively, the interior, the closure, the boundary, and the convex closure of $\mathcal{C} \subset \mathbb{R}^n$;
- $\text{He}(S) \coloneqq S^\top + S$, for a square matrix $S \in \mathbb{R}^{n\times n}$;

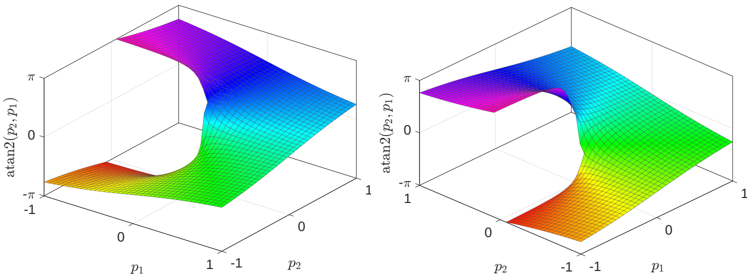

Figure 1: Graph of $\arctan_2$. The color gradient indicates the value of the function, going from red (for $-\pi$) to violet (for π).

- $\lambda_M(S), \lambda_m(S)$ for, respectively, the largest and smallest eigenvalues of S, for $S \in \mathbb{R}^{n\times n}$ symmetric;
- $\mathcal{P} = \{\tau \colon \mathbb{R}_{\geq 0} \to \mathbb{R}_{\geq 0} : \ \tau(0) = 0, \tau(s) > 0 \ \forall s \neq 0, \tau \text{ continuous}\}$ for the class of positive definite functions;
- $\mathcal{K} = \{\tau \in \mathcal{P} : \tau(s) < \tau(r), \forall s, r \in \mathbb{R}_{\geq 0} \text{ such that } s < r\}$ for the set of class-$\mathcal{K}$ functions;
- $\mathcal{K}_\infty = \{\tau \in \mathcal{K} : \lim_{s\to\infty} \tau(s) = \infty\}$ for the set of class-$\mathcal{K}_\infty$ functions;
- $\mathcal{KL} = \{\beta : \mathbb{R}_{\geq 0} \times \mathbb{R}_{\geq 0} \to \mathbb{R}_{\geq 0} : \beta(\cdot, r) \in \mathcal{K} \ \forall r \in \mathbb{R}_{\geq 0}, \beta(s, \cdot) \text{ is continuous and strictly decreasing } \forall s \in \mathbb{R}_{\geq 0}, \beta(s, r) \to 0 \text{ as } s \to \infty\}$ for the set of class-$\mathcal{KL}$ functions;
- $R(\theta)$ for the rotation matrix corresponding to the angle $\theta \in \mathbb{R}$

$$R(\theta) = \begin{bmatrix} \cos(\theta) & -\sin(\theta) \\ \sin(\theta) & \cos(\theta) \end{bmatrix};$$

- $\arctan_2 : \mathbb{R}^2 \setminus \{0\} \to (-\pi, \pi]$ for the function

$$\arctan_2(p_2, p_1) = \begin{cases} \arctan(\frac{p_2}{p_1}) & \text{if } p_1 > 0, \\ \arctan(\frac{p_2}{p_1}) + \pi & \text{if } p_1 < 0 \text{ and } p_2 \geq 0, \\ \arctan(\frac{p_2}{p_1}) - \pi & \text{if } p_1 < 0 \text{ and } p_2 < 0, \\ \frac{\pi}{2} & \text{if } p_1 = 0 \text{ and } p_2 > 0, \\ -\frac{\pi}{2} & \text{if } p_1 = 0 \text{ and } p_2 < 0, \\ \text{undefined} & \text{if } p_1 = 0 \text{ and } p_2 = 0, \end{cases}$$

and we compactly write $\arctan_2(p) := \arctan_2(p_2, p_1)$ for $p = [p_1 \ p_2]^\top \in \mathbb{R}^2$. We remark, as shown in Figure 1, that the $\arctan_2$ function is discontinuous on the half-line $\{(p_1, p_2) \in \mathbb{R}^2 : p_2 = 0, p_1 < 0\}$.

CHAPTER 1

INTRODUCTION

1.1 MOTIVATION AND CONTRIBUTIONS

The use of unmanned vehicles (UVs) has spread across a wide range of applications, among which surveillance, emergency rescue operations, industrial automation, construction, intervention in extreme environments, transportation, and medical care [1].

Early advancements in UVs control were often rooted in practical, application-driven solutions, with a strong emphasis on empirical methods and experimental validation. For unmanned ground vehicles (UGVs), simple proportional-integral-derivative (PID) controllers and path-following algorithms were often sufficient for basic tasks in structured environments [2]. The challenge of navigating in unknown or dynamic environments led to the development of a wide range of obstacle avoidance algorithms [3, 4], focusing on achieving real-time performances. These approaches prioritized practical implementation and, while successful in demonstrating the potential of autonomous systems, paving the way for industrial applications, they often lacked rigorous guarantees.

As these systems became more complex and were deployed in more challenging environments, the limitations of purely heuristic control strategies became apparent. For instance, following the proliferation of unmanned aerial vehicles (UAVs), the need for control design methodologies providing theoretical guarantees of the behavior of the closed-loop system become more prominent, as failure of the controller could result in unrepairable damage to the vehicle. Due to the complexity of controlling this type of vehicles, as highlighted in the seminal survey [5], heuristic solutions are in this sense inadequate. Similarly,

theoretical guarantees are desirable in applications involving human-robot interaction due to the paramount importance of ensuring safety, since a failure could lead to harm or injury to humans working alongside or interacting with the robot [6, 7].
The need to ensure safety and predictability of performance has thus motivated the implementation of control strategies providing theoretical guarantees. The design methodologies developed in the control theory literature provide a useful tool to address these problems, as they allow for the rigorous analysis of the properties of a system and the synthesis of control laws that guarantee the closed-loop system's behavior, even in the presence of uncertainties and disturbances [8, 9]. While general control design techniques are available for fully actuated unmanned vehicles [9, 10], in practice fully actuating an unmanned vehicle is often impractical due to constraints on cost, weight, and complexity, and the design of feedback controllers for underactuated UVs is still an active topic of research.
In this thesis, we adopt this rigorous control-theoretic perspective to design and analyze control strategies for specific classes of UVs. We restrict our attention to two types of underactuated vehicles: unmanned ground vehicles (UGVs), such as wheeled mobile robots, and unmanned surface vehicles (USVs), such as hovercrafts.

In the context of wheeled ground robots, control strategies often exploit a kinematic approximation of the full dynamics of the robot, commonly referred to as the "unicycle model" [11]. Despite the apparent simplicity of the model, stabilization has proven to be a nontrivial task. Indeed, a well-known negative result by Brockett [12, 13] states that a target pose can not be globally stabilized by means of a continuous feedback. Control approaches overcoming these limitations go beyond continuity, using path planning combined with reference tracking [14], discontinuous dynamic feedback laws [15, 16], discontinuous time-invariant [17–19] or discontinuous time-varying sample-and-hold control laws [20, 21], exploiting a discontinuous coordinate transformation, the so-called σ-process [22] to write the system in a convenient set of coordinates. Robust global exponential stability of the origin has also been achieved by a combination of local and global control laws using the equivalent representation of the unicycle dynamics as a chained system [23, 24].
For unmanned surface vehicles, the modeling and control challenges are even more significant. In this context, we focus on hovercraft vehicles, for which, starting from the general dynamic description in [25], a simplified nonlinear model was proposed in [26] to capture the relevant hydrodynamic effects, and has since become the reference model in the majority of the works addressing the stabilization of hovercrafts. The synthesis of stabilizing controllers for this model is a difficult problem, for two main reasons. First, as it is the case with

the unicycle model for wheeled ground robots, there exists no continuous state feedback asymptotically stabilizing a target pose [27]. Second, unlike the case of wheeled ground robots, no simplified kinematic model has been proposed to adequately approximate the equations of the full dynamic model. Using the full model of [26], the authors of [28] achieved global practical exponential stabilization of a reference position trajectory by means of a Lyapunov-based control design. Discontinuous control strategies were proposed in [29] and [27] achieving, respectively, asymptotic stabilization of a reference trajectory and of a reference configuration. Other approaches focus on path following using a Line-of-Sight (LoS) control scheme, where the control input steers the robot towards a moving target point along a desired path, thus ensuring tracking of the reference path [30–32].

All the design solutions discussed so far, for ground wheeled robots and marine surface vessels, use a model describing the robot's dynamics with respect to a fixed reference frame, and rely on measurements of the robot pose in the absolute reference frame, which we call in this work the *Cartesian coordinates* or *Cartesian state* of the robot, to close the loop with a feedback. There are, however, relevant scenarios in which knowledge of the robot pose in the absolute reference frame is not available, and only relative measurements can be used to perform the stabilization task. This is the case, for example, when only on-board sensors, like sonars or cameras, providing range and heading errors, are available to localize the robot [33–35], or in multi-robot systems employing decentralized control strategies, where each robot can measure the relative position of nearby robots with respect to itself [36, 37]. Another example is given by LoS control strategies. In [30], for instance, the control input is defined so that the robot is always pointing towards the target point with a desired speed. This control action can be equivalently described as driving a suitably defined relative heading error angle to zero.

As discussed in [33, 37], an appropriately defined set of *polar coordinates* can be used to model these relative measurements, resulting in an alternative "polar model" for the dynamics of the robot that, noticeably, for wheeled ground robots, does not violate Brockett's condition [12] and can thus be stabilized by smooth time-invariant feedback [37–39]. Nevertheless, the stability properties resulting from these polar-based stabilizers are usually not fully characterized from the point of view of the Cartesian coordinates, nor is the role played by the coordinate transformation mapping the two sets of coordinates into each other discussed. When the coordinate transformation is discontinuous, as in the nominal results of [37, eq. (2), (9)], it is then not possible to extrapolate robustness properties of the Cartesian state. Moreover, when only low-cost sensors are available, such as cameras with a narrow field of view, the measurements coming from multiple devices must be combined to achieve global stabilization.

To ensure that the control strategies we propose in this thesis are widely

applicable, they should be implementable on vehicles equipped with low-cost hardware having limited computational capabilities. Methods that steer a vehicle using full SLAM rely on building a map of the environment from the measurements coming from on-board sensors. In some scenarios, however, (e.g., open sea for marine surface vehicles) building a useful map is impractical or impossible. Moreover, the computational cost of creating and maintaining such map is non-trivial [40, 41]. To steer a vehicle to a desired target we therefore choose to consider, in the context of this thesis, only relative measurements that can be retrieved with minimal computational cost and, in particular, we focus on on-board cameras mounted on the vehicle. A calibrated monocular camera provides a measurement of the bearing (relative heading error) angle to a visible target at a minimum computation cost directly from the image, while the radial distance can, in general, be recovered only up to a global scale factor [42]. This scale factor can be easily estimated online under light assumptions (for example, known target size or a constant camera height), allowing one to retrieve a measurement of the true radial distance [43]. Estimating the relative orientation of the vehicle with respect to the target is computationally efficient when the target is equipped with fiducial markers (e.g., AprilTag) and a PnP solver is used [44]. Conversely, markerless pose estimation for arbitrary objects requires feature extraction and matching and is therefore computationally heavier [45].
These considerations motivated our work in [46, 47]. In [46], we use the polar coordinates representation introduced in [38] to model measurements coming from on-board devices with limited sensing capabilities, described as two cameras with a limited field of view mounted on the robot. We propose a control strategy combining the measurements coming from the two cameras to achieve global stabilization, using the formalism of hybrid dynamical systems [48–50]. We show robustness of the stability properties of the closed-loop system both in the Cartesian and polar coordinates, and we clarify the role played by the coordinate transformations mapping the two sets of coordinates into each other. In [47], we propose a kinematic model approximating the full dynamic model of marine surface robots given in [26]. We then extend the control architecture of [46] to this new kinematic model, and we verify that it adequately approximates the full dynamic model via numerical simulations. Since the control design is based on this simplified kinematic model, its construction and the stability proofs are noticeably simpler than those relying on the full dynamic model.

In the past decades, significant effort has also been devoted to the problem of endowing stabilization with some safety properties. In its most general from, safety is intended as the property of a system to avoid certain unsafe states, and is usually described, in the control theory literature, as forward invariance of a set in which the state is allowed to evolve. Examples of safety-critical cyber-physical systems are, among many, applications with human-robot interaction, assisted driving algorithms such as adaptive cruise control and lane keeping in the automotive industry, and obstacle avoidance for autonomous navigation [51–55]. Several general design methodologies have been proposed to address this problem.

In the robotic literature, artificial potential fields have been introduced in [56, 57]. Within this framework, the target configuration is described as the minimum of a scalar function (the artificial potential energy) and the control input is generated by a combination of the negative gradient of attractive and repulsive functions, pushing the robot towards the target and away from the obstacles, respectively. This approach has been used, for instance, to achieve autonomous robot navigation with obstacle avoidance [58], in the context of robot formation control [59], and to steer the end-effector of a robot manipulator in a cluttered environment [57].

Another successful design methodology, developed in the past decade, originated from the idea proposed in [60] to use a Lyapunov-like function, called barrier function (BF), to certify forward invariance of a safe set. The natural extension of a barrier function to a system with a control input is a control barrier function (CBF) [61], that can be used to enforce invariance of the safe set by selecting a control input satisfying a Lyapunov-like condition on the derivative of the control barrier function. A design combining stabilization, via a control Lyapunov function (CLF), and safety, via a control barrier function (CBF), into a single Lyapunov-like function called a control Lyapunov barrier function (CLBF), was proposed in [62]. Noticeably, due to the similarities between control barrier functions and control Lyapunov functions, standard Lyapunov-based design tools can be applied to synthesize a controller starting from a control Lyapunov barrier function [63–65], among which Sontag's universal formula [66]. More recently, [67] proposed an optimization-based selection of the control input, where the role of the optimization problem is to mediate between the stabilization and safety tasks, prioritizing the latter when the two are conflicting.

As a last widely used tool to handle stabilization with guaranteed safety, expressed using state constraints, we mention model predictive control (MPC) [68, 69]. For the case of linear systems subject to constraints on the input and state that are linear and convex, explicit solutions have been derived [70–72]. While the nonlinear extension of MPC is well-developed [73], and has been applied, for instance, to steer Unmanned Aerial Vehicles while avoiding dynamic obstacles [74] and for collision avoidance of quadruped robots [75], the need to solve a nonlinear optimization problem makes it difficult to derive theoretical guarantees. When the collision avoidance is implemented as a soft constraint with a penalty function in the cost of the optimization problem, small violations of the constraints may occur and avoidance is not guaranteed [76]. On the other hand, when avoidance is encoded as a hard constraint, the

resulting feasibile set is necessarily non-convex and the optimization problem NP-hard in general [77], making the problem particularly challenging even in the linear setting.
Since our goal is to provide theoretical guarantees for stabilization with safety, the first two design methodologies are the most relevant. When safety is expressed in terms of obstacle avoidance, *i.e.*, as avoidance of the union of some bounded unsafe sets, it has been shown [78, 79] that artificial potential fields introduce at least a number of saddle points equal to the number of obstacles, thus making global stabilization topologically impossible. Similarly, as discussed in [80, 81], the design based on CLBF induces additional equilibria on the boundary of the unsafe set, and again global stabilization is not possible. These two design methodologies share the same intrinsic limitation, in that they produce a continuous state feedback selection. To achieve stabilization with obstacle avoidance, (or dynamic or time-varying) input selection is in general needed [82], [83, Section 3.2]. Intuitively, this corresponds to the need to make a "going left" or "going right" decision when navigating around an obstacle in the two dimensional space. The need for a discontinuous control selection, to achieve global stabilization with obstacle avoidance, poses a significant challenge, as arbitrarily small perturbations can induce chattering [84–86], jeopardizing the nominal properties of the controller, and existence of solutions is in general not guaranteed under a discontinuous feedback selection [87].
A design methodology that has proven successful at implementing discontinuous control actions is to combine global and local controllers using the framework of hybrid dynamical systems [48–50], for which existence of solutions and robustness are guaranteed under some regularity assumptions on the system. This approach has been developed in several works, among which [88–90]. Recently, [91, 92] proposed a hybrid control architecture capable of switching between a nominal feedback and an avoidance controller, achieving global stabilization and obstacle avoidance for linear systems.
In our work [93], we adopt this last design methodology and extend it to the class of input-affine nonlinear systems to achieve global stabilization and obstacle avoidance with robustness guarantees. The construction we propose is based on the observation that a Lyapunov function, certifying asymptotic stability of the set of interest, implicitly defines a set of control inputs that do not affect convergence of solutions. This set consists of all inputs generating a velocity component that is orthogonal to the gradient of the given Lyapunov function. When this set is non-empty, one can modify the nominal input, by adding an extra term belonging to this set of inputs, to reshape trajectories, potentially avoiding a given obstacle, while preserving the convergence properties certified by the Lyapunov function. In this sense, the stabilization and avoidance tasks are independent. For the class of input-affine nonlinear systems, this set of values can be easily characterized and, under a

mild assumption on the input matrix, is guaranteed to be non-empty. We propose a redesign strategy based on a hybrid control architecture, switching between a nominal stabilizing feedback and a modified control input, ensuring avoidance of an arbitrary number of point-obstacles, arbitrarily placed in the state space, while preserving the nominal stabilization task.

As discussed above, stabilization under state constraints has received significant attention in the last decades, due to the need to ensure safety in several applications. Similarly, stabilization under input constraints is also a well-studied problem [94–97], due to the relevance of solving stabilization in the presence of input saturation [98–101]. Less attention has been given to the problem of stabilization with reverse input saturation constraints, such as avoidance of specific values of the input. A relevant case study where unwanted input values should be avoided is the stabilization problem for underactuated UAVs where the attitude dynamics is fully actuated, but the position dynamics is not, and the control force can be applied only along certain directions of the airframe. Changing the attitude of the platform to align the delivered force along the direction needed for position control requires specifying a reference attitude that becomes singular in free-falling conditions [102, 103], when the commanded thrust is zero. Existing designs either impose conservative saturation bounds on the control force [102, 104] or modify the reference attitude in the neighborhood of the singularity [105]. The former solution imposes performance limitations since aggressive maneuvers, such as flips to push the UAV downward with a large thrust, are discarded by design. Instead, the latter solution precludes achieving a global stability result. Another potential application example is spacecraft stabilization by means of control moment gyros, where the gimbal-locking condition is problematic [106]. Avoiding certain input values could resolve the associated singularity issue instead of modifying the gimbal rates allocation algorithm when passing through singularities, which locally perturbs the torque commanded by the attitude controller [107].
For a single-input system, avoidance of an unwanted value of the control input necessarily requires a discontinuous action. Motivated by this observation, solutions based on the formalism of hybrid dynamical systems have been proposed to solve the problem. Among the few existing works that deal with this design challenge, [108] addresses the case of avoiding an unwanted value of an m-dimensional control input for a linear plant. Recently, [109, 110] considered reverse polytopic input constraints for linear systems based on hybrid switching.
Inspired by these works, in [111] we propose a simple hybrid redesign for single-input linear systems, which naturally extends to the class of single-input, input-affine nonlinear systems, achieving robust stabilization with avoidance of unwanted input values, thus paving the way to a future extension

to multi-input, input-affine nonlinear systems such as UAVs.

1.2 THESIS OUTLINE

The thesis is structured as follows.

- Chapter 2 introduces the modeling framework of hybrid dynamical systems and discusses asymptotic stability and Lyapunov-based analysis tools for this class of systems.

- Chapter 3 addresses the problem of stabilization of a target configuration for two classes of planar unmanned vehicles, mobile ground robots and marine surface vessels, using relative measurements of the vehicle pose coming from on-board sensors, modelled by a suitably defined set of polar coordinates. We propose a hybrid control architecture, combining measurements coming from different sensors to achieve robust global stabilization. The content of this chapter is based on the author's works:

  – R. Ballaben, A. Astolfi, P. Braun, and L. Zaccarian. "Orchestrating on-board sensors for global hybrid robust stabilization of unicycles". To appear in Automatica. 2025. URL: `https://hal.science/hal-05004452`

  – R. Ballaben, A. Astolfi, P. Braun, and L. Zaccarian. "Towards global stabilization of a hovercraft model using hybrid systems and discontinuous feedback laws". To appear in Proceedings of the IEEE Conference on Decision and Control (CDC), 2025

- Chapter 4 is dedicated to the problem of augmenting stabilization with avoidance. Given a stabilizing feedback and a Lyapunov function, certifying the stability properties of the closed-loop system, we propose two hybrid control redesigns that preserve the stabilization task while ensuring obstacle avoidance, *i.e.*, solutions never get "too close" to a set of obstacles in the state space, or input avoidance, *i.e.*, the control input never gets "too close" to an unwanted value. The content of this chapter is based on the author's works:

  – R. Ballaben, P. Braun, and L. Zaccarian. "Lyapunov-Based Avoidance Controllers With Stabilizing Feedback". In: *IEEE Control Systems Letters* 8 (2024), pp. 862–867

  – R. Ballaben, U. Sutulovic, D. Invernizzi, and L. Zaccarian. "A Hybrid Redesign for Robust Stabilization Without Unit Input". In: *IEEE Control Systems Letters* 7 (2023), pp. 2575–2580

- Chapter 5 concludes the thesis, summarizing the original contributions of this work and discussing possible directions for future research to extend the results presented here.

CHAPTER 2

THE HYBRID DYNAMICAL SYSTEMS FRAMEWORK

This first chapter is dedicated to introducing the main modeling tool that we will use to describe the evolution in time of the physical systems of interest, which is the hybrid dynamical systems framework. Most of the definitions and results we include here are based on the following references [48–50]. Solutions to a hybrid system and their properties are defined in Section 2.1. Section 2.2 presents some key regularity properties of hybrid dynamical systems, which are assumed in Sections 2.3 and 2.4 when discussing, respectively, asymptotic stability notions and Lyapunov-based analysis for hybrid dynamical systems.

A hybrid dynamical system, loosely speaking, is a dynamical system whose solutions are allowed to evolve according to a continuous-time dynamics (we say that the solutions *flow*) or a discrete-time dynamics (we say that the solutions *jump*), depending on where the solutions are in the state space. In its most general form, a hybrid dynamical system is defined as follows

$$(\mathcal{H}) \qquad \begin{aligned} \dot{x} &\in F(x), \qquad & x \in \mathcal{C}, \\ x^+ &\in G(x), \qquad & x \in \mathcal{D}, \end{aligned} \tag{2.1}$$

where F and G are *set-valued maps* defining, respectively, a *differential inclusion* ($\dot{x} \in F(x)$) and a *difference inclusion* ($x^+ \in G(x)$). A set-valued map M associates subsets of $\mathbb{R}^n$ to points of $\mathbb{R}^n$, and can thus be seen as a generalization of singled-valued maps (meaning standard functions). We use the notation $M : \mathbb{R}^n \rightrightarrows \mathbb{R}^n$ to distinguish a set-valued map from a function.

The collection $(\mathcal{C}, F, \mathcal{D}, F)$ is commonly referred to as the *data* of the hybrid system (2.1).

Definition 2.0.1 (Data of a hybrid system [48, Definition 2.1]). *The* data of *a hybrid system $\mathcal{H}$ consists of four elements:*

- *a set $\mathcal{C} \subset \mathbb{R}^n$, called the* flow set*;*
- *a set-valued map $F : \mathbb{R}^n \rightrightarrows \mathbb{R}^n$, called the* flow map*;*
- *a set $\mathcal{D} \subset \mathbb{R}^n$, called the* jump set*;*
- *a set-valued map $G : \mathbb{R}^n \rightrightarrows \mathbb{R}^n$, called the* jump map*.*

We identify a hybrid system defined with the data as above by saying that $\mathcal{H}$ *is a hybrid system on* $\mathbb{R}^n$.
Continuous-time and discrete-time systems can be understood as special cases of hybrid dynamical systems, defined in the following way

$$(\mathcal{H}_c) \quad \begin{array}{rll} \dot{x} & \in F(x), & x \in \mathcal{C}, \\ x^+ & \in *, & x \in \emptyset, \end{array} \qquad (\mathcal{H}_d) \quad \begin{array}{rll} \dot{x} & \in *, & x \in \emptyset, \\ x^+ & \in G(x), & x \in \mathcal{D}, \end{array}$$

where $\mathcal{C}$ and $\mathcal{D}$ may coincide with $\mathbb{R}^n$, if no constraints on the state are imposed, and $*$ is a placeholder for any function, since the constraint $x \in \emptyset$ implies that such a function is never evaluated.
It is clear then that all the results we will state for hybrid dynamical systems also hold for continuous/discrete-time systems. Hence, to avoid duplication of theorems and definitions, in the following we will always refer to the statements presented in this chapter for a generic hybrid dynamical system, and implicitly consider the above representation when applying them to continuous/discrete-time systems.

2.1 SOLUTIONS AND THEIR PROPERTIES

Solutions to continuous-time systems are parametrized by the continuous-time variable $t \in \mathbb{R}_{\geq 0}$, while solutions to discrete-time systems are parametrized by the discrete-time variable $j \in \mathbb{N}$. The, solutions to hybrid systems should be parametrized by both t, the continuous-time elapsed, and j, the number of jumps that have occurred. The following definition clarifies the structure required for a set to be a valid domain of a solution.

Definition 2.1.1 (Hybrid time domains [48, Definition 2.3]). *A subset $E \subset \mathbb{R}^n \times \mathbb{N}$ is a* compact hybrid time domain *if*

$$E = \bigcup_{j=0}^{J-1} [t_j, t_{j+1}] \times \{j\}$$

for some finite sequence of times $0 = t_0 \leq t_1 \leq \ldots \leq t_J$ *and* $t_1, \ldots, t_{J-1}$ *are called jump times. Set* E *is a* hybrid time domain *if for all* $(T, J) \in E$, $E \cap ([0, T] \times \{0, 1, \ldots, J\})$ *is a compact hybrid domain.*

Intuitively speaking, we can say that a hybrid time domain is a subset of $\mathbb{R}_{\geq 0} \times \mathbb{N}$ defining a sequential order of flows and jumps. For instance, given a hybrid evolution consisting of a jump, followed by one second of flow, which can be described by the hybrid time domain $E = (\{0\} \times \{0\}) \cup ([0, 1] \times \{1\})$, it makes no sense to ask what is happening at continuous-time $t = 1$ before any jump has occurred, *i.e.*, $j = 0$, and therefore $(t, j) = \{1\} \times \{0\}$ should not belong to the hybrid domain E.
Given a hybrid time domain, we define a *hybrid arc* in the following way.

Definition 2.1.2 (Hybrid arc [48, Definition 2.4])**.** *A function* $\phi : E \to \mathbb{R}^n$ *is a* hybrid arc *if* E *is a hybrid time domain and if for each* $j \in \mathbb{N}$, *the mapping* $t \mapsto \phi(t, j)$ *is locally absolutely continuous on the interval* $I^j = \{t : (t, j) \in E\}$.

The regularity condition imposed on ϕ by the above definition ensures that on each interval I^j that has nonempty interior (*i.e.*, I^j is not a single point) the function $t \mapsto \phi(t, j)$ is differentiable for almost all $t \in I^j$, allowing us to take its time derivative $\dot{\phi}(t, j) = \frac{d}{dt}\phi(t, j)$ and think of ϕ as a function satisfying a differential equation/inclusion for almost all times.
The notation in (2.1) suggests that solutions to a hybrid system can flow only in the flow set $\mathcal{C}$ and can jump only from the jump set $\mathcal{D}$. This is made precise in the following definition. The domain of a solution ϕ, which we denote as

$$\operatorname{dom} \phi = \{(t, j) \in \mathbb{R}_{\geq 0} \times \mathbb{N} : \phi(t, j) \neq \emptyset\},$$

should obviously be a hybrid time domain.

Definition 2.1.3 (Solution to a hybrid system [48, Definition 2.6])**.** *Let* $\mathcal{H}$ *be a hybrid system on* $\mathbb{R}^n$. *A hybrid arc* ϕ *is a* solution to $\mathcal{H}$ *if* $\phi(0, 0) \in \mathcal{C} \cup \mathcal{D}$, *and*

- *for all* $j \in \mathbb{N}$ *such that* $I^j := \{t : (t, j) \in \operatorname{dom} \phi\}$ *has nonempty interior*

$$\begin{array}{lll} \phi(t, j) \in \mathcal{C} & \textit{for all} & t \in I^j, \\ \dot{\phi}(t, j) \in F(\phi(t, j)) & \textit{for almost all} & t \in I^j; \end{array}$$

- *for all* $(t, j) \in \operatorname{dom} \phi$ *such that* $(t, j+1) \in \operatorname{dom} \phi$,

$$\begin{array}{ll} \phi(t, j) & \in \mathcal{D}, \\ \phi(t, j+1) & \in G(\phi(t, j)). \end{array}$$

Clearly, a solution should start inside $\mathcal{C} \cup \mathcal{D}$. When the continuous-time variable t of $\operatorname{dom} \phi$ increases, meaning that we are considering an interval I^j

that is not just a point, the solution must be in the flow set $\mathcal{C}$ and, according to the standard notion of "Carathéodory solutions" to differential inclusions (see, for example, the introduction of [112, Chapter 5]), its time derivative should exist for almost all times and belong to $F(\phi(t,j))$. When the discrete-time variable j of $\operatorname{dom}\phi$ increases, then the solution must be jumping from the jump set $\mathcal{D}$, and its value after the jump, $\phi(t,j+1)$, must be described by the jump map evaluated at the jump time, $G(\phi(t,j))$.

It is worth highlighting that, when $\mathcal{C} \cap \mathcal{D} \neq \emptyset$, Definition 2.1.3 potentially allows for the existence of solutions that flow and solutions that jump starting from every point of the set $\mathcal{C} \cap \mathcal{D}$, even if F and G are single-valued maps. Thus, non-uniqueness of solutions is a reasonable property of hybrid dynamical systems. For this reason, when characterizing the properties of a set based on the qualitative behavior of solutions to a hybrid system, we will distinguish between *weak* and *strong* properties, *i.e.*, properties that hold for at least one solution, or, respectively, all solutions. Stability, attractivity, and asymptotic stability are always intended here as strong properties. The distinction will become relevant when talking about invariance of sets in Section 2.4.

Solutions to hybrid systems can be classified based on their domain. We state some definitions that will be relevant for us in the following.

Definition 2.1.4 (Types of solutions [48, Definition 2.5, 2.7])**.** *Let $\mathcal{H}$ be a hybrid system on $\mathbb{R}^n$. A solution ϕ to $\mathcal{H}$ is said to be*

- nontrivial *if* $\operatorname{dom}\phi$ *contains at least two points;*
- complete *if* $\operatorname{dom}\phi$ *is unbounded;*
- Zeno *if it is complete and* $\sup_t \operatorname{dom}\phi < \infty$*;*
- maximal *if there does not exist another solution ψ to $\mathcal{H}$ such that* $\operatorname{dom}\phi$ *is a proper (strict) subset of* $\operatorname{dom}\psi$ *and $\phi(t,j) = \psi(t,j)$ for all $(t,j) \in \operatorname{dom}\phi$.*

Generally speaking, completeness of solutions is a desirable property when one wishes to model a physical system, as solutions should describe the evolution of the real system at all times and hence should be defined at all times. On the contrary, existence of Zeno solutions is generally undesirable, as the continuous-time elapsed between consecutive jumps, $t_{j+1} - t_j$, asymptotically goes to zero as j goes to infinity (or, even worse, becomes identically zero in finite time). If a jump in the solution corresponds to a discontinuous action from the actuators, chattering is induced. Maximal solutions are solutions that can not be extended. All complete solutions are maximal, but the converse is not necessarily true.

Another important property of solutions is the existence of a positive lower bound on the elapsed continuous-time between two consecutive jumps, called *dwell-time*.

Definition 2.1.5 (Dwell-time)**.** *Let $\mathcal{H}$ be a hybrid system on $\mathbb{R}^n$ and ϕ be a solution to $\mathcal{H}$. We say that ϕ* has a dwell-time $\tau > 0$ *if $t_{j+1} - t_j \geq \tau$ for all pairs of consecutive jump times t_j, t_{j+1}.*

Proving that all solutions to a hybrid system possess a non-zero dwell-time is a way to prove the absence of Zeno solutions, since a solution with a non-zero dwell-time can not be a Zeno solution.
We postpone the discussion on existence of solutions to the next chapter, after we introduce some key regularity assumptions on the data of hybrid systems.

2.2 WELL-POSEDNESS

A fundamental concept in the development of the stability theory for hybrid dynamical systems is the notion of *well-posedness*. A hybrid system is said to be well-posed if, loosely speaking, the limit of a converging sequence of solutions is a solution to the hybrid system, and this is true for all converging sequences of solutions.
We do not give the formal definition here, as the technical notions required to properly state it go beyond the scope of our discussion (for instance, defining a meaningful notion of distance between solutions to characterize convergence is already a non-trivial matter, as different solutions need not have the same hybrid time domain). We refer the reader to [48, Definition 6.2], for the precise definition, and [48, Chapter 5.3 & 5.4], for the discussion on graphical convergence of solutions.
This brief discussion on well-posedness is motivated by the fact that all the hybrid systems we will consider in the following chapters turn out to be well-posed, and that, under the assumption of well-posedness, it is possible to prove several important and useful results for stability analysis (which we discuss in Section 2.3) including the fact that asymptotic stability is uniform and robust.
To prove well-posedness of a hybrid system we will make use of the following result, providing a simple set of conditions on the data $(\mathcal{C}, F, \mathcal{D}, G)$ of a hybrid system, commonly referred to as *Hybrid Basic Conditions*.

Definition 2.2.1 (Hybrid Basic Conditions [48, Assumption 6.5])**.** *Let $\mathcal{H}$ be a hybrid system on $\mathbb{R}^n$. We say that $\mathcal{H}$ satisfies the* Hybrid Basic Conditions *if*

- *$\mathcal{C}$ and $\mathcal{D}$ are closed;*
- *$F : \mathbb{R}^n \rightrightarrows \mathbb{R}^n$ is outer semicontinuous and locally bounded relative to $\mathcal{C}$, $\mathcal{C} \subset \operatorname{dom} F$, and $F(x)$ is convex for every $x \in \mathcal{C}$;*
- *$G : \mathbb{R}^n \rightrightarrows \mathbb{R}^n$ is outer semicontinuous and locally bounded relative to $\mathcal{D}$, and $\mathcal{D} \subset \operatorname{dom} G$.*

Proposition 2.2.2 (Hybrid Basic Conditions imply well-posedness [48, Theorem 6.30])**.** *Let $\mathcal{H}$ be a hybrid system on $\mathbb{R}^n$ such that $(\mathcal{C}, F, \mathcal{D}, G)$ satisfy the Hybrid Basic Conditions in Definition 2.2.1. Then, $\mathcal{H}$ is well-posed.*

We recall the following definitions for set-valued maps for the reader's convenience.

Definition 2.2.3. *Given a closed set $\mathcal{U} \subset \mathbb{R}^n$, a set-valued map $M : \mathbb{R}^n \rightrightarrows \mathbb{R}^n$ is said to be*

- outer semicontinuous relative to $\mathcal{U}$ *if its graph $\mathcal{U} \times M(\mathcal{U})$ is closed;*
- locally bounded relative to $\mathcal{U}$ *if $M(K)$ is bounded for any bounded $K \subset \mathcal{U}$.*

For the precise definition of these properties see, for example, [112, Chapter 2.2].

Remark 1. *In the hybrid systems literature, a distinction is made between* nominal well-posedness*, which is a property of a given hybrid system, and* well-posedness*, which is a property of the perturbation of the hybrid system. To simplify the exposition, this distinction is not made here.*

Remark 2. *In the case of F being single-valued, $F = f : \mathbb{R}^n \to \mathbb{R}^n$, the conditions in Definition 2.2.3 simply ask for f to be continuous. The same is true also for the case $G = g : \mathbb{R}^n \to \mathbb{R}^n$.*

In the remainder of this section we look at two results that can be proven for hybrid systems satisfying the Hybrid Basic Conditions, pertaining existence and completeness of solutions to a hybrid system and existence of a positive dwell-time.
We remarked in Section 2.1 how, in general, it is desirable for solutions to a hybrid system to be complete, according to Definition 2.1.4. An obstruction to completeness of solutions, inherited from continuous-time systems by the flow dynamics, is finite-time blow up of solutions. Other obstructions, unique to hybrid systems, arise from the constraints imposed by the flow set $\mathcal{C}$ and jump set $\mathcal{D}$. If, while flowing, a solution reaches the boundary of $\mathcal{C}$ with a velocity pushing the solution outside $\mathcal{C}$, then the solution can not be extended in continuous-time, since solutions, according to Definition 2.1.3, can not exit the flow set while flowing. Similarly, if after a jump from $\mathcal{D}$ the solution would land outside $\mathcal{C} \cup \mathcal{D}$, then the solution can not be further extended.
A similar observation is true for existence of solutions. The regularity of the flow map F plays a key role in existence of solutions starting in the flow set $\mathcal{C}$, as the regularity of the vector field f does for ordinary differential equations, and the constraints imposed by $\mathcal{C}$ and $\mathcal{D}$ may prevent existence of solutions if the flow and jump maps F and G would bring solutions outside $\mathcal{C}$ or $\mathcal{D}$.

For hybrid systems satisfying the Hybrid Basic Conditions, a simple set of requirements on the data of $\mathcal{H}$ can be given to ensure existence and, under the additional assumption of boundedness, completeness of solutions.
Before we proceed by stating the result, we need the following definition.

Definition 2.2.4 (Tangent cone [48, Def. 5.12])**.** *The* tangent cone to a set $\mathcal{C} \subset \mathbb{R}^n$ at a point $x \in \mathcal{C}$*, denoted* $T_{\mathcal{C}}(x)$*, is the set*

$$T_{\mathcal{C}}(x) := \left\{ v \in \mathbb{R}^n : \exists x_i \to x, \lambda_i \searrow 0, x_i \in \mathcal{C}, \textit{so that } \frac{x_i - x}{\lambda_i} \to v \right\}.$$

Intuitively speaking, the tangent cone $T_{\mathcal{C}}(x)$ is the set of all vectors, starting from the point x, that do not "point outside" $\mathcal{C}$. This set includes all the vectors belonging to the tangent space to $\mathcal{C}$ at x, when $\mathcal{C}$ is a smooth surface.

Theorem 2.2.5 (Existence and completeness of solutions under Hybrid Basic Conditions [48, Proposition 6.10])**.** *Let $\mathcal{H}$ be a hybrid system on $\mathbb{R}^n$, satisfying the Hybrid Basic Conditions according to Definition 2.2.1, such that $G(\mathcal{D}) \subset \mathcal{C} \cup \mathcal{D}$ and*

$$F(x) \subset T_{\mathcal{C}}(x), \tag{2.2}$$

for all $x \in \mathcal{C} \setminus \mathcal{D}$. Then, there exists a nontrivial solution ϕ to $\mathcal{H}$ for every $\phi(0,0) \in \mathcal{C} \cup \mathcal{D}$. Moreover, all bounded maximal solutions to $\mathcal{H}$ are complete.

The regularity conditions imposed on the flow map F by the Hybrid Basic Conditions in Definition 2.2.1 ensure existence of solutions starting from all points in the interior of $\mathcal{C}$. Moreover, any maximal solution that remains in the interior of $\mathcal{C}$ either blows up in finite time or is complete (see, for example, [112, Corollary 5.16]). Boundedness of solutions prevents finite-time blow up. The additional conditions on G and F address the behavior of solutions in $\mathcal{D}$ and $\mathcal{C} \setminus \mathcal{D}$. Condition $G(\mathcal{D}) \subset \mathcal{C} \cup \mathcal{D}$ in Theorem 2.2.5 ensures that, after a jump from $\mathcal{D}$, the solution is still inside $\mathcal{C} \cup \mathcal{D}$, and therefore it can be extended, either in continuous-time by flowing or in discrete-time by jumping. The condition involving the tangent cone of $\mathcal{C}$ at every $x \in \mathcal{C} \setminus \mathcal{D}$ only becomes relevant if x is also in the boundary of $\mathcal{C}$, since for all $x \in \operatorname{int} \mathcal{C}$ one has, by Definition 2.2.4, $T_{\mathcal{C}}(x) = \mathbb{R}^n$, and therefore the condition is trivially satisfied. If $F(x) \subset T_{\mathcal{C}}(x)$ for every $x \in (\mathcal{C} \setminus \mathcal{D}) \cap \partial\mathcal{C}$, then for all possible velocity vectors $f \in F(x)$ solutions either move in the interior of $\mathcal{C}$ or "slide" on the boundary of $\mathcal{C}$. This ensures that solutions can be extended in continuous-time from all points in $(\mathcal{C} \setminus \mathcal{D}) \cap \partial\mathcal{C}$.
The last result we present in this section ensures existence of a dwell-time for all bounded solutions to a hybrid system satisfying the Hybrid Basic Conditions, under an additional requirement on the jump map G and jump set $\mathcal{D}$.

Theorem 2.2.6 (Dwell-time from boundedness under Hybrid Basic Conditions [113, Lemma 2.7])**.** *Let $\mathcal{H}$ be a hybrid system on $\mathbb{R}^n$ satisfying the Hybrid Basic Conditions in Definition 2.2.1, such that $G(\mathcal{D}) \cap \mathcal{D} = \emptyset$. Let ϕ be a bounded solution to $\mathcal{H}$. Then, there exists $\gamma > 0$ such that $t_{j+1} - t_j \geq \gamma$ for all $j \geq 1, (t_{j+1}, j), (t_j, j) \in \operatorname{dom} \phi$.*

Intuitively speaking, boundedness of the solution ϕ and local boundedness of F (item 2 of Definition 2.2.1) ensure that the velocity vector $\dot{\phi}(t, j) \in F(\phi(t, j))$, when it exists, is uniformly bounded in norm along the solution. Then, the amount of continuous-time it takes the solution to travel the non-zero distance between the closed sets $G(\mathcal{D})$ (closedness of $G(\mathcal{D})$ follows from outer semicontinuity of G) and $\mathcal{D}$, while flowing, is lower bounded by a positive constant, which is the dwell-time τ.
We point out that the version of Theorem 2.2.6 stated in [113, Lemma 2.7] assumes boundedness and completeness of solutions, but only boundedness is actually needed in the proof.

2.3 STABILITY, UNIFORMITY, AND ROBUSTNESS

The goal of the control synthesis carried out in the following chapters is to steer the solutions to a hybrid system $\mathcal{H}$ to a compact set of interest, denoted from here on as

$$\mathcal{A} \subset \mathbb{R}^n,$$

which is not necessarily the origin. Then, to characterize the behavior of solutions with respect to this set, we need the following definition of distance.

Definition 2.3.1 (Distance to a compact set)**.** *Let $\mathcal{A} \subset \mathbb{R}^n$ be compact and $x \in \mathbb{R}^n$. The* distance of x to $\mathcal{A}$ *is the function*

$$|x|_{\mathcal{A}} := \min_{y \in \mathcal{A}} |x - y|,$$

where $|\cdot|$ denotes the Euclidean norm $|x| := \sqrt{x^\top x}$.

In the special case where $\mathcal{A} = \{0\} \in \mathbb{R}^n$, the distance $|\cdot|_{\mathcal{A}}$ becomes the Euclidean norm, $|x|_{\mathcal{A}} = |x|$ for all $x \in \mathbb{R}^n$.
We restrict our attention to a compact set $\mathcal{A}$ for two reasons. First, all the sets of interest that we will consider in the following chapters are compact. Secondly, additional useful results can be proven under the assumption of compactness of $\mathcal{A}$.
Moreover, since all the hybrid systems that we will consider in the following chapters are well-posed, in the sense that they satisfy the Hybrid Basic Conditions in Definition 2.2.1, all the results that we present in this section and in the following, for a hybrid system $\mathcal{H}$ and a set of interest $\mathcal{A}$, are formulated under the following standing assumption.

Assumption 2.3.2 (Standing assumption). *The hybrid system $\mathcal{H}$ satisfies the Hybrid Basic Conditions in Definition 2.2.1 and the set $\mathcal{A} \subset \mathbb{R}^n$ is compact.*

The main property we are interested in is asymptotic stability of a set for a hybrid system.

Definition 2.3.3 ((Local) pre-asymptotic stability (pAS) [48, Definition 3.6 and 7.1]). *Let $\mathcal{H}$ be a hybrid system on $\mathbb{R}^n$. A compact set $\mathcal{A} \subset \mathbb{R}^n$ is said to be*

- (Lyapunov) stable *for $\mathcal{H}$ if for every $\varepsilon > 0$ there exists $\delta > 0$ such that every solution ϕ to $\mathcal{H}$ with $|\phi(0,0)|_{\mathcal{A}} \leq \delta$ satisfies $|\phi(t,j)|_{\mathcal{A}} \leq \varepsilon$ for all $(t,j) \in \operatorname{dom}\phi$;*

- (locally) pre-attractive *for $\mathcal{H}$ if there exists $\mu > 0$ such that every solution ϕ to $\mathcal{H}$ with $|\phi(0,0)|_{\mathcal{A}} \leq \mu$ is bounded and, if ϕ is complete, then also $\lim_{t+j\to\infty} |\phi(t,j)|_{\mathcal{A}} = 0$;*

- (locally) pre-asymptotically stable *for $\mathcal{H}$ if it is both stable and (locally) pre-attractive for $\mathcal{H}$;*

Remark 3. *Following the notation used in [48], we add the suffix "pre-" to properties that are stated without the assumption of completeness of maximal solutions. When all maximal solutions are complete, we drop the "pre-" suffix.*

Given a (locally) pre-asymptotically stable set $\mathcal{A}$, we define its basin of pre-attraction as follows.

Definition 2.3.4 (Basin of pre-attraction, [48, Definition 7.3]). *Let $\mathcal{H}$ be a hybrid system on $\mathbb{R}^n$ and $\mathcal{A} \subset \mathbb{R}^n$ be locally pre-asymptotically stable for $\mathcal{H}$. The* basin of pre-attraction *of $\mathcal{A}$, denoted $\mathcal{B}^p_{\mathcal{A}}$, is the set of points $\xi \in \mathbb{R}^n$ such that every solution ϕ to $\mathcal{H}$ with $\phi(0,0) = \xi$ is bounded and, if it is complete, then also $\lim_{t+j\to\infty} |\phi(t,j)|_{\mathcal{A}} = 0$.*

When the basin of pre-attraction of $\mathcal{A}$ is $\mathbb{R}^n$, we say that the set $\mathcal{A}$ is *globally* pre-asymptotically stable.

Definition 2.3.5 (Global pre-asymptotic stability (GpAS)). *Let $\mathcal{H}$ be a hybrid system $\mathcal{H}$ on $\mathbb{R}^n$. A compact set $\mathcal{A} \subset \mathbb{R}^n$ is said to be* globally pre-asymptotically stable *if it is locally pre-asymptotically stable with basin of pre-attraction $\mathcal{B}^p_{\mathcal{A}} = \mathbb{R}^n$.*

Remark 4. *The basin of pre-attraction automatically includes all the points in $\mathbb{R}^n$ outside $\mathcal{C} \cup \mathcal{D}$. Indeed, according to Definition 2.1.3, solutions to a hybrid system $\mathcal{H}$ only exist starting in the set $\mathcal{C} \cup \mathcal{D}$, and therefore the boundedness and convergence requirements in Definition 2.3.4 are vacuously satisfied for all points $\xi \in \mathbb{R}^n \setminus (\mathcal{C} \cup \mathcal{D})$, as no solution exists starting from those points.*

The observation in Remark 4 has two consequences. The first one is that the basin of pre-attraction is open even when $\mathcal{C} \cup \mathcal{D}$ is not. According to the Hybrid Basic Conditions in Definition 2.2.1, $\mathcal{C}$ and $\mathcal{D}$ should be closed, and therefore their union $\mathcal{C} \cup \mathcal{D}$ may not be open if any of the two sets is bounded in some direction. If all solutions to $\mathcal{H}$ starting in $\mathcal{C} \cup \mathcal{D}$ are bounded and all complete solutions asymptotically converge to a set $\mathcal{A}$, the above remark clarifies that $\mathcal{B}^p_{\mathcal{A}} = \mathbb{R}^n$, which is open. The proof that, under the Hybrid Basic Conditions, the basin of pre-attraction is an open set can be found in [48, Proposition 7.4]. The second consequence of Remark 4 is that we can meaningfully use global definitions to describe stability properties that hold everywhere also when $\mathcal{C} \cup \mathcal{D} \neq \mathbb{R}^n$.
As mentioned in the previous section, one consequence of well-posedness is that pre-asymptotic stability is uniform, according to the following definition.

Definition 2.3.6 (Uniform (global) pre-asymptotic stability)**.** *Let $\mathcal{H}$ be a hybrid system on $\mathbb{R}^n$, $\mathcal{A} \subset \mathbb{R}^n$ a compact set, and $\mathcal{U} \subset \mathbb{R}^n$ an open set such that $\mathcal{A} \subset \mathcal{U}$. $\mathcal{A}$ is said to be*

- uniformly stable (US) *if there exists a class-$\mathcal{K}_\infty$ function*[1] α *such that*

$$|\phi(t, j)|_{\mathcal{A}} \leq \alpha\left(|\phi(0, 0)|_{\mathcal{A}}\right)$$

  for all $(t, j) \in \operatorname{dom} \phi$, for all $\phi(0, 0) \in \mathcal{U}$;

- uniformly pre-attractive (UpA) *if for every compact set $K \subset \mathcal{U}$ and $\varepsilon > 0$ there exists $T > 0$ such that all solutions ϕ to $\mathcal{H}$ with $\phi(0, 0) \in K$ satisfy $|\phi(t, j)|_{\mathcal{A}} \leq \varepsilon$ for all $(t, j) \in \operatorname{dom} \phi$ with $t + j \geq T$;*

- uniformly pre-asymptotically stable (UpAS) *if it is uniformly stable and uniformly pre-attractive.*

Moreover, $\mathcal{A}$ is said to be uniformly globally *stable (UGS), uniformly* globally *pre-attractive (UGpA), and uniformly* globally *pre-asymptotically stable (UGpAS) if the above conditions hold with $\mathcal{U} = \mathbb{R}^n$.*

Uniformity is to be understood with respect to initial conditions, and intuitively says that solutions that start in the same bounded set have the same qualitative behavior in terms of overshoot and convergence speed.
An equivalent characterization of uniform pre-asymptotic stability can be given in terms of existence of a $\mathcal{KL}$ bound on the distance of solutions to the set $\mathcal{A}$. It is equivalent since existence of the $\mathcal{KL}$ bound implies uniform stability and uniform pre-attractivity, as in Definition 2.3.6, and uniform stability and uniform pre-attractivity imply existence of the $\mathcal{KL}$ bound (see [48, Lemma 7.11]).

[1] For the definition see, for example, [114, Definition 2].

The second important consequence of well-posedness of a hybrid system is robustness of pre-asymptotic stability. To properly state this result, we first need to define perturbed hybrid systems.

Definition 2.3.7 (Perturbed hybrid system [48, Definition 6.27])**.** *Let $\mathcal{H}$ be a hybrid system on $\mathbb{R}^n$ and $\rho : \mathbb{R}^n \to \mathbb{R}_{\geq 0}$. We denote with $\mathcal{H}_\rho$ the* ρ-perturbation of $\mathcal{H}$, *defined as follows*

$$\begin{aligned} x &\in F_\rho(x), & x &\in \mathcal{C}_\rho, \\ x &\in G_\rho(x), & x &\in \mathcal{D}_\rho, \end{aligned} \tag{2.3a}$$

where

$$\begin{aligned} \mathcal{C}_\rho &= \{x \in \mathbb{R}^n : (x + \rho(x)\mathbb{B}) \cap \mathcal{C} \neq \emptyset\}, \\ F_\rho(x) &= \overline{con} F((x + \rho(x)\mathbb{B}) \cap \mathcal{C}) + \rho(x)\mathbb{B}, \quad \forall x \in \mathbb{R}^n, \\ \mathcal{D}_\rho &= \{x \in \mathbb{R}^n : (x + \rho(x)\mathbb{B}) \cap \mathcal{D} \neq \emptyset\}, \\ G_\rho(x) &= \{v \ \in \mathbb{R}^n : v \in g + \rho(g)\mathbb{B}, g \in G((x + \rho(x)\mathbb{B}) \cap \mathcal{D})\}, \quad \forall x \in \mathbb{R}^n. \end{aligned} \tag{2.3b}$$

Remark 5. *If $\mathcal{H}$ in* (2.1) *satisfies the Hybrid Basic Conditions in Definition 2.2.1 and $\rho : \mathbb{R}^n \to \mathbb{R}_{\geq 0}$ is continuous, then, by construction, also $\mathcal{H}_\rho$* (2.3) *satisfies the Hybrid Basic Conditions.*

The effect of the extra terms introduced by the perturbation function ρ in the data of (2.3a) is quite general, in the sense that it captures external perturbations acting on the system, via the additive term in F_ρ and G_ρ, measurement errors in the feedback control law, via the extra term in the argument of F_ρ and G_ρ, and uncertainties in the jump time, via the inflation of $\mathcal{C}$ and $\mathcal{D}$ generated by ρ in $\mathcal{C}_\rho$ and $\mathcal{D}_\rho$.
We say that pre-asymptotic stability of $\mathcal{A}$ for the hybrid system $\mathcal{H}$ is robust if there exist a nontrivial perturbation function ρ such that $\mathcal{A}$ is pre-asymptotically stable for the perturbed system $\mathcal{H}_\rho$.

Definition 2.3.8 (Robust pre-asymptotic stability (RpAS) [48, Definition 7.15])**.** *Let $\mathcal{H}$ be a hybrid system on $\mathbb{R}^n$, $\mathcal{A}, \mathcal{U} \subset \mathbb{R}^n$, and $\mathcal{A}$ be locally pre-asymptotically stable for $\mathcal{H}$, with $\mathcal{U} \subset \mathcal{B}^p_{\mathcal{A}}$ such that $\mathcal{A} \subset \mathcal{U}$. We say that $\mathcal{A}$ is* robustly pre-asymptotically stable on $\mathcal{U}$ *if there exists a continuous $\rho : \mathbb{R}^n \to \mathbb{R}_{\geq 0}$, positive on $\mathcal{U} \setminus \mathcal{A}$, such that $\mathcal{A}$ is locally pre-asymptotically stable for $\mathcal{H}_\rho$, defined as in* (2.3)*, and $\mathcal{U}$ is a subset of the basin of pre-attraction of $\mathcal{A}$ for $\mathcal{H}_\rho$. We say that $\mathcal{A}$ is* robustly globally pre-asymptotically stable (RGpAS) *if the above holds with $\mathcal{B}^p_{\mathcal{A}} = \mathbb{R}^n$.*

Having defined uniformity and robustness of pre-asymptotic stability, we can now state the main theorem of this section.

Theorem 2.3.9 (Pre-asymptotic stability is uniform and robust [48, Theorem 7.12 & 7.21])**.** *Let $\mathcal{H}$ be a hybrid system on $\mathbb{R}^n$ and $\mathcal{A}$,$\mathcal{U} \subset \mathbb{R}^n$ such that Assumption 2.3.2 holds. Suppose that $\mathcal{A}$ is locally pre-asymptotically stable with basin of pre-attraction $\mathcal{B}^p_{\mathcal{A}}$. Then, $\mathcal{A}$ is robustly uniformly locally pre-asymptotically stable (RUpAS) with basin of pre-attraction $\mathcal{B}^p_{\mathcal{A}}$. In particular, if $\mathcal{B}^p_{\mathcal{A}} = \mathbb{R}^n$, then $\mathcal{A}$ is* robustly uniformly globally pre-asymptotically stable (RUGpAS)*.*

2.4 LYAPUNOV-BASED ANALYSIS AND CONTROL DESIGN

The main tool we will use for control design and stability analysis are Lyapunov methods. The definition of a Lyapunov function candidate for hybrid systems is akin to the usual one for continuous-time systems.

Definition 2.4.1 (Lyapunov function candidate [49, Definition 3.17])**.** *Let $\mathcal{A} \subset \mathbb{R}^n$ and $\mathcal{H}$ be a hybrid system on $\mathbb{R}^n$. The function $V : \operatorname{dom} V \to \mathbb{R}_{\geq 0}$ and the set $\mathcal{U} \subset \mathbb{R}^n$ define a* Lyapunov function candidate on $\mathcal{U}$ with respect to $\mathcal{A}$ for the hybrid system $\mathcal{H}$ *if the following conditions hold:*

- $(\mathcal{C} \cup \mathcal{D} \cup G(\mathcal{D})) \cap \mathcal{U} \subset \operatorname{dom} V$*;*
- *$\mathcal{U}$ contains an open neighborhood of $\mathcal{A} \cap (\mathcal{C} \cup \mathcal{D} \cup G(\mathcal{D}))$;*
- *V is continuous on $\mathcal{U}$ and continuously differentiable*[2] *on an open set containing $\mathcal{C} \cap \mathcal{U}$;*
- *V is positive definite with respect to $\mathcal{A}$,* i.e., *$V(x) = 0$ for all $x \in \mathcal{A}$, and $V(x) > 0$ otherwise;*
- *The sublevel sets of V over $\mathcal{U}$ are compact,* i.e., *$\{x \in \mathcal{U} : V(x) \leq \mu\}$ is compact for all $\mu \in \mathbb{R}_{\geq 0}$.*

The first requirement ensures that we can evaluate the Lyapunov function along solutions to $\mathcal{H}$ that belong to the set $\mathcal{U}$, while the second requirement is needed to be able to characterize the behavior of solutions starting in a neighborhood of $\mathcal{A}$ using V. The third requirement allows us to describe the change of V, when solutions flow, using the directional derivative of V. The fourth and fifth requirements allow us to conclude convergence of solutions to $\mathcal{A}$ from the decrease to zero of V. Moreover, the fifth requirement allows us to conclude that solutions living in a sublevel set of V are bounded, thus enabling the use of invariance-based arguments, such as Corollary 2.4.6. The property of radial unboundedness, which is usually asked of Lyapunov

[2] A function $V : \mathbb{R}^n \to \mathbb{R}_{\geq 0}$ is continuously differentiable if all of its partial derivatives exist and are continuous on $\mathbb{R}^n$.

function candidates to certify global stability properties when $\mathcal{U} = \mathbb{R}^n$, implies boundedness of the sublevel sets of V, which is the property we are interested in.

In the following, to simplify the notation, when defining Lyapunov function candidates we will often not specify the set $\mathcal{U}$ or the set $\mathcal{A}$, when they are clear from the context.

Given a Lyapunov function candidate, the following theorem provides a set of sufficient conditions under which a set $\mathcal{A}$ is locally pre-asymptotically stable for a given hybrid system $\mathcal{H}$, defined as in (2.1).

Theorem 2.4.2 (Sufficient Lyapunov conditions [49, Theorem 3.18])**.** *Let $\mathcal{H}$ be a hybrid system on $\mathbb{R}^n$ and $\mathcal{A} \subset \mathbb{R}^n$ be such that Assumption 2.3.2 is satisfied and $G(\mathcal{D} \cap \mathcal{A}) \subset \mathcal{A}$. Let $V : \operatorname{dom} V \to \mathbb{R}_{\geq 0}$ and the set $\mathcal{U} \subset \mathbb{R}^n$ define a Lyapunov function candidate on $\mathcal{U}$ with respect to $\mathcal{A}$ for $\mathcal{H}$ that satisfies*

$$\begin{aligned} \langle \nabla V(x), f \rangle &< 0 \qquad \forall x \in (\mathcal{C} \cap \mathcal{U}) \setminus \mathcal{A}, \forall f \in F(x), \\ V(g) - V(x) &< 0 \qquad \forall x \in (\mathcal{D} \cap \mathcal{U}) \setminus \mathcal{A}, \forall g \in G(x). \end{aligned} \tag{2.4}$$

Then, the set $\mathcal{A}$ is locally pre-asymptotically stable. If, additionally, $\mathcal{U} = \mathbb{R}^n$, then the set $\mathcal{A}$ is globally pre-asymptotically stable.

Remark 6. *Often times, Lyapunov-based results such as Theorem 2.4.2 require a function V satisfying bounds*

$$\alpha_1(|x|_{\mathcal{A}}) \leq V(x) \leq \alpha_2(|x|_{\mathcal{A}}),$$

for all $x \in \mathcal{C} \cup \mathcal{D} \cup G(\mathcal{D})$ and for some functions $\alpha_1, \alpha_2 \in \mathcal{K}$. Such bounds automatically hold for a Lyapunov function candidate V defined as in Definition 2.4.1 (see, for example, [115, Lemma 4.3]).

Remark 7. *We say that a Lyapunov function candidate V for a hybrid system $\mathcal{H}$ on $\mathbb{R}^n$ is a* Lyapunov function for $\mathcal{H}$ *if it satisfies* (2.4)*.*

The set of sufficient conditions given in Theorem 2.4.2 apply to hybrid systems without inputs, defined as in (2.1). Given a hybrid system with a control input $u \in \mathbb{R}^m$,

$$\begin{aligned} \dot{x} &\in F(x, u), \qquad & x \in \mathcal{C}, \\ x^+ &\in G(x), \qquad & x \in \mathcal{D}, \end{aligned} \tag{2.5}$$

that we wish to use to steer the solutions by affecting the set of velocities $F(x, u)$, the autonomous system (2.1) can be seen as the closed-loop system obtained by substituting the feedback selection $u = \kappa(x)$, $\kappa : \mathbb{R}^n \to \mathbb{R}^m$ in (2.5)

$$\begin{aligned} \dot{x} &\in F(x, \kappa(x)), \qquad & x \in \mathcal{C}, \\ x^+ &\in G(x), \qquad & x \in \mathcal{D}. \end{aligned} \tag{2.6}$$

Then, given a system with a control input as in (2.5), and a target set $\mathcal{A} \subset \mathbb{R}^n$ that we wish to render pre-asymptotically stable, the control design methodology we follow is to look for a pair of functions, κ and V, such that

- The closed-loop system (2.6) satisfies the Hybrid Basic Conditions in Definition 2.2.1;
- V is a Lyapunov function candidate on some set $\mathcal{U} \subset \mathbb{R}^n$ with respect to $\mathcal{A}$ for (2.6);
- V satisfies the conditions (2.4).

Remark 8. *Given a hybrid system $\mathcal{H}$ on $\mathbb{R}^n$ and a function $V : \operatorname{dom} V \to \mathbb{R}_{\geq 0}$, we will sometimes make use of the shorthand notation*

$$\begin{aligned} \dot{V}(x) &\coloneqq \max_{f \in F(x)} \langle \nabla V(x), f \rangle, \quad \forall x \in \mathcal{C} \cap \mathcal{U}, \\ \Delta V(x) &\coloneqq \max_{g \in G(x)} V(g) - V(x), \quad \forall x \in \mathcal{D} \cap \mathcal{U}, \end{aligned} \tag{2.7}$$

defined in [49, Definition 3.18].

Remark 9. *Conditions* (2.4) *and* (2.7) *can be weakened by only considering the subset of velocities $f \in (F(x) \cap T_{\mathcal{C}}(x))$ in the inner product $\langle \nabla V(x), f \rangle$. Indeed, all velocities $f \in F(x) \setminus T_{\mathcal{C}}(x)$ would push solutions outside of the set $\mathcal{C}$. Since, according to Definition 2.1.3, solutions can not leave the flow set $\mathcal{C}$ while flowing, the velocities $f \in F(x) \setminus T_{\mathcal{C}}(x)$ can never be selected by a flowing solution and do not play any role in the stability properties of $\mathcal{A}$, and can thus be discarded when evaluating the change of a Lyapunov function candidate along solutions to a hybrid system.*

It is often the case, as we will see in the next chapters, that it is easier to satisfy (2.4) with non-strict inequalities. Under this weaker set of conditions, convergence of complete solutions to the set $\mathcal{A}$ can no longer be concluded. Stability, on the other hand, still follows from V being non-increasing along solutions of the closed-loop hybrid system.

Theorem 2.4.3 (Stability from nonincreasing Lyapunov function)**.** *Let $\mathcal{H}$ be a hybrid system on $\mathbb{R}^n$ and $\mathcal{A} \subset \mathbb{R}^n$ be such that Assumption 2.3.2 is satisfied. Let $V : \operatorname{dom} V \to \mathbb{R}_{\geq 0}$ and $\mathcal{U} \subset \mathbb{R}^n$ define a Lyapunov function candidate on $\mathcal{U}$ with respect to $\mathcal{A}$ for $\mathcal{H}$ that satisfies*

$$\begin{aligned} \langle \nabla V(x), f \rangle \leq 0 \qquad & \forall x \in (\mathcal{C} \cap \mathcal{U}), \forall f \in F(x), \\ V(g) - V(x) \leq 0 \qquad & \forall x \in (\mathcal{D} \cap \mathcal{U}), \forall g \in G(x). \end{aligned} \tag{2.8}$$

Then, the set $\mathcal{A}$ is (Lyapunov) stable. If, additionally, $\mathcal{U} = \mathbb{R}^n$, then the set $\mathcal{A}$ is uniformly globally stable according to Definition 2.3.6.

The first conclusion of Theorem 2.4.3 comes from [49, Theorem 3.19]. The second conclusion comes from strong forward pre-invariance (defined below) and compactness of all sublevel sets of V, implied by, respectively, conditions (2.8) and the last requirement in Definition 2.4.1.

Definition 2.4.4 (Invariance [49, Definition 3.12 & 3.13])**.** *Let $\mathcal{H}$ be a hybrid system on $\mathbb{R}^n$. A nonempty set $K \subset \mathbb{R}^n$ is said to be*

- weakly forward pre-invariant *for $\mathcal{H}$ if for each $x \in K$ there exists at least one maximal solution ϕ to $\mathcal{H}$ that satisfies $\phi(0,0) = x$ and $\phi(t,j) \in K$ for all $(t,j) \in \operatorname{dom}\phi$;*

- strongly forward pre-invariant *for $\mathcal{H}$ if all maximal solutions ϕ to $\mathcal{H}$ starting in K satisfy $\phi(t,j) \in K$ for all $(t,j) \in \operatorname{dom}\phi$;*

- weakly backward invariant *if for each $x \in K$, every $\tau > 0$, there exists at least one maximal solution ϕ to $\mathcal{H}$ such that for some $(t^*,j^*) \in \operatorname{dom}\phi$, $t^* + j^* \geq \tau$, it is the case that $\phi(t^*,j^*) = x$ and $\phi(t,j) \in K$ for all $(t,j) \in \operatorname{dom}\phi$ with $t + j \leq t^* + j^*$;*

- weakly invariant *if it is both weakly forward invariant and weakly backward invariant.*

Remark 10. *Given a hybrid system $\mathcal{H}$ on $\mathbb{R}^n$, $\mathcal{A},\mathcal{U} \subset \mathbb{R}^n$, and V a Lyapunov function candidate on $\mathcal{U}$ with respect to $\mathcal{A}$ for $\mathcal{H}$ such that the assumptions in Theorem 2.4.3 are satisfied, all sublevel sets of V over $\mathcal{U}$ are strongly forward pre-invariant.*

Once stability is established, convergence of all bounded complete solutions to the set of interest can be concluded using a hybrid version of the famous Krasovskii-LaSalle's Invariance Principle [116, Theorem 5.3.77], thus proving pre-asymptotic stability. In its most general form, the theorem can be stated as follows.

Theorem 2.4.5 (Hybrid Invariance Principle [49, Theorem 3.23])**.** *Let $\mathcal{H}$ be a hybrid system on $\mathbb{R}^n$ and $\mathcal{A}, \subset \mathbb{R}^n$, be such that Assumption 2.3.2 is satisfied. Let $V : \operatorname{dom} V \to \mathbb{R}_{\geq 0}$ and $\mathcal{U} \subset \mathbb{R}^n$, with $\mathcal{U}$ open, define a Lyapunov function candidate on $\mathcal{U}$ with respect to $\mathcal{A}$ for $\mathcal{H}$ such that (2.8) holds, $r \in \mathbb{R}_{\geq 0}$, and denote*

$$
\begin{aligned}
V^{-1}(r) &:= \{x \in (\mathcal{C} \cup \mathcal{D} \cup G(\mathcal{D})) \cap \mathcal{U} : V(x) = r\}, \\
\dot{V}^{-1}(0) &:= \{x \in \mathcal{C} \cap \mathcal{U} : \dot{V}(x) = 0\}, \\
\Delta V^{-1}(0) &:= \{x \in \mathcal{D} \cap \mathcal{U} : \Delta V(x) = 0\}.
\end{aligned}
$$

Let ϕ be a complete and bounded solution to $\mathcal{H}$ such that $\overline{\phi(E)} \subset \mathcal{U}$, where $E = \operatorname{dom}\phi$. Then, for some $r \in \mathbb{R}_{\geq 0}$, ϕ converges to the largest weakly *invariant set in*

$$V^{-1}(r) \cap \mathcal{U} \cap \left[\dot{V}^{-1}(0) \cup \left(\Delta V^{-1}(0) \cap G(\Delta V^{-1}(0))\right)\right]. \tag{2.9}$$

Each bounded complete solution to a hybrid system asymptotically converges to some set (commonly referred to as *its ω-limit set* in the literature), which is, among other properties, weakly invariant [48, Proposition 6.21]. A function non-increasing along solutions, such as a Lyapunov function V satisfying the conditions (2.8), is constant in this set. Then, each complete bounded solution converges to some level set of V in which V remains constant, as described by (2.9).

Theorem 2.4.5 admits convergence of different solutions to different sets, contained in suitable level sets of V satisfying (2.9). This can be useful, for instance, when characterizing the evolution of the opinions of different agents in a network, as different subsystems may converge to a different consensus.

In the context of this thesis, we seek to use the hybrid formulation of the Invariance Principle to prove convergence of all complete solutions to the set of interest $\mathcal{A}$. To this end, we exploit the fact that, given a weakly invariant set $\mathcal{S} \subset \mathbb{R}^n$, for each $x \in S$ there exists at least one complete solution ϕ to $\mathcal{H}$ such that $\phi(t^*, j^*) = x$, for some $(t^*, j^*) \in \operatorname{dom} \phi$, and $\phi(t, j) \in S$ for all $(t, j) \in \operatorname{dom} \phi$ (see the discussion below [48, Definition 6.19]). In other words, a weakly invariant set $\mathcal{S}$ inside which a Lyapunov function V is constant can be described as the image of complete solutions along which V is constant.

Therefore, if one can show that the only complete solution ϕ to $\mathcal{H}$ along which V remains constant satisfies $\phi(t, j) \in \mathcal{A}$ for all $(t, j) \in \operatorname{dom} \phi$ (*i.e.*, V is identically zero along ϕ), then all complete solutions to $\mathcal{H}$ converge to $\mathcal{A}$.

Corollary 2.4.6 ([117, Theorem 23])**.** *Let $\mathcal{H}$ be a hybrid system on $\mathbb{R}^n$ and $\mathcal{A} \subset \mathbb{R}^n$, be such that Assumption 2.3.2 is satisfied. Let $V : \operatorname{dom} V \to \mathbb{R}_{\geq 0}$ and $\mathcal{U} \subset \mathbb{R}^n$, with $\mathcal{U}$ open, define a Lyapunov function candidate on $\mathcal{U}$ with respect to $\mathcal{A}$ for $\mathcal{H}$ such that (2.8) holds. If each complete solution ϕ to $\mathcal{H}$, with $\overline{\phi(E)} \subset \mathcal{U}$, $E = \operatorname{dom} \phi$, along which V is constant satisfies*

$$V(\phi(t, j)) = 0, \ \forall (t, j) \in \operatorname{dom} \phi,$$

then all complete solutions to $\mathcal{H}$ contained in $\mathcal{U}$ asymptotically converge to $\mathcal{A}$.

CHAPTER 3

ROBUST GLOBAL STABILIZATION OF PLANAR UNMANNED VEHICLES USING RELATIVE MEASUREMENTS

Chapter 3 addresses the problem of stabilization for planar unmanned vehicles using relative measurements of the robot pose coming from on-board sensors. We start by introducing the sensors set-up, consisting of two cameras mounted on the robot, one facing forward and one facing backward, with limited fields of view, and the set of polar coordinates we use to model the relative measurements coming from the cameras. In Section 3.1 we define the coordinate transformations mapping the two sets of coordinates into each other and discuss their properties. Section 3.2 focuses on ground wheeled robots whose dynamics can be approximated by the kinematic model of the unicycle. The equations of motion in the polar coordinates are derived in Section 3.2.1, and two pairs of stabilizers, one for each camera, stabilizing the position and the full pose of the robot, are introduced in Section 3.2.2, and then combined in Section 3.2.3 using a hybrid control architecture to achieve global stabilization. Robustness of the nominal stability properties in the polar coordinates is proven in Section 3.2.4, and we conclude in Section 3.2.5 by discussing stability and robustness of the proposed control architecture as seen in the Cartesian coordinates. Numerical simulations in Section 3.2.6 illustrate the performances of the proposed solution and its robustness to perturbations and measurement noises. Section 3.3, extends the construction of Section 3.2 to unmanned surface vessels. After introducing the full dynamic model, we propose an approximated kinematic model in the Cartesian coordinates, in Section 3.3.1, and in the camera-based coordinates, in Section 3.3.2. Extend-

ing the construction carried out in Section 3.2.3, we propose two camera-based controllers, stabilizing the robot position using measurements from either the front or rear camera, and we combine the two control laws into a hybrid global stabilizer in Section 3.3.3. We discuss a heuristic extension of the control architecture to the full dynamic of the hovercraft in Section 3.3.4, and verify that the kinematic model is a valid approximation of the full equations of dynamics via numerical simulations in Section 3.3.5.

Given a planar unmanned vehicle, we denote with $p := [p_1\ p_2]^\top \in \mathbb{R}^2$ and $\phi \in \mathbb{R}$, respectively, its position in the Cartesian plane and its orientation with respect to a reference frame that, without loss of generality, can be identified with the zero position and orientation (*i.e.*, the origin). We call the state vector $x := [p_1\ p_2\ \phi]^\top \in \mathbb{R}^3$ the *Cartesian coordinates* of the robot. Given the kinematic equations of a generic planar robot

$$\dot{x} = \begin{bmatrix} \dot{p}_1 \\ \dot{p}_2 \\ \dot{\phi} \end{bmatrix} = f(x, u), \tag{3.1}$$

we identify as the control input the vector $u := [u_1\ u_2]^\top \in \mathbb{R}^2$, where u_1 is the forward linear velocity and u_2 the angular velocity. Knowledge of the pose of the robot in the absolute reference frame, *i.e.*, a set of sensors allowing for recovering the state x, is required to design a feedback control law stabilizing the origin of (3.1).

In this chapter we assume that only relative measurements of the robot pose, coming from on-board sensors, are available, and consider the problem of asymptotically stabilizing a target position or pose using only these relative measurements.

We consider the set-up illustrated in Figure 3.1, of a unmanned vehicle equipped with a set of two cameras, one facing forward and one facing backwards, providing measurements of the distance of the robot, r, and of its misalignment, defined by the two angles α and β, with respect to a reference target. We combine these measurements into the state vector

$$z = \begin{bmatrix} r \\ \beta \\ \alpha \end{bmatrix}, \tag{3.2}$$

which we call the *polar* (or *camera-based, on-board*) *coordinates*, and we write z_F and z_R to identify the measurements coming from the front and rear camera, respectively.

We assume the field of view of each camera to be $[-\frac{\pi}{2} - \delta, \frac{\pi}{2} + \delta]$, where $\delta \in (0, \frac{\pi}{2})$ is an arbitrary parameter defining an overlapping of the fields of view of the two cameras. This overlapping will be used later to combine the two cameras and obtain a global stabilizer.

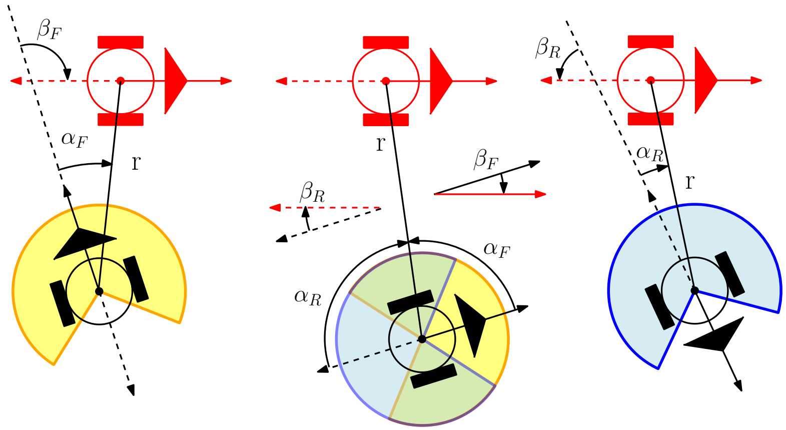

Figure 3.1: A robot equipped two cameras with overlapping fields of view (blue and yellow), providing measurements $(r, \alpha_\mathrm{F}, \beta_\mathrm{F})$ and $(r, \alpha_\mathrm{R}, \beta_\mathrm{R})$, each available only when the target depicted in red is in the camera's field of view $\alpha_i \in [-\frac{\pi}{2} - \delta, \frac{\pi}{2} + \delta]$, $i \in \{\mathrm{F}, \mathrm{R}\}$, $\delta > 0$.

The fields of view of both front and rear cameras satisfy

$$\alpha_\mathrm{F}, \alpha_\mathrm{R} \in \left[-\frac{\pi}{2} - \delta, \frac{\pi}{2} + \delta\right], \tag{3.3}$$

for $\delta \in (0, \frac{\pi}{2})$, by definition. Thus, since $\delta > 0$ and by pointing in opposite directions, the front and rear cameras have a combined field of view covering 360°, ensuring that the target is always in the field of view of at least one camera.

Remark 11. *For practical implementations, the field of view of the front and rear cameras in Figure 3.1 can be thought of as the combined field of view of multiple cameras, each one with a smaller field of view. Considering multiple cameras with a smaller field of view, grouped together into "front cameras" and "rear cameras", would result in the same control strategy that we propose in the following. Thus, considering only two cameras with a field of view greater than* 180° *in our setup is not restrictive, and it is motivated by notational convenience.*

The angle α in (3.2) is commonly referred to, in the context of monocular visual odometry, as "bearing angle", and it can be directly measured from the image provided by a single camera. A measurement of the distance to

the target r in (3.2) can also be obtained from the image, up to an unknown scaling factor which, if the camera is well-calibrated, is constant. This scaling factor can be estimated directly from the images provided by the camera, thus recovering the real distance r, if, for example, the true dimension of the target is known. This is the case, for instance, when the target to reach is a known vehicle or a person. Recovering the relative orientation β in (3.2) is instead more challenging, usually requiring the use of special markers on the target or features-extraction algorithms.
Given the considerations above, in the following sections we propose control strategies relying on knowledge of (r, α), when no measurement of the relative orientation β is available, to stabilize the position of the vehicle, and on knowledge of the full state z, when measuring β is possible, to stabilize the full pose of the vehicle.

3.1 CARTESIAN AND POLAR COORDINATES

Let us consider a planar unmanned vehicle equipped with sensors providing the relative measurements $z_i, i \in \{\mathrm{F}, \mathrm{R}\}$, as illustrated in Figure 3.1.

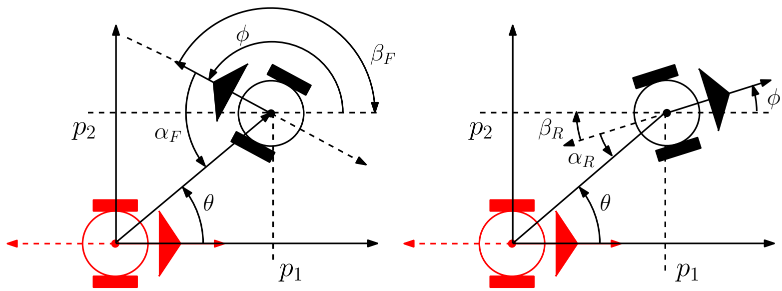

Figure 3.2: Transformation from the Cartesian coordinates $x = [p_1\ p_2\ \phi]^\top$ to the on-board camera-based (polar) coordinates $z = [r\ \beta_i\ \alpha_i]^\top, i \in \{\mathrm{F}, \mathrm{R}\}$. The angle θ can be expressed using the measurements coming from the front camera (left), as $\theta = \alpha_\mathrm{F} - \beta_\mathbb{R} - \pi$, or rear camera (right), as $\theta = \alpha_\mathrm{R} - \beta_\mathrm{R}$.

Before we introduce the two coordinate transformations mapping one set of coordinates into the other, we define the domains of the two sets of coordinates. The Cartesian coordinates x are defined over the domain

$$\mathcal{X} := \mathbb{R}^2 \times \left[-\frac{3}{2}\pi - \delta, \frac{3}{2}\pi + \delta\right]. \tag{3.4}$$

where the orientation ϕ is restricted from $\mathbb{R}$ to the set $[-\frac{3}{2}\pi - \delta, \frac{3}{2}\pi + \delta]$. This restriction of the interval of ϕ is introduced to avoid angular unwinding, and it is not restrictive since all possible orientations of the robot in the

plane can be represented using any interval including $(-\pi, \pi]$ as the domain of ϕ. The particular choice of domain for ϕ used in (3.4) is motivated by Lyapunov-based arguments used in Section 3.2.2. For the discussion presented in this section, the interval $[-\frac{3}{2}\pi - \delta, \frac{3}{2}\pi + \delta]$ can be replaced by any interval $I_\phi \supseteq (-\pi, \pi]$.
The camera-based polar coordinates $z_i, i \in \{\mathrm{F}, \mathrm{R}\}$ are defined on the domain

$$\mathcal{Z} := \mathbb{R}_{\geq 0} \times \left[-\frac{3}{2}\pi - \delta, \frac{3}{2}\pi + \delta\right] \times \left[-\frac{\pi}{2} - \delta, \frac{\pi}{2} + \delta\right], \tag{3.5}$$

for $\delta \in (0, \frac{\pi}{2})$, where the third component α evolves as defined in (3.3), while the second one β evolves in the set $[-\frac{3}{2}\pi - \delta, \frac{3}{2}\pi + \delta]$ to match the domain of ϕ in (3.4).
Via trigonometric considerations, illustrated in Figure 3.2, one obtains the first coordinate transformation, mapping the camera-based coordinates into the Cartesian coordinates

$$\begin{aligned} \begin{bmatrix} p_1 \\ p_2 \\ \phi \end{bmatrix} &= \gamma_{\mathrm{R}}(z_{\mathrm{R}}) := \begin{bmatrix} r\cos(\alpha_{\mathrm{R}} - \beta_{\mathrm{R}}) \\ r\sin(\alpha_{\mathrm{R}} - \beta_{\mathrm{R}}) \\ -\beta_{\mathrm{R}} \end{bmatrix}, \\ \begin{bmatrix} p_1 \\ p_2 \\ \phi \end{bmatrix} &= \gamma_{\mathrm{F}}(z_{\mathrm{F}}) := \begin{bmatrix} r\cos(\alpha_{\mathrm{F}} - \beta_{\mathrm{F}} - \pi) \\ r\sin(\alpha_{\mathrm{F}} - \beta_{\mathrm{F}} - \pi) \\ -\beta_{\mathrm{F}} \end{bmatrix}, \end{aligned} \tag{3.6}$$

where F and R refer to the front and rear camera, respectively. Observe that the coordinate transformation (3.6) is well-defined for every $z_i \in \mathcal{Z}, i \in \{\mathrm{F}, \mathrm{R}\}$. When the target is in the field of view of both cameras (middle sketch in Fig. 3.1), simple geometric considerations yield

$$\begin{aligned} \alpha_{\mathrm{F}} &= \alpha_{\mathrm{R}} - \pi \mathrm{sign}(\alpha_{\mathrm{R}}), \qquad & \beta_{\mathrm{F}} &= \beta_{\mathrm{R}}, \\ \alpha_{\mathrm{R}} &= \alpha_{\mathrm{F}} - \pi \mathrm{sign}(\alpha_{\mathrm{F}}), \qquad & \beta_{\mathrm{R}} &= \beta_{\mathrm{F}}. \end{aligned} \tag{3.7}$$

Moreover, since $\delta > 0$ and the cameras point in opposite directions, the combined field of view of the two cameras covers 360°, and for $r \neq 0$, *i.e.*, $|p| \neq 0$, the robot pose can be equivalently represented in the Cartesian coordinates or through at least one of the on-board coordinates $z_i, i \in \{\mathrm{F}, \mathrm{R}\}$. Indeed, given the two subsets of $\mathcal{X}$ from which the front, respectively, the rear, camera sees the target

$$\begin{aligned} \mathcal{X}_{\mathrm{R}} &:= \gamma_{\mathrm{R}}(\mathcal{Z}) = \{x \in \mathcal{X} \colon |p| \neq 0, \arctan_2(R(\phi)^\top p) \in [-\tfrac{\pi}{2} - \delta, \tfrac{\pi}{2} + \delta]\}, \\ \mathcal{X}_{\mathrm{F}} &:= \gamma_{\mathrm{F}}(\mathcal{Z}) = \{x \in \mathcal{X} \colon |p| \neq 0, \arctan_2(-R(\phi)^\top p) \in [-\tfrac{\pi}{2} - \delta, \tfrac{\pi}{2} + \delta]\}, \end{aligned} \tag{3.8}$$

one has $\mathcal{X}_{\mathrm{R}} \cup \mathcal{X}_{\mathrm{F}} = \mathcal{X} \backslash (\{0\}^2 \times \mathbb{R})$, and therefore for any $x \in \mathcal{X}$ there always exists one $i \in \{\mathrm{F}, \mathrm{R}\}$ and $z \in \mathcal{Z}$ such that $x = \gamma_i(z)$.

The following lemma introduces the inverse coordinate transformation, mapping the Cartesian into the camera-based coordinates, and summarizes its properties.

Lemma 3.1.1. *For any* $\delta \in (0, \frac{\pi}{2})$*, consider the sets* $\mathcal{Z}$*,* $\mathcal{X}$*,* $\mathcal{X}_R$*,* $\mathcal{X}_F$ *in* (3.5), (3.4), (3.8). *Then, the coordinate transformations* $\varrho_R : \mathcal{X}_R \to \mathcal{Z}\backslash(\{0\} \times \mathbb{R}^2)$*,* $\varrho_F : \mathcal{X}_F \to \mathcal{Z}\backslash(\{0\} \times \mathbb{R}^2)$*, defined as*

$$\begin{aligned} \begin{bmatrix} r \\ \beta_R \\ \alpha_R \end{bmatrix} &= \varrho_R(x) := \begin{bmatrix} |p| \\ -\phi \\ \arctan_2(R(\phi)^\top p) \end{bmatrix}, \\ \begin{bmatrix} r \\ \beta_F \\ \alpha_F \end{bmatrix} &= \varrho_F(x) := \begin{bmatrix} |p| \\ -\phi \\ \arctan_2(-R(\phi)^\top p) \end{bmatrix}, \end{aligned} \tag{3.9}$$

are bijective and continuous mappings with inverse given by (3.6)*. In addition,* $\mathcal{X}\backslash(\{0\}^2 \times \mathbb{R}) = (\mathcal{X}_F \cup \mathcal{X}_R)$*.*

Proof of Lemma 3.1.1. Consider the first two equations in (3.9), namely $r = |p|, \beta_i = -\phi, i \in \{\mathrm{F}, \mathrm{R}\}$, mapping x onto $(r, \beta_i), i \in \{\mathrm{F}, \mathrm{R}\}$. These are trivially the definition of r and the inverse of the third equation in (3.6). The rest of the proof focuses on the third equation, related to $\alpha_i, i \in \{\mathrm{F}, \mathrm{R}\}$. To this end, focus on the rear camera angle α_R. Since $x = (p, \phi) \in \mathcal{X}_\mathrm{R}$ implies $p \neq 0$, by the expression of $(p_1, p_2) = (r\cos(\alpha_\mathrm{R} - \beta_\mathrm{R}), r\sin(\alpha_\mathrm{R} - \beta_\mathrm{R}))$ in (3.6), using the angle differences identities one obtains

$$\begin{aligned} r\cos(\alpha_\mathrm{R}) &= r\cos(\alpha_\mathrm{R} - \beta_\mathrm{R} + \beta_\mathrm{R}) &&= p_1\cos(\beta_\mathrm{R}) - p_2\sin(\beta_\mathrm{R}), \\ r\sin(\alpha_\mathrm{R}) &= r\sin(\alpha_\mathrm{R} - \beta_\mathrm{R} + \beta_\mathrm{R}) &&= p_1\sin(\beta_\mathrm{R}) + p_2\cos(\beta_\mathrm{R}). \end{aligned}$$

From the identities above we have that

$$\begin{aligned} \arctan_2\left(\begin{bmatrix} r\cos(\alpha_\mathrm{R}) \\ r\sin(\alpha_\mathrm{R}) \end{bmatrix}\right) &= \arctan_2\left(\begin{bmatrix} \cos(\beta_\mathrm{R}) & -\sin(\beta_\mathrm{R}) \\ \sin(\beta_\mathrm{R}) & \cos(\beta_\mathrm{R}) \end{bmatrix}\begin{bmatrix} p_1 \\ p_2 \end{bmatrix}\right) \\ &= \arctan_2(R(\phi)^\top p), \end{aligned}$$

where we have used $\phi = -\beta_\mathrm{R}$. Due to the definition of $\mathcal{X}_\mathrm{R}$, $\arctan_2(R(\phi)^\top p) \in [-\frac{\pi}{2} - \delta, \frac{\pi}{2} + \delta]$, which implies, due to the properties of $\arctan_2$, that $\alpha_\mathrm{R} = \arctan_2(R(\phi)^\top p)$ is a valid selection of the inverse of (3.6), for any $x \in \mathcal{X}_\mathrm{R}$. Similar steps can be followed to derive the expression for α_F.
To prove bijectivity of $\rho_\mathrm{R}(\cdot)$, consider an arbitrary $x = (p, \phi) \in \mathcal{X}_\mathrm{R}$. We first observe that the second equation in (3.9) defines a bijective mapping, uniquely determining $\beta_\mathrm{R} = -\phi$. Then, there is exactly one pair $(r, \alpha_\mathrm{R}) \in \mathbb{R}_{\geq 0} \times [-\frac{\pi}{2} - \delta, \frac{\pi}{2} + \delta]$ such that $r = |p|$, and $\alpha_\mathrm{R} = \arctan_2(R(\phi)^\top p) = \arctan_2(R(\beta)p)$, with $z_\mathrm{R} = [r\ \beta_\mathrm{R}\ \alpha_\mathrm{R}]^\top \in \mathcal{Z}_\mathrm{R}$. Bijectivity of $\rho_\mathrm{F}(\cdot)$ can be proven following similar steps.

To conclude the proof, observe that the function $p \mapsto \arctan_2(p)$ is discontinuous over the set $\Upsilon = \{p \in \mathbb{R}^2 : p_2 = 0, p_1 < 0\}$. For any converging sequence $\{x_j\} \in \mathcal{X}_{\mathrm{R}}$, $x_j \to x_\infty$ for $j \to \infty$, the sequence $\{R(\phi_j)^\top p_j\} \to R(\phi_\infty)^\top p_\infty$ is bounded away from Υ. This follows from the definition of $\mathcal{X}_{\mathrm{R}}$ and the fact that $\delta \in (0, \frac{\pi}{2})$, since, for any $\{x_j\} \in \mathcal{X}_{\mathrm{R}}$, $|\arctan_2(R(\phi_j)^\top p_j)| \leq \frac{\pi}{2} + \delta < \pi$. Hence, $\lim_{j\to\infty} \arctan_2(R(\phi_j)^\top p_j) = R(\phi_\infty)^\top p_\infty$, namely $x \mapsto \arctan_2(R(\phi)^\top p)$ used in (3.9) is continuous in $\mathcal{X}_{\mathrm{R}}$. The same reasoning shows that the function $x \mapsto \arctan_2(-R(\phi)^\top p)$ in (3.9) is continuous in $\mathcal{X}_{\mathrm{F}}$. $\square$

We conclude this section with the following observation. The coordinate transformation $x \mapsto z_i, i \in \{\mathrm{F}, \mathrm{R}\}$ defined in (3.9) is not a homeomorphism, that is, neighborhoods of the origin in $\mathcal{X}$ are not mapped into neighborhoods of the origin in $\mathcal{Z}$. To see this, observe that, for example, $z_{\mathrm{R}} \to 0$ implies $x \to 0$ according to (3.6), but the opposite is not necessarily true. Indeed, consider, for example, the sequence $\{x_k\}_{k\in\mathbb{N}}, x_k \in \mathcal{X}, x_k = [0\ \frac{1}{k}\ 0]^\top$, satisfying $x_k \to 0$ for $k \to \infty$. Applying the coordinate transformation (3.9) one has that $z_R(x_k) = [0\ 0\ \frac{\pi}{2}]^\top$ for all $k \in \mathbb{N}$, and therefore $\lim_{k\to\infty}(x_k) = [0\ 0\ \frac{\pi}{2}]^\top$, *i.e.*, the limit is not the origin $0 \in \mathcal{Z}$.
The consequences of this property of the coordinate transformation (3.9) will be discussed in Section 3.2.5, where we discuss stability results in the Cartesian coordinates.

3.2 GROUND WHEELED ROBOTS

In this section we focus on ground wheeled robots whose dynamics in the Cartesian coordinates can be approximated by the unicycle kinematic model

$$\dot{x} = \begin{bmatrix} \dot{p}_1 \\ \dot{p}_2 \\ \dot{\phi} \end{bmatrix} = f(x, u) := \begin{bmatrix} u_1 \cos(\phi) \\ u_1 \sin(\phi) \\ u_2 \end{bmatrix}, \tag{3.10}$$

and we address the following points:
(a) By hybridly merging two camera-based stabilizers, each one using only the measurements coming from one camera, we derive a united global feedback stabilizer from on-board sensors, globally asymptotically stabilizing the origin of the unicycle dynamics in the polar coordinates, not suffering from any angular unwinding phenomena.
(b) We establish links between the polar coordinates and the classical Cartesian coordinates representation of the system, clearly illustrating why Brockett's necessary condition is not violated by our stability proof.
(c) We prove robustness properties of the proposed hybrid feedback, with respect to measurement noise and unmodeled dynamics as seen by the on-board representation, and with respect to external perturbations as seen in the Cartesian coordinates representation.

3.2.1 KINEMATIC EQUATIONS IN POLAR COORDINATES

Given equation (3.10), describing the evolution in time of the Cartesian coordinates under the input u, we now combine (3.6) and (3.10) to show that the dynamics in the camera-based coordinates is

$$\begin{aligned} \dot{z}_{\mathrm{R}} &= f_{\mathrm{R}}(z_{\mathrm{R}}, v) := \begin{bmatrix} v_1 r \cos(\alpha_{\mathrm{R}}) \\ -v_2 \\ -v_1 \sin(\alpha_{\mathrm{R}}) - v_2 \end{bmatrix}, \\ \dot{z}_{\mathrm{F}} &= f_{\mathrm{F}}(z_{\mathrm{F}}, v) := \begin{bmatrix} -v_1 r \cos(\alpha_{\mathrm{F}}) \\ -v_2 \\ v_1 \sin(\alpha_{\mathrm{F}}) - v_2 \end{bmatrix}, \end{aligned} \quad \text{with} \quad \begin{aligned} v_1 r &= u_1, \\ v_2 &= u_2, \end{aligned} \tag{3.11}$$

with a transformed input $v = [v_1 \ v_2]^\top \in \mathbb{R}^2$.

Lemma 3.2.1. *Whenever $r \neq 0$, the dynamics* (3.10) *can be equivalently represented through* (3.11)*.*

Proof. We start by deriving f_{R}. Let $r \neq 0$ in the remainder of the proof and define the angle $\theta = \alpha_{\mathrm{R}} - \beta_{\mathrm{R}}$ (see Figure 3.2). Proceeding as in [118, eq. (41)], we use the fact that the derivative of a function $g(p) = p$ satisfies $\frac{dg}{dp}(p) = \frac{dp}{dp} = I$ (with I the identity matrix). Using the definition of θ as well as (3.6), the matrix can be written as

$$\begin{aligned} \frac{dp}{dp} &= \begin{bmatrix} \frac{\partial r}{\partial p_1} \cos(\theta) & \frac{\partial r}{\partial p_2} \cos(\theta) \\ \frac{\partial r}{\partial p_1} \sin(\theta) & \frac{\partial r}{\partial p_2} \sin(\theta) \end{bmatrix} + r \begin{bmatrix} -\sin(\theta) \frac{\partial \theta}{\partial p_1} & -\sin(\theta) \frac{\partial \theta}{\partial p_2} \\ \cos(\theta) \frac{\partial \theta}{\partial p_1} & \cos(\theta) \frac{\partial \theta}{\partial p_2} \end{bmatrix} \\ &= \begin{bmatrix} \cos(\theta) \\ \sin(\theta) \end{bmatrix} \frac{dr}{dp} + r \begin{bmatrix} -\sin(\theta) \\ \cos(\theta) \end{bmatrix} \frac{d\theta}{dp}. \end{aligned}$$

With the definition $J = \left[\begin{smallmatrix} 0 & -1 \\ 1 & 0 \end{smallmatrix}\right]$ and the observations that

$$\frac{p}{r} = \begin{bmatrix} \cos(\theta) \\ \sin(\theta) \end{bmatrix} \quad \text{and} \quad Jp = r \begin{bmatrix} -\sin(\theta) \\ \cos(\theta) \end{bmatrix}, \tag{3.12}$$

for $r \neq 0$, the calculations above yield

$$I = \frac{dp}{dp} = \frac{d}{dp} \left(r \begin{bmatrix} \cos(\theta) \\ \sin(\theta) \end{bmatrix} \right) = \frac{1}{r} p \frac{dr}{dp} + Jp \frac{d\theta}{dp}. \tag{3.13}$$

Note that $p^\top Jp = 0$, hence, left-multiplying (3.13) by $p^\top$ gives

$$p^\top = \frac{1}{r} p^\top p \frac{dr}{dp} + p^\top Jp \frac{d\theta}{dp} = \frac{r^2}{r} \frac{dr}{dp} = r \frac{dr}{dp}.$$

Similarly, the equation

$$(Jp)^\top I = \frac{1}{r} p^\top J^\top p \frac{dr}{dp} + p^\top p \frac{d\theta}{dp} = r^2 \frac{d\theta}{dp}$$

holds, which leads to the expressions $\frac{dr}{dp} = \frac{1}{r} p^\top$ and $\frac{d\theta}{dp} = \frac{1}{r^2}(Jp)^\top$. With these calculations, the definition of the function f_R follows from (3.10), that is

$$\begin{aligned}
\dot{r} &= \frac{\partial r}{\partial p}\dot{p} = \frac{1}{r} p^\top \dot{p} = \frac{1}{r}\begin{bmatrix} r\cos(\theta) & r\sin(\theta) \end{bmatrix}\begin{bmatrix} u_1\cos(\phi) \\ u_1\sin(\phi) \end{bmatrix} \\
&= u_1[\cos(\theta)\cos(\phi) + \sin(\theta)\sin(\phi)] = v_1 r\cos(\phi - \theta) \\
&= v_1 r\cos(-\beta_\mathrm{R} - \alpha_\mathrm{R} + \beta_\mathrm{R}) = v_1 r\cos(\alpha_\mathrm{R}) \\
\dot{\theta} &= \frac{\partial \theta}{\partial p}\dot{p} = \frac{1}{r^2} p^\top J^\top \dot{p} = \frac{1}{r^2}\begin{bmatrix} r\cos(\theta) & r\sin(\theta) \end{bmatrix}\begin{bmatrix} u_1\sin(\phi) \\ -u_1\cos(\phi) \end{bmatrix} \\
&= \frac{u_1}{r}(\cos(\theta)\sin(\phi) - \sin(\theta)\cos(\phi)) = -v_1\sin(\phi - \theta) \\
&= -v_1\sin(\alpha_\mathrm{R}) \\
\dot{\beta}_\mathrm{R} &= -\dot{\phi} = -v_2 \\
\dot{\alpha}_\mathrm{R} &= \dot{\beta}_\mathrm{R} + \dot{\theta} = -v_2 - v_1\sin(\alpha_\mathrm{R}).
\end{aligned}$$

The expression of f_F can be obtained by following similar steps, using the definition $\theta = \alpha_\mathrm{F} - \beta_\mathrm{F} - \pi$. □

3.2.2 CAMERA-BASED STABILIZERS

We now derive control laws for the dynamics (3.11) rendering the target set $\mathcal{A} \subset \mathcal{Z}$, defined as

$$\mathcal{A} := \{0\} \times \left[-\frac{3}{2}\pi - \delta, \frac{3}{2}\pi + \delta\right] \times \{0\}, \tag{3.14}$$

as well as the origin of $\mathcal{Z}$, asymptotically stable, *globally relative to $\mathcal{Z}$*. Stabilizing the set (3.14) corresponds to asymptotically reaching the origin $p = 0$ of the plane in Fig. 3.2 with a non-specified orientation, while stabilizing the origin also imposes a constraint on the orientation ϕ (which is equivalent to the constraints on β_F or β_R, respectively). This follows from the coordinates transformations (3.6) by observing that $r \to 0$ implies $(p_1, p_2) \to 0$, and $\beta_i \to 0$, $i \in \{\mathrm{F}, \mathrm{R}\}$, implies $\phi \to 0$.
Since the control laws proposed here use only measurements coming either from the rear camera, $z_\mathrm{R} \in \mathcal{Z}$, or the front camera, $z_\mathrm{F} \in \mathcal{Z}$, the resulting trajectories may stop at the boundary of $\mathcal{Z}$ with a bounded time domain, and therefore, given the presence of maximal but not complete solutions, we

use the notions of "pre-asymptotic stability" and "pre-attractivity" defined in Section 2.3. Non-completeness of solutions is a consequence of the fact that, when only one camera is available, it is possible to use the measurements coming from the on-board sensors to steer the robot only if that camera sees the target, *i.e.*, only if $x \in \mathcal{X}_i, i \in \{\mathrm{F}, \mathrm{R}\}$. Thus, any result obtained using only one camera is *local* from the Cartesian point of view, in the sense that it holds in the set $\mathcal{X}_i, i \in \{\mathrm{F}, \mathrm{R}\}$.
In the next section we will see how, by using a hybrid control architecture combining the measurements coming from the two cameras, we can ensure completeness of maximal solutions, so that the prefix "pre" can be dropped, and achieve stability results that are truly global in both Cartesian and camera-based coordinates.

Proposition 3.2.2. *Let the feedback gains $k_r, k_\alpha \in \mathbb{R}_{>0}$ be arbitrary. Consider the z_R-dynamics* (3.11) *with $z_R \in \mathcal{Z}$ defined as in* (3.5)*. Then, for $v = v_R$, with*

$$v_R := \begin{bmatrix} v_{R_1} \\ v_{R_2} \end{bmatrix} = \begin{bmatrix} -k_r \cos(\alpha_R) \\ k_r \cos(\alpha_R)\sin(\alpha_R) + k_\alpha \alpha_R \end{bmatrix}, \tag{3.15}$$

the set $\mathcal{A}$ in (3.14) *is globally pre-asymptotically stable. Moreover, $V_\phi(z_R) = \frac{1}{2}(r^2 + \alpha_R^2)$ is a Lyapunov function for the closed-loop dynamics.*

Proof. First observe that $V_\phi(z_\mathrm{R}) = \frac{1}{2}|z_\mathrm{R}|^2_{\mathcal{A}}$, and therefore V_ϕ satisfies all requirements of Definition 2.4.1. The directional derivative of V_ϕ along the dynamics (3.11) is

$$\begin{aligned} \dot{V}_\phi(z_\mathrm{R}) &= \langle \nabla V_\phi(z_\mathrm{R}), f_\mathrm{R}(z_\mathrm{R}, v_\mathrm{R}) \rangle \\ &= r^2 v_{\mathrm{R}_1} \cos(\alpha_\mathrm{R}) + \alpha_\mathrm{R}(-v_{\mathrm{R}_2} - v_{\mathrm{R}_1}\sin(\alpha_\mathrm{R})) \\ &= -k_r r^2 \cos^2(\alpha_\mathrm{R}) - k_\alpha \alpha_\mathrm{R}^2, \end{aligned}$$

which is negative for all $z \in \mathcal{Z}_\mathrm{R} \setminus \mathcal{A}$, and thus global pre-asymptotic stability of $\mathcal{A}$ follows from Theorem 2.4.2. □

Following parallel steps it is possible to prove a similar result for the coordinates z_F, formalized below.

Corollary 3.2.3. *Let the gains $k_r, k_\alpha \in \mathbb{R}_{>0}$ be arbitrary. Consider the z_F-dynamics* (3.11) *with $z_F \in \mathcal{Z}$. Then, for $v = v_F$, with*

$$v_F := \begin{bmatrix} k_r \cos(\alpha_F) \\ k_r \cos(\alpha_F)\sin(\alpha_F) + k_\alpha \alpha_F \end{bmatrix}, \tag{3.16}$$

the set $\mathcal{A}$ in (3.14) *is globally pre-asymptotically stable. Moreover, $V_\phi(z_F) = \frac{1}{2}(r^2 + \alpha_F^2)$ is a Lyapunov function for the closed-loop dynamics.*

We now focus on the origin of $\mathcal{Z}$, to ensure that $\beta_{\mathrm{R}}(t) \to 0$ for $t \to \infty$. To also guarantee convergence of the orientation to $\beta = 0$, we include an additional term in the feedback law v_{R} and in the Lyapunov function.

Proposition 3.2.4. *Let $k_r, k_\alpha, k_\beta \in \mathbb{R}_{>0}$ be arbitrary. Consider the z_R-dynamics* (3.11) *with $z_R \in \mathcal{Z}$. Then the control law $v = v_R$, with*

$$v_R := \begin{bmatrix} -k_r \cos(\alpha_R) \\ k_r \cos(\alpha_R)\sin(\alpha_R) + k_\alpha \alpha_R + k_\beta(\alpha_R - \beta_R)\frac{\cos(\alpha_R)\sin(\alpha_R)}{\alpha_R} \end{bmatrix} \tag{3.17}$$

is well-defined for all $z_R \in \mathcal{Z}$ and globally pre-asymptotically stabilizes the origin. Moreover, $V(z_R) = \frac{1}{2}(r^2 + \frac{k_\beta}{k_r}(\alpha_R - \beta_R)^2 + \alpha_R^2)$ satisfies $\langle \nabla V(z_R), f_R(z_R, v_R)\rangle \leq 0$, for all $z_R \in \mathcal{Z}$.

Proof. First note that $\lim_{\alpha_{\mathrm{R}} \to 0} \frac{\sin(\alpha_{\mathrm{R}})}{\alpha_{\mathrm{R}}} = 1$ and thus the feedback law is well-defined.
The expression of V can be rewritten as

$$\begin{aligned} V(z_{\mathrm{R}}) &= \frac{1}{2}(r^2 + \frac{k_\beta}{k_r}(\alpha_{\mathrm{R}} - \beta_{\mathrm{R}})^2 + \alpha_{\mathrm{R}}^2) \\ &= \frac{1}{2}r^2 + \frac{1}{2k_r}\left(k_\beta(\alpha_{\mathrm{R}}^2 + \beta_{\mathrm{R}}^2 - 2\alpha_{\mathrm{R}}\beta_{\mathrm{R}}) + k_r\alpha_{\mathrm{R}}^2\right) \\ &= \frac{1}{2}r^2 + \frac{1}{2k_r}\left((k_r + k_\beta)\alpha_{\mathrm{R}}^2 + k_\beta\beta_{\mathrm{R}}^2 - 2k_\beta\alpha_{\mathrm{R}}\beta_{\mathrm{R}}\right), \end{aligned}$$

where the second term at the right-hand-side is the quadratic form in $(\alpha_{\mathrm{R}}, \beta_{\mathrm{R}})$ corresponding to the positive definite matrix $\begin{bmatrix} k_\beta + k_r & -k_\beta \\ -k_\beta & k_\beta \end{bmatrix}$. Thus, V is positive definite with respect to the origin and radially unbounded, which in turn implies that its sublevel sets are compact. It is straightforward to verify that V also satisfies the remaining requirements of Definition 2.4.1, and therefore V is a Lyapunov function candidate on $\mathcal{Z}$ with respect to the origin for the z_{R} dynamics (3.11), (3.17).
Extending the derivations in Proposition 3.2.2 with the additional terms in (3.17), one obtains

$$\begin{aligned} \langle \nabla V(z_{\mathrm{R}}), f_{\mathrm{R}}(z_{\mathrm{R}}, v_{\mathrm{R}})\rangle =& r^2 v_{\mathrm{R}_1}\cos(\alpha_{\mathrm{R}}) + \alpha_{\mathrm{R}}(-v_{\mathrm{R}_2} - v_{\mathrm{R}_1}\sin(\alpha_{\mathrm{R}})) \\ &+ \frac{k_\beta}{k_r}(-v_{\mathrm{R}_2} - v_{\mathrm{R}_1}\sin(\alpha_{\mathrm{R}}) + v_{\mathrm{R}_2})(\alpha_{\mathrm{R}} - \beta_{\mathrm{R}}) \\ =& -k_r r^2\cos^2(\alpha_{\mathrm{R}}) - k_\alpha\alpha_{\mathrm{R}}^2 \\ &+ k_\beta(\alpha_{\mathrm{R}} - \beta_{\mathrm{R}})\cos(\alpha_{\mathrm{R}})\sin(\alpha_{\mathrm{R}}) \\ &- \alpha_{\mathrm{R}}k_\beta(\alpha_{\mathrm{R}} - \beta_{\mathrm{R}})\left(\cos(\alpha_{\mathrm{R}})\frac{\sin(\alpha_{\mathrm{R}})}{\alpha_{\mathrm{R}}}\right) \\ =& -k_r r^2\cos^2(\alpha_{\mathrm{R}}) - k_\alpha\alpha_{\mathrm{R}}^2 \leq 0 \quad \forall\, z_{\mathrm{R}} \in \mathcal{Z}, \end{aligned} \tag{3.18}$$

showing that the sublevel sets of V are strongly forward pre-invariant. Lyapunov stability of the origin follows from Theorem 2.4.3. Boundedness of solutions follows from forward pre-invariance and compactness of the sublevel sets of V. Moreover, for all $z_{\mathrm{R}} \in \mathcal{Z}$ for which (3.18) is zero, one has that the z_{R} closed-loop dynamics (3.11), (3.17) becomes $\dot{z}_{\mathrm{R}} = \begin{bmatrix} 0 & k_\beta \beta_{\mathrm{R}} & k_\beta \beta_{\mathrm{R}} \end{bmatrix}^\top$. Since (3.18) is zero only when $r = \alpha_{\mathrm{R}} = 0$, one has that the only complete solution along which the Lyapunov derivative is identically zero is $z_{\mathrm{R}} = [0\ 0\ 0]^\top$, for all $t \geq 0$. Hence, global pre-attractivity of the origin relative to $\mathcal{Z}$ follows from Corollary 2.4.6. Global pre-asymptotic stability of the origin then follows from stability and global pre-attractivity. $\square$

Observe that through $k_\beta = 0$, Proposition 3.2.4 covers the result of Proposition 3.2.2 as a special case, because (3.17) reduces to (3.15). For the z_{F}-dynamics in (3.11), using the same ideas, a result equivalent to Proposition 3.2.4 can be derived, as follows.

Corollary 3.2.5. *Let $k_r, k_\alpha, k_\beta \in \mathbb{R}_{>0}$ be arbitrary. Consider the z_F-dynamics* (3.11) *with $z_F \in \mathcal{Z}$. The control law $v = v_F$, with*

$$v_F := \begin{bmatrix} k_r \cos(\alpha_F) \\ k_r \cos(\alpha_F)\sin(\alpha_F) + k_\alpha \alpha_F + k_\beta(\alpha_F - \beta_F)\frac{\cos(\alpha_F)\sin(\alpha_F)}{\alpha_F} \end{bmatrix} \tag{3.19}$$

is well-defined for all $z_F \in \mathcal{Z}$ and globally pre-asymptotically stabilizes the origin. Moreover, $V(z_F) = \frac{1}{2}(r^2 + \frac{k_\beta}{k_r}(\alpha_F - \beta_F)^2 + \alpha_F^2)$ satisfies $\langle \nabla V(z_F), f_F(z_F, v_F)\rangle \leq 0$, for all $z_F \in \mathcal{Z}$.

3.2.3 HYBRID GLOBAL STABILIZERS

Since the measurements of both cameras are needed to cover all the possible robot configurations (recall from Lemma 3.1.1 that $\gamma_{\mathrm{F}}(\mathcal{Z}) \cup \gamma_{\mathrm{R}}(\mathcal{Z}) = \mathcal{X}$), we hybridly combine the two camera-based controllers of Section 3.2.2 to ensure completeness of maximal solutions and achieve global robust asymptotic stability.

To combine the two controllers (3.17), (3.19) we introduce an additional logic variable $q \in \{-1, 1\}$, where $q = -1$ represents the rear camera R and $q = 1$ represents the front camera F. In the overall system representation we consider the hybrid state

$$\xi = [r\ \beta\ \alpha\ q]^\top \in \Xi := \mathcal{Z} \times \{-1, 1\} \tag{3.20a}$$

where (α, β) can either represent $(\alpha_{\mathrm{R}}, \beta_{\mathrm{R}})$ when $q = -1$ or $(\alpha_{\mathrm{F}}, \beta_{\mathrm{F}})$ when $q = 1$. Accordingly, q is responsible for the selection of the camera measurements used to define the input.

With this notation, the dynamics (3.11) can be unified, by using the state q, in the flow map

$$\dot{\xi} = \begin{bmatrix} \dot{r} \\ \dot{\beta} \\ \dot{\alpha} \\ \dot{q} \end{bmatrix} = f(\xi, v) := \begin{bmatrix} -qv_1 r\cos(\alpha) \\ -v_2 \\ -v_2 + qv_1 \sin(\alpha) \\ 0 \end{bmatrix}, \quad \xi \in \mathcal{C}, \tag{3.20b}$$

with the flow set $\mathcal{C} = \Xi$ as in (3.20a). The feedback laws (3.17) and (3.19) are unified as $v = \kappa(\xi)$, with

$$\kappa(\xi) := \begin{bmatrix} qk_r \cos(\alpha) \\ k_r \cos(\alpha)\sin(\alpha) + k_\alpha \alpha + k_\beta(\alpha - \beta)\cos(\alpha)\frac{\sin(\alpha)}{\alpha} \end{bmatrix}. \tag{3.20c}$$

The jump map and the jump set ensure completeness of maximal solutions inspired by (3.7), by jumping from the boundary of $\mathcal{C}$ to its interior. Define the functions

$$g_\beta(\xi) = \begin{bmatrix} r \\ \beta - 2\pi\mathrm{sign}(\beta) \\ \alpha \\ q \end{bmatrix}, \; g_\alpha(\xi) = \begin{bmatrix} r \\ \beta \\ \alpha - \pi\mathrm{sign}(\alpha) \\ -q \end{bmatrix}, \tag{3.20d}$$

the first one encompassing 2π wraps of the angle β and the second one stemming from the relationship between α_{F} and α_{R} in (3.7). In addition, we define jump sets

$$\begin{aligned} \mathcal{D}_\alpha &:= \left\{\xi \in \Xi : |\alpha| \geq \frac{\pi}{2} + \delta\right\}, \\ \mathcal{D}_\beta &:= \left\{\xi \in \Xi : |\beta| \geq \frac{3}{2}\pi + \delta\right\}, \\ \mathcal{D} &:= \mathcal{D}_\beta \cup \mathcal{D}_\alpha, \end{aligned} \tag{3.20e}$$

covering the boundary of $\mathcal{C}$. Finally, the jump map (which is set-valued) is defined as

$$\xi^+ \in G(\xi) = \begin{cases} \{g_\beta(\xi)\}, & \text{if } \xi \in \mathcal{D}_\beta \backslash \mathcal{D}_\alpha, \\ \{g_\alpha(\xi)\}, & \text{if } \xi \in \mathcal{D}_\alpha \backslash \mathcal{D}_\beta, \\ \{g_\alpha(\xi)\} \cup \{g_\beta(\xi)\}, & \text{if } \xi \in \mathcal{D}_\alpha \cap \mathcal{D}_\beta. \end{cases} \tag{3.20f}$$

Note that $\beta^+ = \beta - 2\pi\mathrm{sign}(\beta)$, defined through g_β, guarantees that β^+ and β differ by a multiple of 2π and $|\beta^+| < |\beta|$ for all $\xi \in \mathcal{D}_\beta$ (wherein $|\beta| \geq \frac{3}{2}\pi + \delta$). Thus, β^+ and β describe the same information with respect to the position of the robot but β^+ is closer to the target orientation $\beta = 0$. Similarly, $\alpha^+ = \alpha - \pi\mathrm{sign}(\alpha)$, defined through g_α, captures the properties in (3.7) when the perspective of the cameras is switched. We compactly write the closed-loop hybrid system (3.20) as

$$\mathcal{H}: \left\{ \begin{array}{rcll} \dot{\xi} & = & f(\xi, \kappa(\xi)), & \xi \in \mathcal{C}, \\ \xi^+ & \in & G(\xi), & \xi \in \mathcal{D}. \end{array} \right. \tag{3.21}$$

System (3.21) satisfies the Hybrid Basic Conditions in Definition 2.2.1, therefore asymptotic stability of any compact set is robust in the general sense discussed in Definition 2.3.8.

Remark 12. *Let κ_0 be the stabilizer in* (3.20c) *evaluated for $k_\beta = 0$. Then,* (3.21) *returns the expression of the hybrid closed-loop system without angular stabilization, that is*

$$\mathcal{H}_\phi: \left\{ \begin{array}{rcll} \dot{\xi} & = & f(\xi, \kappa_0(\xi)), & \xi \in \mathcal{C}, \\ \xi^+ & \in & G(\xi), & \xi \in \mathcal{D}, \end{array} \right. \tag{3.22}$$

where the rationale is to globally asymptotically stabilize the robot position (r, α), but not its orientation β. In the coordinates (3.10)*, this maps back to only focusing on the position p and disregarding the orientation ϕ.*

Before presenting the stability properties of the closed-loop systems (3.21) and (3.22), we present a preliminary result stating that any solution switches between the front and rear cameras or vice versa at most once.

Lemma 3.2.6. *Let $\delta \in (0, \frac{\pi}{2})$, $k_r, k_\alpha \in \mathbb{R}_{>0}$, $k_\beta \in \mathbb{R}_{\geq 0}$ be arbitrary. Then, the set Ω is strongly forward invariant for* (3.21) *and* (3.22)*. Moreover, for each $\xi \in \mathcal{D}_\alpha$, g_α defined in* (3.20d) *satisfies $g_\alpha(\xi) \in \Omega := \{\xi \in \Xi : |\alpha| \leq \frac{\pi}{2}\} = \mathbb{R}_{\geq 0} \times [-\frac{3}{2}\pi - \delta, \frac{3}{2}\pi + \delta] \times [-\frac{\pi}{2}, \frac{\pi}{2}] \times \{-1, 1\}$.*

Remark 13. *By definition of Ω we have that $\mathcal{D}_\alpha \cap \Omega = \emptyset$. This, combined with the results of Lemma 3.2.6, stating that Ω is strongly forward invariant and that $g_\alpha(\xi) \in \Omega$ for $\xi \in \mathcal{D}_\alpha$, imply that along every solution of* (3.21), (3.22) *there can be at most one jump from the front to the rear camera, or vice versa.*

Proof of Lemma 3.2.6. To prove the first statement we show that solutions starting in Ω can not exit the set while flowing in $\mathcal{C} \cap \Omega$ or by jumping from $\mathcal{D}_\beta \cap \Omega$. This, together with Remark 13, ensures that solutions can not leave the set Ω once they enter it. Consider the function $V_{\mathrm{B}}(\xi) = \frac{1}{2}\alpha^2$ and consider a time $(t, j) \in \mathrm{dom}(\xi)$, where a solution $\xi(\cdot, \cdot)$ starting in Ω is flowing. Under this assumption, for $\xi(t, j) \in \mathcal{C} \cap \Omega$, the directional derivative of V_{B} along $f(\xi, \kappa(\xi))$ in (3.21) (which also covers (3.22) for $k_\beta = 0$) is

$$\begin{aligned} \dot{V}_{\mathrm{B}}(\xi) &= \langle \nabla V_{\mathrm{B}}(\xi), f(\xi, \kappa(\xi)) \rangle \\ &= -k_\alpha \alpha^2 - k_\beta \alpha \cos(\alpha) \sin(\alpha) + k_\beta \beta \cos(\alpha) \sin(\alpha), \end{aligned}$$

which implies that

$$\xi(t,j) \in \mathcal{C} \cap \Omega \text{ and } |\alpha| = \frac{\pi}{2} \quad \Longrightarrow \quad \dot{V}_{\mathrm{B}}(\xi) = -k_\alpha \frac{\pi^2}{4} < 0.$$

This inequality implies that $\frac{d}{dt}|\alpha| < 0$ when $|\alpha| = \frac{\pi}{2}$ in Ω. Therefore, solutions can not exit Ω while flowing. Consider now solutions jumping from $\mathcal{D}_\beta \cap \Omega$. Since the jump map (3.20d) does not change the α component of ξ we have that $\xi(t, j+1) = g_\beta(\xi(t,j))$ is still inside Ω. These two results combined with Remark 13 ensure that solutions can not leave the set Ω once they enter it, which proves the first statement. Consider now a solution $\xi(\cdot,\cdot)$ and $(t,j) \in \operatorname{dom}(\xi)$, such that $\xi(t,j) \in \mathcal{D}_\alpha$. From (3.20d) we have

$$\begin{aligned}
|\alpha(t,j+1)| &= |\alpha(t,j) - \pi \operatorname{sign}(\alpha(t,j))| \\
&= |\operatorname{sign}(\alpha(t,j))(|\alpha(t,j)| - \pi)| = |(|\alpha(t,j)| - \pi)| \\
&= \left|\tfrac{\pi}{2} + \delta - \pi\right| = \left|\delta - \tfrac{\pi}{2}\right| < \tfrac{\pi}{2},
\end{aligned}$$

and thus $\xi(t, j+1) = g_\alpha(\xi(t,j)) \in \Omega$, which proves the second statement. □

We now characterize the stability properties of the set

$$\mathcal{A}_q = \{0\} \times \{0\} \times \{0\} \times \{-1, 1\}, \tag{3.23}$$

for $\mathcal{H}$ in (3.21) and of the set

$$\mathcal{A}_{q,\phi} = \{0\} \times \left[-\frac{3}{2}\pi - \delta, \frac{3}{2}\pi + \delta\right] \times \{0\} \times \{-1, 1\}, \tag{3.24}$$

for $\mathcal{H}_\phi$ in (3.22). Here, $\mathcal{A}_q$ specifies zero orientation (for β), while $\mathcal{A}_{q,\phi}$ does not enforce any asymptotic orientation β.

Theorem 3.2.7. *Let $\delta \in (0, \frac{\pi}{2})$, $k_r, k_\alpha \in \mathbb{R}_{>0}$ be arbitrary and $k_\beta = 0$. Then, all maximal solutions of the hybrid closed-loop system* (3.22) *are complete and the set $\mathcal{A}_{q,\phi}$ in* (3.24) *is uniformly globally robustly asymptotically stable for* (3.22)*.*

Proof. We start by observing that the hybrid system (3.22) satisfies the Hybrid Basic Conditions in Definition 2.2.1.
Consider the Lyapunov function candidate $V_\phi(\xi) = \frac{1}{2}(r^2 + \alpha^2)$. It is immediate to check that V_ϕ satisfies the requirements in Definition 2.4.1. From the results presented in Proposition 3.2.2 and in Corollary 3.2.3 it follows that the directional derivative of V_ϕ is negative definite with respect to $\mathcal{A}_{q,\phi}$ along flowing solutions. Moreover for $\xi \in \mathcal{D}_\alpha$ we have that

$$\begin{aligned}
V_\phi(\xi^+) - V_\phi(\xi) &= \tfrac{1}{2}(\alpha^+)^2 - \tfrac{1}{2}\alpha^2 \\
&= \tfrac{1}{2}[(\alpha - \pi \operatorname{sign}(\alpha))^2 - \alpha^2] \\
&= \tfrac{1}{2}[\alpha^2 + \pi^2 - 2\pi|\alpha| - \alpha^2] \\
&= \tfrac{1}{2}(\pi^2 - 2\pi|\alpha|) < 0,
\end{aligned}$$

where the last inequality holds because, for $\xi \in \mathcal{D}_\alpha$, $|\alpha| \geq \frac{\pi}{2} + \delta > \frac{\pi}{2}$, according to the definition of $\mathcal{D}_\alpha$ in (3.20e). Additionally, for any $\xi \in \mathcal{D}_\beta$, $V_\phi(\xi^+) - V_\phi(\xi) = 0$, because V_ϕ does not depend on β. Since $V_\phi(\cdot)$ is non-increasing along solutions to (3.22), Theorem 2.4.3 implies that the set $\mathcal{A}_{q,\phi}$ is uniformly globally stable, and thus all solutions are bounded. Moreover, since V_ϕ remains constant, outside $\mathcal{A}_{q,\phi}$, only when the solutions jump from $\mathcal{D}_\beta$, and since $\xi^+ = g_\beta(\xi) \notin \mathcal{D}_\beta$, we can conclude that the only complete solutions $\xi(t,j)$ along which V_ϕ remains identically constant satisfy $V_\phi(\xi(t,j)) = 0$ for all $(t,j) \in \operatorname{dom} \xi$. Then, Corollary 2.4.6 implies that all complete solutions converge to $\mathcal{A}_{q,\phi}$, proving global pre-attractivity of $\mathcal{A}_{q,\phi}$, and therefore, combined with stability, proving that $\mathcal{A}_{q,\phi}$ is globally pre-asymptotic stable for (3.22). Uniformity and robustness follow from Theorem 2.3.9.
We conclude the proof by showing completeness of all maximal solutions. Since we have that (3.22) satisfies the Hybrid Basic Conditions in Definition 2.2.1, all solutions are bounded, and $G(\mathcal{D}) \subset \mathcal{C} \cup \mathcal{D}$, the only condition to check in Theorem 2.2.5 is the fact that $f(\xi, \kappa(\xi)) \subset T_\mathcal{C}(\xi)$ holds for all $\xi \in C \setminus \mathcal{D}$. Before we verify that condition $f(\xi, \kappa(\xi)) \subset T_\mathcal{C}(\xi)$ holds, we observe that, since the q component of ξ in (3.20a) is a logic variable satisfying $q \in \{-1, 1\}$, we have $T_\mathcal{C}(\xi) \subset \mathbb{R}^3 \times \{0\}$ for all $\xi \in \mathcal{C}$. This fact follows directly from Definition 2.2.4, by observing that any sequence of points $\{\xi_j\} \in \mathcal{C}$, converging to some $\overline{\xi} \in \mathcal{C}$ with $\overline{q} \in \{-1, 1\}$, satisfies $q_j \in \{-1, 1\}$, and therefore the ratio $\frac{\overline{q} - q_j}{\lambda_j}$ converges to zero for any sequence $\lambda_j \searrow 0$. This is in accordance to the fact that, during flow, the value of q is kept constant, and so $\dot{q} = 0$. The only points in $\mathcal{C} \setminus \mathcal{D}$ that are not in the interior of $\mathcal{C}$ (for those points one has $T_\mathcal{C}(\xi) = \mathbb{R}^3 \times \{0\}$) are those in the set $\{\xi \in \Xi : r = 0, |\alpha| < \frac{\pi}{2} + \delta, |\beta| < \frac{3}{2}\pi + \delta\}$, for which $T_\mathcal{C}(\xi) = \{0\} \times \mathbb{R}^2 \times \{0\}$. Substituting $r = 0$ in (3.20b) yields $\dot{r} = f_r(\xi, \kappa(\xi))|_{r=0} = 0$. Then, $f(\xi, \kappa(\xi)) \in T_\mathcal{C}(\xi)$ for all $\xi \in \mathcal{C} \setminus \mathcal{D}$, and therefore all maximal solutions to (3.22) are complete from Theorem 2.2.5.

$\square$

Theorem 3.2.8. *Let $\delta \in (0, \frac{\pi}{2})$, $k_r, k_\alpha, k_\beta \in \mathbb{R}_{>0}$ be arbitrary. Then all solutions of the hybrid closed-loop system* (3.21) *are complete and the set $\mathcal{A}_q$ in* (3.23) *is robustly uniformly globally asymptotically stable for* (3.21).

Before we give the proof of Theorem 3.2.8, note that this is not a simple extension of the proof of Theorem 3.2.7. The function

$$V(\xi) = \frac{1}{2}\left(r^2 + \frac{k_\beta}{k_r}(\alpha - \beta)^2 + \alpha^2\right) \tag{3.25}$$

is non-increasing along solutions flowing in $\mathcal{C}$. This is an immediate consequence of Proposition 3.2.4 and Corollary 3.2.5, and the selection of f in (3.20b) and of κ in (3.20c).

Note also that solutions jumping from $\xi \in \mathcal{D}_\beta$ satisfy

$$\begin{aligned} V(\xi^+) - V(\xi) &= \tfrac{k_\beta}{2k_r}(\alpha^+ - \beta^+)^2 - \tfrac{k_\beta}{2k_r}(\alpha - \beta)^2 \\ &= \tfrac{k_\beta}{2k_r}\left[4(\alpha - \beta)\mathrm{sign}(\beta)\pi + 4\pi^2\right] \\ &= 2\tfrac{k_\beta}{k_r}\left[\alpha\mathrm{sign}(\beta)\pi - \beta\mathrm{sign}(\beta)\pi + \pi^2\right] \\ &\leq 2\tfrac{k_\beta}{k_r}\left[(\tfrac{\pi}{2} + \delta)\pi - (\tfrac{3}{2}\pi + \delta)\pi + \pi^2\right] = 0, \end{aligned}$$

by the choice of domain $[-\frac{3}{2}\pi - \delta, \frac{3}{2}\pi + \delta]$ for β. On the other hand, non-increase of V across jumps from $\xi \in \mathcal{D}_\alpha$ is not guaranteed. Indeed, the change of V across jumps from $\mathcal{D}_\alpha$ is

$$\begin{aligned} V(\xi^+) - V(\xi) &= \tfrac{k_\beta}{2k_r}(\alpha^+ - \beta)^2 + \tfrac{1}{2}(\alpha^+)^2 - \tfrac{k_\beta}{2k_r}(\alpha - \beta)^2 + \tfrac{1}{2}\alpha^2 \\ &= \tfrac{k_\beta}{k_r}(\alpha - \beta)\mathrm{sign}(\alpha)\pi + \tfrac{k_\beta}{2k_r}\pi^2 - |\alpha|\pi + \tfrac{1}{2}\pi^2 \\ &= -\tfrac{k_\beta}{k_r}|\alpha|\pi + \tfrac{k_\beta}{k_r}\beta\mathrm{sign}(\alpha)\pi + \tfrac{k_\beta}{2k_r}\pi^2 - |\alpha|\pi + \tfrac{1}{2}\pi^2 \\ &\leq -\tfrac{k_\beta}{k_r}(\tfrac{\pi}{2} + \delta)\pi + \tfrac{k_\beta}{k_r}(\tfrac{3}{2}\pi + 2\delta)\pi + \tfrac{k_\beta}{2k_r}\pi^2 - (\tfrac{\pi}{2} + \delta)\pi + \tfrac{1}{2}\pi^2 \\ &\leq -\delta\pi(1 - \tfrac{k_\beta}{k_r}) + \tfrac{3}{2}\tfrac{k_\beta}{k_r}\pi^2, \end{aligned} \tag{3.26}$$

where the last term is a constant upper bound on $V(g_\alpha(\xi)) - V(\xi)$, whose sign depends on the values of the gains k_r, k_β.

By (3.26), for an arbitrary gain selection, V may increase after a jump from $\mathcal{D}_\alpha$. Therefore, the Hybrid Invariance Principle in Corollary 2.4.6 can not be used to conclude global asymptotic stability. For this reason, we present a proof based on two steps, relying on Lemma 3.2.6 and on an intermediate result for the reduced system $\mathcal{H}_\beta := (\mathcal{C}, F, \mathcal{D}_\beta, g_\beta)$, where the original jump dynamics (3.20f) are replaced by

$$\xi^+ = g_\beta(\xi), \quad \xi \in \mathcal{D}_\beta. \tag{3.27}$$

Proof of Theorem 3.2.8. We split the proof in two parts.

Step 1. Stability properties of $\mathcal{A}_q$ for $\mathcal{H}_\beta$: We start by pointing out that $\mathcal{H}_\beta$ satisfies the Hybrid Basic Conditions in Definition 2.2.1, since it shares the same flow data as $\mathcal{H}$, $\mathcal{D}_\beta$ is closed, and g_β is continuous and bounded in $\mathcal{D}_\beta$. Note that there exist solutions of $\mathcal{H}_\beta$ which are maximal but not complete, i.e., solutions that stop in the set $\{\xi \in \Xi : |\alpha| = \frac{\pi}{2} + \delta\}$ with bounded time domain. For this reason we characterize the stability properties of $\mathcal{A}_q$ for $\mathcal{H}_\beta$ in terms of pre-attractivity and global pre-asymptotic stability.

Lyapunov stability of $\mathcal{A}_q$ follows from V in (3.25) being non-increasing in $\mathcal{C} \cup \mathcal{D}_\beta$ (see the proof of Proposition 3.2.4 and Corollary 3.2.5). Moreover, since V is non-increasing along all solutions to $\mathcal{H}_\beta$, Theorem 2.4.3 allow us to conclude uniform global stability of $\mathcal{A}_q$, which in turn implies that all solutions are bounded.

We now show that all complete solutions of $\mathcal{H}_\beta$ asymptotically converge to $\mathcal{A}_q$. Since $\mathcal{H}_\beta$ satisfies the Hybrid Basic Conditions, $\mathcal{D}_\beta \cap g_\beta(\mathcal{D}_\beta) = \emptyset$, and all solutions are bounded, Theorem 2.2.6 ensures that all solutions have a non-zero dwell-time. Since solutions must flow after a jump from $\mathcal{D}_\beta$, we have that any complete solution $\xi(t,j)$ to $\mathcal{H}_\beta$ along which V is constant must satisfy $\dot{V}(\xi(t,j)) = 0$ for almost all $(t,j) \in \operatorname{dom}\xi$ such that $\xi(t,j) \in \mathcal{C}$. This, in turn, implies that such a solution must belong to the set $\dot{V}^{-1}(0) = \{\xi \in \Xi : r = \alpha = 0\}$ for almost all $(t,j) \in \operatorname{dom}\xi$ such that $\xi(t,j) \in \mathcal{C}$. The definition of $\dot{V}^{-1}(0)$ follows from (3.18). As shown in the proof of Proposition 3.2.4, a complete solution to (3.11) can remain in the set $\dot{V}^{-1}(0)$ only if $\beta_{\mathrm{R}} = 0$. The same statement can be made with respect to β_{F} (with reference to Corollary 3.2.5). Therefore, we have that the only complete solutions to $\mathcal{H}_\beta$ along which V is constant must also have $\beta = 0$, and thus satisfy $V(\xi(t,j)) = 0$ for all $(t,j) \in \operatorname{dom}\xi$. Therefore, Corollary 2.4.6 implies that all complete solutions converge to $\mathcal{A}_q$. This, together with the fact that all solutions are bounded, proves global pre-attractivity of $\mathcal{A}_q$. Uniform global pre-asymptotic stability of $\mathcal{A}_q$ follows from Theorem 2.3.9.
Before we continue with the next step of the proof, we point out that all maximal solutions to $\mathcal{H}_\beta$ that do not reach $\mathcal{D}_\alpha$ are complete, since they are bounded. Moreover, in all points of $\mathcal{C} \setminus \mathcal{D} = \{\xi \in \Xi : |\alpha| < \frac{\pi}{2} + \delta, |\beta| < \frac{3}{2}\pi + \delta\}$ condition (2.2) is satisfied, and $g_\beta(\mathcal{D}_\beta \setminus \mathcal{D}_\alpha) \subset \operatorname{int}\mathcal{C}$.
Step 2. Stability properties of $\mathcal{A}_q$ for $\mathcal{H}$: Lyapunov stability of $\mathcal{A}_q$ for $\mathcal{H}$ can be shown using the fact that $\mathcal{D}_\alpha$ is bounded away from $\mathcal{A}_q$, which implies that there exists a neighborhood of $\mathcal{A}_q$ in which V is non-increasing. Additionally, all solutions to $\mathcal{H}$ that do not reach $\mathcal{D}_\alpha$ are also solutions to $\mathcal{H}_\beta$, and therefore are complete, bounded, and asymptotically converge to $\mathcal{A}_q$. Consider now solutions to $\mathcal{H}$ for which there exists a time (t,j) such that $\xi(t,j) \in \mathcal{D}_\alpha$. From Lemma 3.2.6 we have that $\xi(t,j+1) \in \Omega$, and since Ω is strongly forward invariant for both $\mathcal{H}$ and $\mathcal{H}_\beta$, the tail of such solutions to $\mathcal{H}$, from time $(t,j+1)$ onward, coincide with the complete solutions ξ_β to $\mathcal{H}_\beta$ starting at $\xi_\beta(0,0) = \xi(t,j+1)$, and thus asymptotically converge to $\mathcal{A}_q$. Since the increment in (3.26) is upper bounded by a constant and V is non-increasing in Ω, these solutions of $\mathcal{H}$ are also bounded. Since all maximal solutions of $\mathcal{H}$ are complete, bounded, and asymptotically converge to $\mathcal{A}_q$, we have global attractivity of $\mathcal{A}_q$. Uniformity and robustness of global asymptotic stability of $\mathcal{A}_q$ for $\mathcal{H}$ follow from Theorem 2.3.9. □

Remark 14. *The hybrid control architecture proposed in* (3.20) *assumes the same values of control gains $k_r, k_\alpha \in \mathbb{R}_{>0}$, $k_\beta \in \mathbb{R}_{\geq 0}$ for both cameras. Indeed, once the gains k_r, k_α, k_β have been selected, they are used for both values of $q \in \{-1, 1\}$ in* (3.20c). *This is a consequence of the fact that the proofs of Theorem 3.2.7 and 3.2.8 rely on showing that a suitably defined function is*

a common Lyapunov function for both camera-based stabilizers, that is, this function decreases during flow when each camera is used (for each value of q). For the stabilization of the position of the vehicle, considering the Lyapunov function used in the proof of Theorem 3.2.7, $V_\phi(\xi) = \frac{1}{2}(r^2 + \alpha^2)$, it is possible to verify, following steps similar to those presented in the proof of Proposition 3.2.2, that negative definiteness of the directional derivative of V_ϕ is preserved under a different selection of control gains $k_r, k_\alpha \in \mathbb{R}_{>0}$ for the front and rear camera.
For the stabilization of the full pose of the vehicle, instead, non-positivity of the Lyapunov derivative of the function $V = \frac{1}{2}(r^2 + \frac{k_\beta}{k_r}(\alpha - \beta)^2 + \alpha^2)$ is achieved, in the proof of Theorem 3.2.8, by canceling potentially harmful terms via the feedback (3.20c)*. These cancellations rely on the gains k_r and k_β being constant with respect to q. Therefore, for the stabilization of the full pose of the vehicle, the front and rear camera must share the same selection of gains k_r, k_β, while the gain k_α can be selected independently.*

3.2.4 ROBUSTNESS ANALYSIS

Common perturbations considered in the literature are measurement errors in the feedback loop and external additive disturbances affecting the dynamics. The switch between front and rear cameras, modelled by a jump of α, and the reset of the robot orientation angle, modelled by a jump of β, may also be affected by uncertainties. The goal of this section is to characterize the robustness properties of the closed-loop system to these types of uncertainties. Note that in the following analysis we do not consider perturbations affecting the measurement of the logic variable q or its dynamics. This choice is motivated by the fact that the value of q represents which camera is currently being used by the system. Assuming no hardware failure, it is reasonable to think that q is always known exactly. To simplify the notation used in this section and in the next one, we define $\mathbb{B}_q := \mathbb{B} \times \{0\} \subset \mathbb{R}^4$, where $\mathbb{B}$ is the unit ball in $\mathbb{R}^3$.
For $\mathcal{H}$ in (3.21), $\bar{r} > 0$ arbitrary, $\lambda \in \mathbb{R}_{>0}$ and $\mu : \Xi \to \mathbb{R}_{\geq 0}$ positive definite with respect to $\mathcal{A}_q$, we define the perturbed system

$$\mathcal{H}_p : \begin{cases} \dot{\xi} & \in f(\xi, \kappa(\xi + \mu(\xi)\mathbb{B}_q)) + \mu(\xi)\mathbb{B}_q, & \xi \in \mathcal{C}_{\bar{r}} + \lambda\mathbb{B}_q \\ \xi^+ & \in G(\xi) + \mu(\xi)\mathbb{B}_q, & \xi \in \mathcal{D}_{\bar{r}} + \lambda\mathbb{B}_q \end{cases} \tag{3.28a}$$

where

$$\mathcal{C}_{\bar{r}} := \mathcal{C} \cap \{\xi \in \Xi : r \leq \bar{r}\}, \quad \mathcal{D}_{\bar{r}} := \mathcal{D} \cap \{\xi \in \Xi : r \leq \bar{r}\}. \tag{3.28b}$$

The use of a differential (respectively, difference) inclusion in the definition of the perturbed flow (respectively, jump) dynamics in (3.28a) allows capturing the effect of all possible additive disturbances and measurement errors affecting the feedback $\kappa(\cdot)$ that, along a solution $\xi(t,j)$ of (3.28), are contained in the set $\mu(\xi(t,j))\mathbb{B}_q$ for all $(t,j) \in \mathrm{dom}(\xi)$. The constant $\lambda > 0$, defining an inflation of $\mathcal{C}_{\bar{r}}$ and $\mathcal{D}_{\bar{r}}$, generates solutions along which the cameras are switched too early or too late, and the reset of the angle β happens for $|\beta|$ larger or smaller than $\frac{3}{2}\pi + \delta$. Since $\mathbb{B}_q$ is used instead of $\mathbb{B}$ in (3.28a), the perturbations do not affect q or the dynamics of q.

Theorem 3.2.9. *Let $\delta \in (0, \frac{\pi}{2})$, $k_r, k_\alpha, k_\beta \in \mathbb{R}_{>0}$ and $\overline{r} > 0$ be arbitrary. Then, there exist a scalar function $\xi \mapsto \mu(\xi)$, positive definite with respect to $\mathcal{A}_q$, and $\lambda > 0$ such that $\mathcal{A}_q$ is uniformly globally pre-asymptotically stable for* (3.28).

Observe that uniform global pre-asymptotic stability of $\mathcal{A}_q$ for (3.28) implies semi-global robust uniform pre-asymptotic stability of $\mathcal{A}_q$ for (3.21), according to [48, Definition 7.18], due to the restriction $r \leq \bar{r}$ introduced in (3.28b). While it is possible to prove a global robustness result, doing so requires defining λ as a function of ξ. The robustness result we provide here, uniform in λ, is not restrictive for real applications, since $\bar{r}$ can be taken sufficiently large so that the restriction $r \leq \bar{r}$ is not relevant in the physical scale of the real system.

Proof of Theorem 3.2.9. Let us consider the perturbed system defined in (2.3), whose equations are recalled here for the convenience of the reader,

$$\mathcal{H}_\rho : \begin{cases} \dot{\xi} & \in F_\rho(\xi), \quad \xi \in \mathcal{C}_\rho, \\ \xi^+ & \in G_\rho(\xi), \quad \xi \in \mathcal{D}_\rho, \end{cases} \tag{3.29a}$$

where $\rho(\xi) : \Xi \to \mathbb{R}_{\geq 0}$ is a continuous function, positive definite with respect to $\mathcal{A}_q$, for which $\mathcal{A}_q$ is uniformly globally pre-asymptotically stable for system (3.29) and

$$\begin{aligned} \mathcal{C}_\rho &:= \{\xi \in \Xi : (\xi + \rho(\xi)\mathbb{B}) \cap \mathcal{C} \neq \emptyset\}, \\ F_\rho(x) &:= \overline{\mathrm{con}} f((\xi + \rho(\xi)\mathbb{B}) \cap \mathcal{C}, \kappa((\xi + \rho(\xi)\mathbb{B}) \cap \mathcal{C})) + \rho(x)\mathbb{B} \quad \forall x \in \mathbb{R}^n, \\ \mathcal{D}_\rho &:= \{\xi \in \Xi : (\xi + \rho(\xi)\mathbb{B}) \cap \mathcal{D} \neq \emptyset\}, \\ G_\rho(x) &:= \{\xi \in \Xi : \xi \in g + \rho(g)\mathbb{B}, g \in G((\xi + \rho(\xi)\mathbb{B}) \cap \mathcal{D})\} \quad \forall x \in \mathbb{R}^n, \\ \Xi_\rho &:= \mathcal{C}_\rho \cup \mathcal{D}_\rho. \end{aligned} \tag{3.29b}$$

Existence of ρ is guaranteed by Theorem 3.2.8.

To prove Theorem 3.2.9 we show that the data of (3.28) is a subset of the data of (3.29). Then, uniform global pre-asymptotic stability of $\mathcal{A}_q$ for (3.29) implies uniform global pre-asymptotic stability of $\mathcal{A}_q$ for (3.28).

We start by showing that for each $\overline{r} > 0$ there exists $\lambda > 0$ such that $\mathcal{C}_{\bar{r}} + \lambda\mathbb{B}_q \subset \mathcal{C}_\rho$ and $\mathcal{D}_{\bar{r}} + \lambda\mathbb{B}_q \subset \mathcal{D}_\rho$. Consider the set $\Gamma := (\mathcal{C} \cap \mathcal{D}) \cap \{\xi \in \Xi : r \leq \overline{r}\}$. Continuity and positive definiteness with respect to $\mathcal{A}_q$ of $\rho(\cdot)$, together with

the fact that Γ is compact and bounded away from $\mathcal{A}_q$, ensures that there exists $\varepsilon > 0$ sufficiently small such that $\rho(\xi) \geq \varepsilon$ for all $\xi \in \Gamma + \varepsilon\mathbb{B}$. Then, it is sufficient to pick $\lambda = \varepsilon$. We now show that there exist a function $\mu(\cdot)$, positive definite with respect to $\mathcal{A}_q$, such that $f(\xi, \kappa(\xi + \mu(\xi)\mathbb{B}_q)) + \mu(\xi)\mathbb{B}_q \subset F_\rho(\xi)$ and $G(\xi) + \mu(\xi)\mathbb{B}_q \subset G_\rho(\xi)$, for all $\xi \in \Xi_\rho$.
Consider the nominal flow dynamics in (3.21): $\dot{\xi} = f(\xi, \kappa(\xi))$. Continuity of the right-hand side with respect to ξ ensures that for each $\varepsilon > 0$ there exists a sufficiently small $\eta > 0$ such that $f(\xi, \kappa(\xi + \eta\mathbb{B}_q)) + \eta\mathbb{B}_q \subset f(\xi, \kappa(\xi)) + \varepsilon\mathbb{B}_q$ for all $\xi \in \Xi_\rho$. Observe now that from the definition of $F_\rho(\cdot)$ in (3.29b) we have $f(\xi, \kappa(\xi)) + \rho(\xi)\mathbb{B} \subset F_\rho(\xi)$. Since $\rho(\cdot)$ is positive definite with respect to $\mathcal{A}_q$, for each $\xi \in \Xi_\rho \backslash \mathcal{A}_q$ there exists $\varepsilon > 0$ such that $\rho(\xi) \geq \varepsilon$ and $f(\xi, \kappa(\xi)) + \varepsilon\mathbb{B}_q \subset F_\rho(\xi)$, for all $\xi \in \Xi_\rho \backslash \mathcal{A}_q$. Then, we can conclude that there exists $\mu_f : \Xi_\rho \to \mathbb{R}_{\geq 0}$, positive definite with respect to $\mathcal{A}_q$, such that $f(\xi, \kappa(\xi + \mu_f(\xi)\mathbb{B}_q)) + \mu_f(\xi)\mathbb{B}_q \subset f(\xi, \kappa(\xi)) + \rho(\xi)\mathbb{B} \subset F_\rho(\xi)$, for all $\xi \in \Xi_\rho$. Similarly, for the jump dynamics we can conclude the existence of a function $\mu_g : \Xi_\rho \to \mathbb{R}_{\geq 0}$, positive definite with respect to $\mathcal{A}_q$, such that $G(\xi) + \mu_d(\xi)\mathbb{B}_q \subset G_\rho(\xi)$ for all $\xi \in \Xi_\rho$. Accordingly, $\mu(\cdot)$ can be defined as the pointwise minimum between $\mu_f(\cdot)$ and $\mu_g(\cdot)$, for all $\xi \in \Xi_\rho$, i.e., $\mu(\xi) := \min\{\mu_g(\xi), \mu_f(\xi)\}$.
Finally, uniform global pre-asymptotic stability of $\mathcal{A}_q$ for (3.28) can be concluded from [48, Prop. 3.32], since $\mathcal{A}_q$ is uniformly globally pre-asymptotically stable for (3.29) and $\mathcal{C}_{\bar{r}} + \lambda\mathbb{B}_q \subset \mathcal{C}_\rho$, $f(\xi, \kappa(\xi) + \mu(\xi)\mathbb{B}_q) + \mu(\xi)\mathbb{B}_q \subset F_\rho(\xi)$ for all $\xi \in \mathcal{C}_{\bar{r}} + \lambda\mathbb{B}_q$, $\mathcal{D}_{\bar{r}} + \lambda\mathbb{B}_q \subset \mathcal{D}_\rho$, and $G(\xi) + \mu(\xi)\mathbb{B}_q \subset G_\rho(\xi)$ for all $\xi \in \mathcal{D}_{\bar{r}} + \lambda\mathbb{B}_q$. $\square$

3.2.5 STABILITY AND ROBUSTNESS IN THE CARTESIAN COORDINATES

In this section we characterize the behavior of the unicycle, driven by the camera-based stabilizers (3.15) and (3.16), as seen in the absolute reference frame. To this end, we define the Cartesian output of the systems (3.11), for a given solution $t \mapsto z_i(t)$, $i \in \{\mathrm{F}, \mathrm{R}\}$, as

$$x(t) := \gamma_i(z_i(t)),$$

$i \in \{\mathrm{F}, \mathrm{R}\}$, for all $t \in \mathrm{dom}(z_i)$, where $\gamma_i(\cdot)$ denotes the corresponding coordinate transformations in (3.6), and we interpret the Cartesian coordinates x of the unicycle during its motion as an output of a dynamical system. This is a natural "on-board" perspective.
The first observation we make is that the Cartesian output does not satisfy a ϱ-ε stability bound. Due to the lack of a homeomorphism between the coordinates systems, as observed at the end of Section 3.1, while uniform pre-asymptotic stability in the camera-based polar coordinates z_F, z_R implies

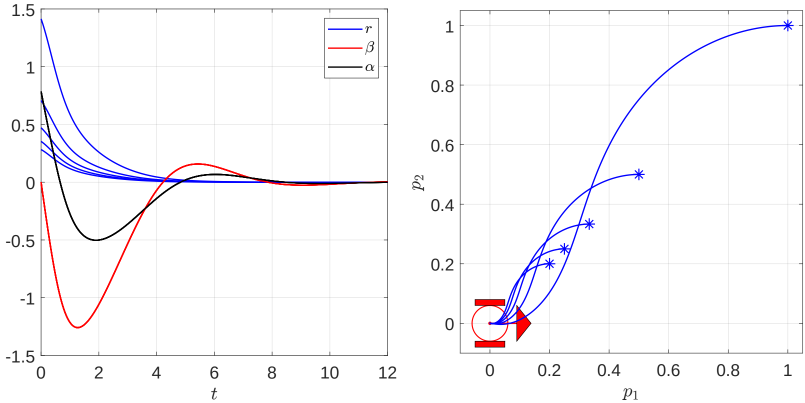

Figure 3.3: Closed-loop solutions of (3.11), (3.17) for different initial conditions $z_{\rm R}(0)$: time histories of $z_{\rm R}$ (left) Cartesian output responses (right). Recall from (3.6) that $\phi = -\beta_{\rm R}$.

the existence of $\beta \in \mathcal{KL}$ such that $|z_i(t)| \leq \beta(|z_i(0)|, t)$ for all $t \geq 0$, such a $\mathcal{KL}$ bound does not exist for the evolution of the Cartesian output $x = \gamma_i(z_i), i \in \{\mathrm{F}, \mathrm{R}\}$. More precisely, the Cartesian output does not satisfy a ϱ-ε stability bound (see [119, Definition 3] and [120] for definitions of output stability properties), because for any sufficiently small $\varepsilon > 0$ there exists no $\varrho > 0$ such that $|x(0)| \leq \varrho$ implies $|x(t)| \leq \varepsilon$ for all $t \geq 0$. This property of the Cartesian output is illustrated in Fig. 3.3, where the family of curves represents trajectories of the unicycle, obtained using the rear-camera stabilizer (3.17), starting from different initial conditions $z_{\rm R}(0)$ mapping to $p_1(0) = p_2(0) = \frac{\varrho}{\sqrt{2}}, \phi(0) = 0$, for decreasing values of $\varrho > 0$. As shown by the red and black curves at the left of Fig. 3.3, the trajectories all share the same time evolution of $\phi(t) = -\beta_{\rm R}(t)$ and $\alpha_{\rm R}(t)$, whose amplitudes do not decrease as ϱ goes to zero. Then, given an arbitrary $\varepsilon \in \mathbb{R}_{>0}$, there exists no $\varrho \in \mathbb{R}_{>0}$ such that $|x(0)| \leq \varrho$ implies $|x(t)| \leq \varepsilon$ for all $t \geq 0$.
However, since $r \to 0$ and $\beta_{\rm R} \to 0$ imply $x \to 0$, we can still prove convergence to zero of the Cartesian output, as stated below.
Lemma 3.2.10. *Let $k_r, k_\alpha, k_\beta \in \mathbb{R}_{>0}$ be arbitrary. Then, for any solution $z(t)$ of the z_R-system* (3.11), (3.15) *(or z_F-system* (3.11), (3.16)*), the Cartesian output $x(t) = \gamma_R(z(t))$ (or $x(t) = \gamma_F(z(t))$), is bounded, and, if the solution is complete, it asymptotically converges to the set $\{0\}^2 \times [-\frac{3}{2}\pi - \delta, \frac{3}{2}\pi + \delta] \subset \mathcal{X}$.*

The proof follows trivially from continuity of (3.6). A similar statement can be made using the feedback laws (3.17) or (3.19), for convergence to the origin of $\mathcal{X}$.

The control laws (3.15) and (3.16) use, respectively, measurements coming from the rear camera, $z_{\mathrm{R}} \in \mathcal{Z}$, and the front camera, $z_{\mathrm{F}} \in \mathcal{Z}$. Then, as discussed in Section 3.2.2, any result obtained using only one camera is *local* from the Cartesian point of view, in the sense that it holds in the set $\mathcal{X}_i, i \in \{\mathrm{F}, \mathrm{R}\}$, defined in (3.8). By using the hybrid control architecture (3.21), combining the measurements coming from both cameras, we can obtain *global* results that hold in the set $\mathcal{X}$.
Consider now the Cartesian output of the hybrid system (3.21), defined, for a given solution $\xi(t,j) = [z(t,j)^\top \ q(t,j)]^\top$ to (3.21), as

$$x(t,j) := \gamma_{q(t,j)}(z(t,j)),$$

for all $(t,j) \in \mathrm{dom}(\xi)$, where $\gamma_q(\cdot)$ combines the two coordinates transformations in (3.6) through the use of the logic variable q. We first show that uniformity of asymptotic stability of $\mathcal{A}_q$ for (3.21) implies uniformity of convergence of the Cartesian output. Similar results hold for system (3.22) and convergence of the Cartesian output to the set $\{0\}^2 \times [-\frac{3}{2}\pi - \delta, \frac{3}{2}\pi + \delta] \subset \mathcal{X}$.

Theorem 3.2.11. *Let $\delta \in (0, \frac{\pi}{2}), k_r, k_\alpha, k_\beta \in \mathbb{R}_{>0}$ be arbitrary. Then, for any solution $\xi(t,j)$ of (3.21), the Cartesian output $x(t,j) = \gamma_{q(t,j)}(z(t,j))$ satisfies the following property. For each $\epsilon, \varrho \in \mathbb{R}_{>0}$ there exists $T(\epsilon,\varrho) > 0$ such that $|x(0,0)| \leq \varrho$ implies $|x(t,j)| \leq \epsilon$ for all $(t,j) \in \mathrm{dom}(x)$ such that $t + j \geq T(\epsilon, \varrho)$.*

Proof. Observe that for any pair $x \in \mathcal{X}, \xi \in \Xi$, satisfying $x = \gamma_q(z)$ (recall the definition given in (3.6)) the inequality

$$|x|^2 = p_1^2 + p_2^2 + \phi^2 = r^2 + \beta^2 \leq r^2 + \alpha_q^2 + \beta^2 = |\xi|_{\mathcal{A}_q}^2 \tag{3.30}$$

holds. Fix an arbitrary $\varrho > 0$ and consider the compact set $\mathcal{X}_\varrho := \{x \in \mathcal{X} : |x| \leq \varrho\}$. From (3.6) we can see that the pre-image of $\mathcal{X}_\varrho$ through $\gamma_q(\cdot)$ is contained in the compact set $\Xi_\varrho := \{\xi \in \Xi : r \leq \varrho, \beta \leq \varrho, \alpha \in [-\frac{\pi}{2} - \delta, \frac{\pi}{2} + \delta], q \in \{-1, 1\}\}$. Since Ξ_ϱ is compact, there exists $\overline{\varrho} > 0$ sufficiently large such that $|\xi|_{\mathcal{A}_q} \leq \overline{\varrho}$ for all $\xi \in \Xi_\varrho$. Then, for any Cartesian output satisfying $|x(0,0)| \leq \varrho$, all solutions $\xi(t,j)$ of (3.21) for which $x(0,0) = \gamma_{q(0,0)}(z(0,0))$ satisfy $|\xi(0,0)|_{\mathcal{A}_q} \leq \overline{\varrho}$. Fix now an arbitrary $\epsilon > 0$. The uniform global attractivity property of $\mathcal{A}_q$ established in Theorem 3.2.8 implies that for each $\epsilon, \overline{\varrho} > 0$ there exists $\bar{T}(\epsilon, \overline{\varrho}) > 0$ such that $|\xi(0,0)|_{\mathcal{A}_q} \leq \overline{\varrho}$ implies $|\xi(t,j)|_{\mathcal{A}_q} \leq \epsilon$ for all $(t,j) \in \mathrm{dom}(\xi)$ such that $t + j \geq \bar{T}(\epsilon, \overline{\varrho})$. Then, from the inequality (3.30) it follows that $|x(0,0)| = |\gamma_{q(0,0)}(z(0,0))| \leq \varrho$ implies $|x(t,j)| \leq |\xi(t,j)|_{\mathcal{A}_q} \leq \epsilon$, for all $(t,j) \in \mathrm{dom}(x)$ such that $t + j \geq \bar{T}(\epsilon, \overline{\varrho})$. As a final step, since $\overline{\varrho}$ depends on ϱ, we can write $\bar{T}(\epsilon, \overline{\varrho}) = \bar{T}(\epsilon, \overline{\varrho}(\varrho)) =: T(\epsilon, \varrho)$. □

Following the results presented in Section 3.2.4, showing semi-global robustness of the asymptotic stability properties of the closed-loop system (3.21), we now derive robustness results for the Cartesian output of the perturbed system (3.28), defined through the relation $x(t,j) = \gamma_{q(t,j)}(z(t,j))$ for a given solution $(t,j) \mapsto \xi(t,j)$ to (3.28). The first result states that a uniform convergence property, as defined in Theorem 3.2.11, holds globally also for the Cartesian output of the perturbed system (3.28), and therefore uniform convergence is robust, semi-globally, for the Cartesian output of system (3.21).

Theorem 3.2.12. *Let the assumptions of Theorem 3.2.9 be satisfied and let $\mu(\cdot)$ and $\bar{r} > 0$ be defined as in Theorem 3.2.9. Then, for any solution $(t,j) \mapsto \xi(t,j)$ of (3.28), the Cartesian output $x(t,j) = \gamma_{q(t,j)}(z(t,j))$ satisfies the following property. For each $\epsilon, \varrho \in \mathbb{R}_{>0}$ satisfying $\varrho \leq \bar{r}$ there exists $T(\epsilon,\varrho) > 0$ such that $|x(0,0)| \leq \varrho$ implies $|x(t,j)| \leq \epsilon$ for all $(t,j) \in \mathrm{dom}(x)$ with $t + j \geq T(\epsilon,\varrho)$.*

While the uniform convergence result presented in Theorem 3.2.11 holds globally, its extension to the perturbed system (3.28), presented in Theorem 3.2.12, holds for $0 < \varrho \leq \bar{r}$. The bound $\varrho \leq \bar{r}$ ensures that $r(0,0)^2 = p_1(0,0)^2 + p_2(0,0)^2 \leq |x(0,0)|^2 \leq \varrho^2 \leq \bar{r}^2$ (recall the coordinates transformation (3.6)), allowing to apply the semi-global result stated in Theorem 3.2.9 to system (3.28) to establish asymptotic convergence to zero of the Cartesian output in the presence of measurement errors and perturbations.
Proof of Theorem 3.2.12. The result follows by applying the same steps as in the proof of Theorem 3.2.11 and using uniform global asymptotic stability of $\mathcal{A}_q$ for (3.28), established in Theorem 3.2.9. □

As a second result, we investigate how the perturbation function $\mu(\cdot)$ in (3.28a) can be recast and interpreted in the Cartesian output. For a given $\mu(\cdot)$ and for each $\xi \in \Xi$, we define the set

$$\Gamma(\xi) = \begin{bmatrix} \frac{\partial}{\partial z}\gamma_q(z) & 0 \end{bmatrix} \left(f(\xi, \kappa(\xi + \mu(\xi)\mathbb{B}_q)) + \mu(\xi)\mathbb{B}_q\right) \subset \mathbb{R}^3 \tag{3.31}$$

where $\frac{\partial}{\partial z}\gamma_q : \mathbb{R}^3 \to \mathbb{R}^{3\times 3}$ (with $q \in \{0,1\}$) denotes the gradient and $0 \in \mathbb{R}^3$ denotes the zero vector. First note that for a solution ξ to (3.28) and a time $(t,j) \in \mathrm{dom}(\xi)$, with ξ differentiable, it holds, when solutions evolve continuously in time, that $\dot{x}(t,j) = \frac{d}{dt}\gamma_{q(t,j)}(z(t,j)) = \frac{\partial}{\partial z}\gamma_{q(t,j)}(z(t,j))\dot{z}(t,j)$ and thus $\dot{x} \in \Gamma(\xi)$. Recalling (3.10), we also know that in the unperturbed setting the Cartesian output satisfies $\dot{x} = h(x,u)$, with $u = \left[\begin{smallmatrix} r & 0 \\ 0 & 1 \end{smallmatrix}\right]\kappa(\xi)$, according to (3.11), and $\kappa(\cdot)$ selected as in (3.20c). Recalling that $\xi = [z^\top \; q]^\top$, the condition $h(\gamma_q(z), u(\xi)) = \dot{x} \in \Gamma(\xi)$ holds. Exploiting this inclusion, we show that there exists a nontrivial perturbation function $\mu_x : \Xi \to \mathbb{R}_{\geq 0}$ such that $h(\gamma_q(z), u(\xi)) + \mu_x(\xi)\mathbb{B} \subset \Gamma(\xi)$, thus illustrating our robustness result also from the viewpoint of the Cartesian output x.

Theorem 3.2.13. *Let the assumptions of Theorem 3.2.9 be satisfied and let $\mu(\cdot)$ and $\bar{r}$ be defined as in Theorem 3.2.9. Then, there exists $\mu_x : \Xi \to \mathbb{R}_{\geq 0}$, positive definite with respect to $\{\xi \in \Xi : r = 0\}$, such that for any pair $(\xi, x) \in (\Xi \times \mathcal{X}) \cap \bar{r}\mathbb{B}$ satisfying $x = \gamma_q(z)$ the relation $h(x, u(\xi)) + \mu_x(\xi)\mathbb{B} \subset \Gamma(\xi)$ holds.*

Proof. By using the notation $\theta_q := \alpha - \beta - \frac{1+q}{2}\pi$ in the coordinates transformation (3.6) it holds that

$$\frac{\partial}{\partial z}\gamma_q(z) = \begin{bmatrix} \cos(\theta_q) & -r\sin(\theta_q) & r\sin(\theta_q) \\ \sin(\theta_q) & r\cos(\theta_q) & -r\cos(\theta_q) \\ 0 & 0 & -1 \end{bmatrix}, \tag{3.32}$$

and for $\xi \in \Xi$ the matrix on the right-hand side is singular if and only if $r = 0$. The set $\Gamma(\xi)$ defined in (3.31) can be rewritten as

$$\Gamma(\xi) = \left[\frac{\partial}{\partial z}\gamma_q(z) \quad 0 \right] f(\xi, \kappa(\xi + \mu(\xi)\mathbb{B}_q)) + \frac{\partial}{\partial z}\gamma_q(z)\mu(\xi)\mathbb{B}.$$

Accordingly, for each $(\xi, x) \in \Xi \times \mathcal{X}$ with $x = \gamma_q(z)$ and $r \neq 0$, there exists $\varepsilon > 0$ such that $\left[\frac{\partial}{\partial z}\gamma_q(z) \; 0\right] f(\xi, \kappa(\xi + \mu(\xi)\mathbb{B}_q)) + \varepsilon\mathbb{B} \subset \Gamma(\xi)$. This, in particular, implies that $h(x, u(\xi)) + \varepsilon\mathbb{B} = \left[\frac{\partial}{\partial z}\gamma_q(z) \; 0\right] f(\xi, \kappa(\xi)) + \varepsilon\mathbb{B} \subset \Gamma(\xi)$. Based on the definition of $\varepsilon > 0$, we can conclude that there exists a function $\mu_x : \Xi \to \mathbb{R}_{\geq 0}$, with $\mu_x(\xi) > 0$ for all $\xi \in \Xi$ with $r \neq 0$, such that $h(x, u(\xi)) + \mu_x(\xi)\mathbb{B} \subset \Gamma(\xi)$. □

The result stated in Theorem 3.2.13 can be interpreted in the following way. If the unicycle dynamics (3.10) is subject to any additive disturbance d satisfying $d \in \mu_x(\xi)\mathbb{B}$, then convergence of the Cartesian output x to the origin is preserved. Clearly, no robust stability bound can be established for the output x because, as already discussed at the beginning of the section (see Fig. 3.3), such a bound does not hold for the nominal case.

3.2.6 NUMERICAL SIMULATIONS

We illustrate the results derived in the preceding sections with two sets of numerical simulations. The feedback gains are selected as $k_r = 2, k_\alpha = 1, k_\beta = 0.3$ for the first set of simulations and $k_r = 1, k_\alpha = 2, k_\beta = 1$ for the second set. To define the field of view of the two cameras we use $\delta = \frac{\pi}{10}$ in the first set of simulations. The second set of simulations compares trajectories obtained using different values of δ. To indicate the pose of the robot $x_0 = [p_0^\top \; \phi_0]^\top$ we place in Figures 3.4 and 3.5 a unicycle icon at the initial position p_0, whose orientation coincides with the initial orientation ϕ_0. When the origin is inside the field of view of both cameras in the initial configuration, we show both trajectories obtained by initializing q_0 through -1 and 1, respectively.

To illustrate the robustness properties of the hybrid stabilizer, in Figure 3.4, we simulate the perturbed system (3.28a) and perform stabilization of the full pose (left plots) and position-only (right plots) by setting the gain k_β to zero. For each $\xi = [z^\top \ q]^\top$ the admissible amplitude of the perturbations in the simulations on the left and right are $\mu(\xi) = \frac{1}{3}|z|$ and $\mu(\xi) = \frac{1}{3}|z|_{\mathcal{A}}$, respectively, where $\mathcal{A}$ is the set in (3.14), so that the perturbations vanish as the pose, respectively, the position, of the robot converges to the origin. The parameter λ, modeling uncertainties affecting the cameras switching and the reset of the angle β, is set to zero. The resulting perturbed flow dynamics is $\dot{\xi} = f(\xi, \kappa(\xi + [e^\top \ 0]^\top)) + [d^\top \ 0]^\top$, where the components of the vectors $e, d \in \mathbb{R}^3$ are sampled from a uniform distribution over the interval $[-\mu(\xi), \mu(\xi)]$ and model possible measurement errors in the feedback and additive perturbations. In the top plots of Figure 3.4 we display two sets of trajectories in the Cartesian plane obtained by plotting the Cartesian output (3.6) of system (3.28a), showing convergence of the robot's position p to the origin. The simulations are obtained by initializing the unicycle at different positions on the unit circle and with a random initial orientation $\phi_0 = -\beta_0$. The trajectories along which the front camera ($q = 1$) is used are shown in red, while blue is used to indicate the rear camera ($q = -1$). In the bottom plots of Figure 3.4 we show the corresponding evolution of $z = [r \ \beta \ \alpha]^\top$ in continuous time for system (3.28a). Since the gain k_β is set to zero in the feedback law for the simulations on the right (recall the definition of κ_0 in Remark 12), the position of the unicycle converges to the origin while the orientation is generic, as expected from Proposition 3.2.2 and Corollary 3.2.3. Along the solutions on the left, instead, both position and orientation converge to zero. Moreover, we can see that increasing k_β from zero (right plot) to $k_\beta = 1$ (left plot) affects noticeably the speed of convergence of r and α, thus suggesting a natural trade-off.

Figure 3.5 shows two sets of simulations obtained using $\delta = \frac{\pi}{10}$ (left plot) and $\delta = \frac{\pi}{4}$ (right plot). The purple area represents the region of the Cartesian plane in which both cameras can see the origin in the initial configuration. When the initial configuration of the unicycle is in the purple region we show the two trajectories generated by selecting $q(0,0) = 1$ (in red) or $q(0,0) = -1$ (in blue).

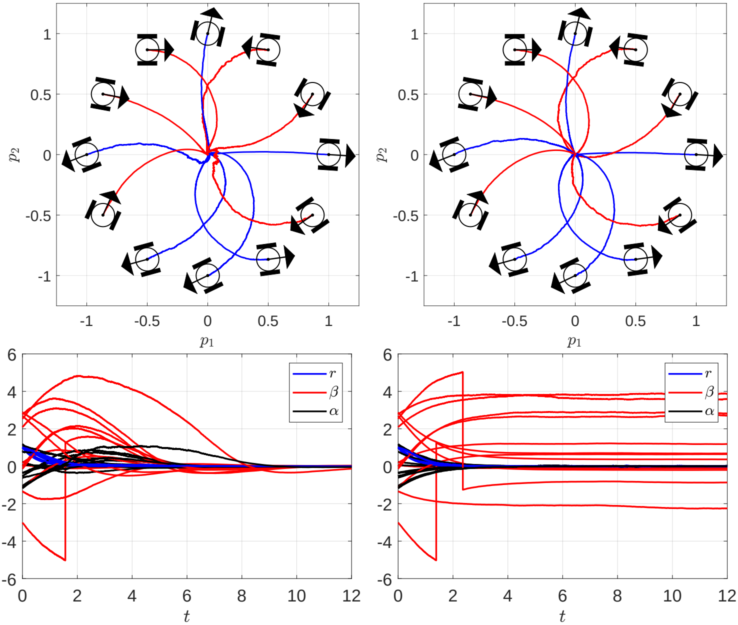

Figure 3.4: Closed-loop solutions of the hybrid system (3.28a) obtained by stabilizing the robot pose (left) and position (right). Top: Trajectories of the unicycle in the Cartesian plane. Bottom: Continuous time evolution of the camera-based coordinates $z = [r\ \beta\ \alpha]$.

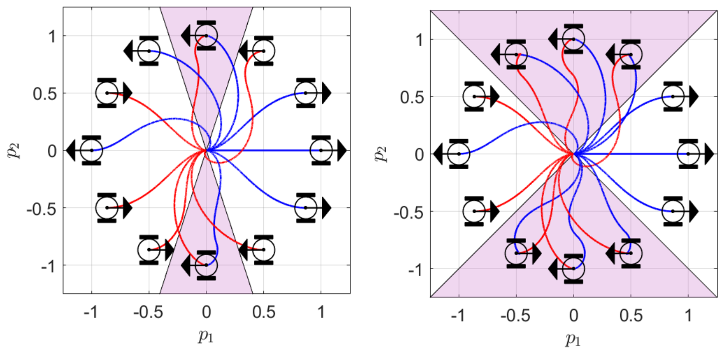

Figure 3.5: Closed-loop trajectories of the hybrid system (3.21) in the Cartesian plane for $\delta = \frac{\pi}{10}$ (left plot) and $\delta = \frac{\pi}{4}$ (right plot). In the purple region, both cameras see the target in the initial configuration.

3.3 MARINE SURFACE VESSELS

In this section we focus on marine surface vessels that can be described, in the Cartesian coordinates, using the dynamic equations proposed in [26]. We derive a kinematic model approximating the full dynamics and extend the results obtained for the unicycle model in Section 3.2 by proposing feedback laws for the simplified kinematic model and for the full dynamic model.

3.3.1 DERIVATION OF A KINEMATIC MODEL OF THE HOVERCRAFT

Let us consider the dynamical system representation of a hovercraft introduced in [26]

$$\begin{aligned} \dot{p}_1 &= v_1 \cos(\phi) - v_2 \sin(\phi), \\ \dot{p}_2 &= v_1 \sin(\phi) + v_2 \cos(\phi), \\ \dot{\phi} &= \omega, \end{aligned} \tag{3.33}$$

where $p = [p_1, p_2]^\top \in \mathbb{R}^2$ and $\phi \in \mathbb{R}$ denote the position and the orientation of the hovercraft; $v_1 \in \mathbb{R}$ and $v_2 \in \mathbb{R}$ denote the surge speed and the sway speed; and ω is the angular velocity. The dynamics of the velocities in the body-reference frame are

$$\begin{aligned} m\dot{v}_1 - m v_2 \omega + d_\nu v_1 &= F, \\ m\dot{v}_2 + m v_1 \omega + d_\nu v_2 &= 0, \\ J\dot{\omega} + d_r \omega &= T, \end{aligned} \tag{3.34}$$

where $F, T \in \mathbb{R}$ are the external force and torque inputs, $m, J \in \mathbb{R}_{>0}$ are the vehicle's mass and moment of inertia, and $d_\nu, d_r \in \mathbb{R}_{>0}$ are the coefficients of viscous and rotational friction.
Starting from the dynamics (3.33)-(3.34), we derive a kinematic model approximation, based on the assumption that v_1 and ω are slowly varying. In fact, when v_1 and ω are constant, from the second equation in (3.34) we observe that the sway speed v_2 converges to the value

$$v_2 = -\mu v_1 \omega := -\frac{m}{d_\nu} v_1 \omega, \tag{3.35}$$

where we have introduced the parameter $\mu := \frac{m}{d_\nu}$ to simplify the notation. Through the definition of the total speed

$$\eta := \sqrt{v_1^2 + v_2^2} \tag{3.36}$$

and by defining ψ through the implicit relationship

$$v_1 = \eta \cos(\psi), \qquad v_2 = \eta \sin(\psi), \tag{3.37}$$

(see Figure 3.6) we can rewrite (3.33), equivalently, as

$$\begin{bmatrix} \dot{p}_1 \\ \dot{p}_2 \end{bmatrix} = R(\phi)R(\psi)\begin{bmatrix} \eta \\ 0 \end{bmatrix} = R(\phi)\begin{bmatrix} \eta\cos(\psi) \\ \eta\sin(\psi) \end{bmatrix}, \tag{3.38}$$

by using an additional rotation matrix $R(\psi)$. Approximating v_2 by (3.35), we obtain from (3.37) the relation

$$\eta\sin(\psi) = v_2 = -\frac{m}{d_\nu}v_1\omega = -\mu\omega\eta\cos(\psi).$$

Substituting this expression in (3.38), and using the first relation in (3.37), allows writing the position dynamics in the form

$$\dot{p} = R(\phi)\begin{bmatrix} \eta\cos(\psi) \\ -\eta\cos(\psi)\mu\omega \end{bmatrix} = R(\phi)\begin{bmatrix} 1 \\ -\mu\omega \end{bmatrix} v_1. \tag{3.39}$$

Accordingly, approximating v_2 as in (3.35), we propose the kinematic model of the hovercraft

$$\dot{x} = f_{\mathrm{kin}}(x, u) \tag{3.40}$$

where the function $f_{\mathrm{kin}} : \mathbb{R}^3 \times \mathbb{R}^2 \to \mathbb{R}^3$ is defined as

$$f_{\mathrm{kin}}(x, u) = \begin{bmatrix} R(\phi) & 0 \\ 0 & 1 \end{bmatrix}\begin{bmatrix} u_1 \\ -\mu u_2 u_1 \\ u_2 \end{bmatrix} \tag{3.41}$$

with state $x = [p_1, p_2, \phi]^\top \in \mathbb{R}^3$ and input $u = [u_1, u_2]^\top = [v_1, \omega]^\top \in \mathbb{R}^2$ describing the surge speed and the angular velocity.

3.3.2 KINEMATIC AND DYNAMIC EQUATIONS IN POLAR COORDINATES

We assume that the hovercraft is equipped with on-board sensors, as depicted in Figure 3.6, and show that the equivalent representation of the equations of motion of the hovercraft (3.38) in the camera-based coordinates $z_i, i \in \{\mathrm{F}, \mathrm{R}\}$ introduced in Section 3.1, is given by

$$\dot{z}_{\mathrm{F}} = f_{\mathrm{F}}(z_{\mathrm{F}}, \nu) = \begin{bmatrix} -\nu_1 r\cos(\alpha_{\mathrm{F}}) - \mu\nu_1\nu_2 r\sin(\alpha_{\mathrm{F}}) \\ -\nu_2 \\ \nu_1\sin(\alpha_{\mathrm{F}}) - \nu_2 + \mu\nu_1\nu_2\cos(\alpha_{\mathrm{F}}) \end{bmatrix} \tag{3.42}$$

$$\dot{z}_{\mathrm{R}} = f_{\mathrm{R}}(z_{\mathrm{R}}, \nu) = \begin{bmatrix} \nu_1 r\cos(\alpha_{\mathrm{R}}) + \mu\nu_1\nu_2\sin(\alpha_{\mathrm{R}}) \\ -\nu_2 \\ -\nu_1\sin(\alpha_{\mathrm{R}}) - \nu_2 - \mu\nu_1\nu_2\cos(\alpha_{\mathrm{R}}) \end{bmatrix} \tag{3.43}$$

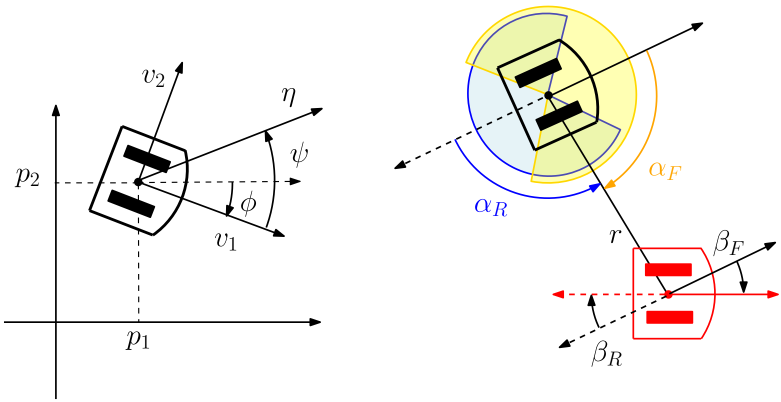

Figure 3.6: A robot equipped with a range sensor and two cameras with overlapping fields of view (blue and yellow), providing measurements $(r, \alpha_{\mathrm{F}}, \beta_{\mathrm{F}})$ and $(r, \alpha_{\mathrm{R}}, \beta_{\mathrm{R}})$. Each measurement is only available when the target depicted in red is in the camera's field of view $\alpha_i \in [-\frac{\pi}{2} - \delta, \frac{\pi}{2} + \delta]$, $i \in \{\mathrm{F}, \mathrm{R}\}$, $\delta > 0$.

where $\nu = [\nu_1 \ \nu_2]^\top \in \mathbb{R}^2$ is a transformed input, given by

$$\begin{aligned} \nu_1 r = u_1 = v_1, \\ \nu_2 = u_2 = \omega. \end{aligned} \tag{3.44}$$

Lemma 3.3.1. *Whenever* $r \neq 0$*, the dynamics* (3.41) *can be equivalently represented through* (3.42)*,* (3.43)*,* (3.44)*.*

Proof. We start by deriving f_{F}. Let $r \neq 0$ and $\theta = \alpha_{\mathrm{F}} - \beta_{\mathrm{F}} - \pi$. Using the coordinate transformation $x = \gamma_{\mathrm{F}}(z_{\mathrm{F}})$ in (3.6) and the definition of θ, following the same steps as in the proof of Lemma 3.2.1, and with the definition $J = \left[\begin{smallmatrix} 0 & -1 \\ 1 & 0 \end{smallmatrix}\right]$, one can show that

$$\dot{r} = \frac{\partial r}{\partial p}\dot{p} = \frac{1}{r}p^\top \dot{p}, \tag{3.45}$$

$$\dot{\theta} = \frac{\partial \theta}{\partial p}\dot{p} = \frac{1}{r^2}p^\top J^\top \dot{p}. \tag{3.46}$$

Using the definition of the transformed input (3.44) and substituting (3.41) into (3.45) and (3.46) one has:

$$
\begin{aligned}
\dot{r} &= \frac{1}{r} p^\top \dot{p} = \frac{1}{r} \begin{bmatrix} r\cos(\theta) & r\sin(\theta) \end{bmatrix} \begin{bmatrix} v_1 \cos(\phi) + \mu v_1 \omega \sin(\phi) \\ v_1 \sin(\phi) - \mu v_1 \omega \cos(\phi) \end{bmatrix} \\
&= v_1 \left(\cos(\theta)\cos(\phi) + \sin(\theta)\sin(\phi) \right) \\
&- v_1 \omega \left(\mu \cos(\theta)\sin(\phi) - \sin(\theta)\cos(\phi) \right) \\
&= v_1 \cos(\phi - \theta) - \mu v_1 \omega \sin(\phi - \theta) \\
&= v_1 \cos(\pi - \alpha_{\mathrm{F}}) - \mu v_1 \omega \sin(\pi - \alpha_{\mathrm{F}}) \\
&= -\nu_1 r \cos(\alpha_{\mathrm{F}}) - \mu \nu_1 \nu_2 r \sin(\alpha_{\mathrm{F}}), \\
\dot{\theta} &= \frac{1}{r^2} p^\top J^\top \dot{p} \\
&= \frac{1}{r^2} \begin{bmatrix} r\cos(\theta) & r\sin(\theta) \end{bmatrix} \begin{bmatrix} v_1 \sin(\phi) - \mu v_1 \omega \cos(\phi) \\ -v_1 \cos(\phi) - \mu v_1 \omega \sin(\phi) \end{bmatrix} \\
&= \frac{1}{r} v_1 \left(\cos(\theta)\sin(\phi) - \sin(\theta)\cos(\phi) \right) \\
&\quad - \frac{1}{r} \mu v_1 \omega \left(\cos(\theta)\cos(\phi) + \sin(\theta)\sin(\phi) \right) \\
&= \frac{1}{r} v_1 \sin(\phi - \theta) - \frac{1}{r} \mu v_1 \omega \cos(\phi - \theta) \\
&= \frac{1}{r} v_1 \sin(\pi - \alpha_{\mathrm{F}}) - \frac{1}{r} \mu v_1 \omega \cos(\pi - \alpha_{\mathrm{F}}) \\
&= \nu_1 \sin(\alpha_{\mathrm{F}}) + \mu \nu_1 \nu_2 \cos(\alpha_{\mathrm{F}}).
\end{aligned}
$$

Finally, using the definition of θ and the third equation of (3.41), we get

$$
\dot{\alpha}_{\mathrm{F}} = \dot{\theta} + \dot{\beta}_{\mathrm{F}} = \nu_1 \sin(\alpha_{\mathrm{F}}) + \mu \nu_1 \nu_2 \cos(\alpha_{\mathrm{F}}) - \nu_2.
$$

Similar computations yield the expression of f_{R} using the relation $\theta = \alpha_{\mathrm{R}} - \beta_{\mathrm{R}}$. □

3.3.3 CAMERA-BASED STABILIZERS FOR THE KINEMATIC MODEL

We now prove that the following selections of controllers

$$
\nu_{\mathrm{F}} = \begin{bmatrix} k_r \cos(\alpha_{\mathrm{F}}) \\ k_\alpha \sin(\alpha_{\mathrm{F}}) \end{bmatrix}, \tag{3.47}
$$

$$
\nu_{\mathrm{R}} = \begin{bmatrix} -k_r \cos(\alpha_{\mathrm{R}}) \\ k_\alpha \sin(\alpha_{\mathrm{R}}) \end{bmatrix}, \tag{3.48}
$$

asymptotically drive the hovercraft's position to the origin in the Cartesian coordinates by locally asymptotically stabilizing the set $\mathcal{A} = \{0\} \times$

$\left[-\frac{3}{2}\pi - \delta, \frac{3}{2}\pi + \delta\right] \times \{0\} \subset \mathcal{Z}$ (where $\mathcal{Z}$ has been defined in (3.5)). To see this, observe from the coordinates transformation (3.6) that $r \to 0$ and $\alpha_i \to 0, i \in \{\mathrm{F}, \mathrm{R}\}$ imply $p \to 0$.
We first need the following preliminary result.

Lemma 3.3.2. *Let $k_\alpha \in \mathbb{R}_{>0}$ and $k_r \in (0, \frac{k_\alpha}{1+\mu k_\alpha})$. Then, the set $\Gamma := \{z \in \mathcal{Z} : |\alpha| \leq \frac{\pi}{2}\}$ is forward pre-invariant for* (3.42), (3.47) *and* (3.43), (3.48), *and all complete solutions reach Γ in finite time.*

Proof. We prove the statement for (3.42), (3.47). The assertion for (3.43), (3.48) follows the same steps. Consider the function

$$W(\alpha) := 1 - \cos(\alpha),$$

and observe that $W(\alpha) \geq 0$ for all $\alpha \in [-\frac{\pi}{2} - \delta, \frac{\pi}{2} + \delta]$ (since $\delta \in (0, \frac{\pi}{2})$ according to (3.5)) and $W(\alpha) = 0$ if and only if $\alpha = 0$. The directional derivative of W along the vector field (3.42), (3.47) is

$$\begin{aligned}
&\langle \nabla W(\alpha_\mathrm{F}), f_\mathrm{F}(z_\mathrm{F}, \nu_\mathrm{F}) \rangle \\
&\quad = \sin(\alpha_\mathrm{F}) \left(\nu_{\mathrm{F}_1} \sin(\alpha_\mathrm{F}) - \nu_{\mathrm{F}_2} + \mu \nu_{\mathrm{F}_1} \nu_{\mathrm{F}_2} \cos(\alpha_F)\right) \\
&\quad = k_r \cos(\alpha_\mathrm{F}) \sin^2(\alpha_\mathrm{F}) - k_\alpha \sin^2(\alpha_\mathrm{F}) \\
&\qquad\quad + \mu k_r k_\alpha \cos^2(\alpha_F) \sin^2(\alpha_F) \\
&\quad = -\sin^2(\alpha_F) \left(k_\alpha - k_r \cos(\alpha_\mathrm{F}) - \mu k_r k_\alpha \cos^2(\alpha_\mathrm{F})\right),
\end{aligned}$$

where we observe that, if $k_\alpha - k_r - k_r k_\alpha \mu > 0$, then the directional derivative is negative definite for $\alpha_\mathrm{F} \in (-\pi, \pi) \setminus \{0\}$. This implies that $|\alpha_\mathrm{F}(t)|$ is strictly decreasing and converging to zero along all complete solutions to (3.42), (3.47). Moreover, solutions do not escape in finite time because ν_F in (3.47) and ν_R in (3.48) are uniformly bounded and the dynamics (3.42), (3.43) are bounded by an affine function of r. Thus, the set Γ is forward pre-invariant and every complete solution reaches Γ in finite-time. The proof is concluded by observing that the above condition on the gains k_r, k_α can be rewritten as $k_\alpha > k_r + \mu k_r k_\alpha$ or equivalently $k_r < \frac{k_\alpha}{1+\mu k_\alpha}$. □

We now prove that the controllers (3.47), (3.48) asymptotically stabilize the set $\mathcal{A} = \{0\} \times \left[-\frac{3}{2}\pi - \delta, \frac{3}{2}\pi + \delta\right] \times \{0\}$, which corresponds to stabilizing the zero position in (3.41).

Theorem 3.3.3. *Let $k_\alpha \in \mathbb{R}_{>0}$ and $k_r \in (0, \frac{k_\alpha}{1+\mu k_\alpha})$. Then, the controller selection* (3.47) *(respectively,* (3.48)*) renders the set $\mathcal{A}$ globally pre-asymptotically stable for* (3.42) *(respectively,* (3.43)*).*

Proof. As for the proof of Lemma 3.3.2, we only show the assertion for (3.42), (3.47), because the proof for (3.43), (3.48) follows similar steps. Consider the function

$$V(z) := \frac{1}{2}r^2 + W(\alpha) = \frac{1}{2}r^2 + (1 - \cos(\alpha)),$$

which is positive definite with respect to $\mathcal{A}$. It is immediate to verify that V satisfies the remaining requirements in Definition 2.4.1, and therefore V is a Lyapunov function candidate on $\mathcal{Z}$ with respect to $\mathcal{A}$ for (3.42), (3.47). Its directional derivative along the vector field (3.42), (3.47) is

$$\begin{aligned} &\langle V(z_{\mathrm{F}}), f_{\mathrm{F}}(z_{\mathrm{F}}, \nu_{\mathrm{F}})\rangle \\ &\quad = -k_r r^2 \cos^2(\alpha_{\mathrm{F}}) - \mu k_r k_\alpha r^2 \cos(\alpha_{\mathrm{F}}) \sin^2(\alpha_{\mathrm{F}}) \\ &\qquad - \sin^2(\alpha_{\mathrm{F}}) \left(k_\alpha - k_r \cos(\alpha_{\mathrm{F}}) - \mu k_r k_\alpha \cos^2(\alpha_{\mathrm{F}})\right). \end{aligned} \tag{3.49}$$

We observe that for $z_{\mathrm{F}} \in \mathcal{Z}$ the first term is negative when $r \neq 0$ and $|\alpha_{\mathrm{F}}| \neq \frac{\pi}{2}$, and the third term is negative when $\alpha_{\mathrm{F}} \neq 0$, as shown in the proof of Lemma 3.3.2, due to the selection of the gains k_r, k_α. The second term is non-positive when $|\alpha_{\mathrm{F}}| \leq \frac{\pi}{2}$, that is, for $z_{\mathrm{F}} \in \Gamma$. This allows concluding Lyapunov stability of the set $\mathcal{A}$ using Theorem 2.4.3, since (3.49) is negative definite in a neighborhood of $\mathcal{A}$. Since no solution escapes in finite-time, as established in the proof of Lemma 3.3.2, either solutions are complete or they stop at the boundary of $\mathcal{Z}$ with a bounded time domain. All complete solutions reach Γ in finite time, due to Lemma 3.3.2, and remain in it forever. Since the Lyapunov derivative (3.49) is negative definite over Γ, and Γ is strongly forward pre-invariant, convergence of all complete solutions to $\mathcal{A}$ can be established using the formulation of the Hybrid Invariance Principle in Corollary 2.4.6. Moreover, all maximal solutions that stop at the boundary of $\mathcal{Z}$ in finite time are bounded. Thus, the set $\mathcal{A}$ is globally pre-attractive, which, combined with Lyapunov stability, proves that $\mathcal{A}$ is globally pre-asymptotically stable. □

We now combine the two camera-based stabilizers (3.47), (3.48), using the hysteresis-based switching logic proposed in Section 3.2.3, to obtain global and robust stability results.
Let $q \in \{-1, 1\}$ be the logic variable identifying what camera measurements are currently being used ($q = 1$ for the front camera F, $q = -1$ for the rear camera R), and consider the hybrid state

$$\xi := [r\ \beta\ \alpha\ q]^\top \in \Xi, \tag{3.50a}$$
$$\Xi := \mathbb{R}_{\geq 0} \times \left[-\tfrac{3}{2}\pi - \delta, \tfrac{3}{2}\pi + \delta\right] \times \left[-\tfrac{\pi}{2} - \delta, \tfrac{\pi}{2} + \delta\right] \times \{-1, 1\},$$

whose values correspond to the measurements z_{F} if $q=1$ or z_{R} if $q=-1$. As we did for system (3.20), we introduce a reset logic for the angle β to prevent the unwinding of the hovercraft's orientation.
The flow map describing the continuous-time evolution of the state ξ is obtained by combining the dynamics (3.42), (3.43) with the logic variable q and leading to the dynamics

$$\dot{\xi} = \begin{bmatrix} \dot{r} \\ \dot{\beta} \\ \dot{\alpha} \\ \dot{q} \end{bmatrix} = f(\xi,\nu) := \begin{bmatrix} -q\nu_1 r\cos(\alpha) - q\mu\nu_1\nu_2 r\sin(\alpha) \\ -\nu_2 \\ q\nu_1\sin(\alpha) - \nu_2 + q\mu\nu_1\nu_2\cos(\alpha) \\ 0 \end{bmatrix}, \quad \xi \in \mathcal{C}, \tag{3.50b}$$

with flow set $\mathcal{C} = \Xi$. The stabilizers (3.47), (3.48) are combined in the feedback law $\nu = \kappa(\xi)$, with

$$\kappa(\xi) := \begin{bmatrix} qk_r\cos(\alpha) \\ k_\alpha\sin(\alpha) \end{bmatrix}. \tag{3.50c}$$

The functions

$$g_\beta(\xi) := \begin{bmatrix} r \\ \beta - 2\pi\mathrm{sign}(\beta) \\ \alpha \\ q \end{bmatrix}, \; g_\alpha(\xi) := \begin{bmatrix} r \\ \beta \\ \alpha - \pi\mathrm{sign}(\alpha) \\ -q \end{bmatrix}, \tag{3.50d}$$

model, respectively, the switch between the front and rear camera measurements z_{F} and z_{R}, and the reset of the orientation angle $\beta_i, i \in \{\mathrm{F},\mathrm{R}\}$. The jump sets

$$\begin{aligned} &\mathcal{D}_\alpha := \{\xi \in \Xi : |\alpha| \geq \tfrac{\pi}{2} + \delta\}, \\ &\mathcal{D}_\beta := \{\xi \in \Xi : |\beta| \geq \tfrac{3}{2}\pi + \delta\}, \quad \mathcal{D} := \mathcal{D}_\beta \cup \mathcal{D}_\alpha, \end{aligned} \tag{3.50e}$$

define the conditions at which the cameras switch, respectively, the reset of β_i, occurs. The reset rules for α_i and β_i, $i \in \{\mathrm{F},\mathrm{R}\}$, discussed above are encompassed by the (set-valued) jump map

$$\xi^+ \in G(\xi) = \begin{cases} \{g_\beta(\xi)\}, & \text{if } \xi \in \mathcal{D}_\beta \backslash \mathcal{D}_\alpha, \\ \{g_\alpha(\xi)\}, & \text{if } \xi \in \mathcal{D}_\alpha \backslash \mathcal{D}_\beta, \\ \{g_\alpha(\xi)\} \cup \{g_\beta(\xi)\}, & \text{if } \xi \in \mathcal{D}_\alpha \cap \mathcal{D}_\beta. \end{cases} \tag{3.50f}$$

The closed-loop hybrid system resulting from (3.50) can then be written as

$$\mathcal{H} : \left\{ \begin{array}{rcll} \dot{\xi} & = & f(\xi,\kappa(\xi)), & \xi \in \mathcal{C}, \\ \xi^+ & \in & G(\xi), & \xi \in \mathcal{D}. \end{array} \right. \tag{3.51}$$

Theorem 3.3.4. *Let $k_\alpha \in \mathbb{R}_{>0}$ and $k_r \in (0, \frac{k_\alpha}{1+\mu k_\alpha})$. Then, the set $\mathcal{A}_q := \{0\} \times [-\frac{3}{2}\pi - \delta, \frac{3}{2}\pi + \delta] \times \{0\} \times \{-1, 1\}$ is robustly globally uniformly asymptotically stable for* (3.51).

Proof. We start by observing that (3.51) satisfies the Hybrid Basic Conditions in Definition 2.2.1.
Consider the Lyapunov function candidate

$$V(\xi) = \frac{1}{2}r^2 + (1 - \cos(\alpha)), \tag{3.52}$$

which is positive definite with respect to $\mathcal{A}_q$. Let $\Omega := \Gamma \times \{-1, 1\} = \{\xi \in \Xi : |\alpha| \leq \frac{\pi}{2}\}$ and observe that $\Omega \cap \mathcal{D}_\alpha = \emptyset$ and that $\mathcal{A}_q \subset \Omega$. For $\xi \in \Omega \setminus \mathcal{A}_q$ arbitrary, it holds that

$$\langle \nabla V(\xi), f(\xi, \kappa(\xi)) \rangle < 0 \quad \text{when } \xi \in (\Omega \cap \mathcal{C}) \setminus \mathcal{A}_q \tag{3.53}$$

(which was shown in the proof of Theorem 3.3.3) and

$$V(g_\beta(\xi)) - V(\xi) = 0 \quad \text{when } \xi \in \Omega \cap \mathcal{D} \tag{3.54}$$

(which follows from the fact that V does not depend on β). Thus, V is non-increasing along solutions in Ω, which proves Lyapunov stability of $\mathcal{A}_q$ via Theorem 2.4.3.
Let $\xi(\cdot, \cdot)$ be an arbitrary solution to (3.51). Suppose that $\xi(0, 0)$ satisfies $|\alpha(0, 0)| \leq \frac{\pi}{2}$. Lemma 3.3.2 ensures that if the solution is flowing at time $(t, j) \in \operatorname{dom} \xi$ then $|\alpha(t, j)| \leq \frac{\pi}{2}$, and, from the definition of the jump map in (3.50d), if $\xi(t, j) \in \mathcal{D}_\beta$ then $\alpha(t, j + 1) = \alpha(t, j)$. Thus, $|\alpha(t, j)| \leq \frac{\pi}{2}$ for all $(t, j) \in \operatorname{dom} \xi$, and therefore $\xi(t, j) \in \Omega$ for all $(t, j) \in \operatorname{dom} \xi$. Moreover, since V is nonincreasing in Ω, ξ is also bounded. Since $\Omega \cap \mathcal{D}_\alpha = \emptyset$ and $g_\beta(\mathcal{D}_\beta \setminus \mathcal{D}_\alpha) \cap \mathcal{D}_\beta = \emptyset$, if ξ jumps from Ω then it lands in the interior of the flow set, and therefore Theorem 2.2.6 implies that ξ has a positive dwell-time. Then, using the hybrid formulation of the invariance principle in Corollary 2.4.6 one has that condition (3.53) implies that $\xi(t, j)$ converges to $\mathcal{A}_q$, if it is complete, since the complete solutions $\xi(t, j)$ along which V remains constant must satisfy $V(\xi(t, j)) = 0$ for all $(t, j) \in \operatorname{dom} \xi$.
Suppose now that $\xi(0, 0)$ is such that $|\alpha(0, 0)| > \frac{\pi}{2}$. If there exists a time $(t, j) \in \operatorname{dom} \xi$ such that $\xi(t, j) \in \mathcal{D}_\alpha$, then from (3.50d) one has that $\xi(t, j + 1) = g_\alpha(t, j)$ satisfies

$$\begin{aligned} |\alpha(t, j + 1)| &= |\alpha(t, j) - \pi \operatorname{sign}(\alpha(t, j))| \\ &= |\operatorname{sign}(\alpha(t, j))(|\alpha(t, j)| - \pi)| = |(|\alpha(t, j)| - \pi)| \\ &= |\tfrac{\pi}{2} + \delta - \pi| = |\delta - \tfrac{\pi}{2}| < \tfrac{\pi}{2}, \end{aligned}$$

and from the discussion above we have that $|\alpha(t', j')| \leq \frac{\pi}{2}$, for all $(t', j') \in \operatorname{dom} \xi$ such that $t' + j + \geq t + j$. Accordingly, the solution will converge to

$\mathcal{A}_q$, if it is complete. If there is no time $(t,j) \in \operatorname{dom} \xi$ such that $\xi(t,j) \in \mathcal{D}_\alpha$, then Lemma 3.3.2 ensures that there exists a time $(\bar{t},\bar{j}) \in \operatorname{dom} \xi$ such that $\xi(\bar{t},\bar{j}) \in \Omega$, and the above discussion implies that the solution asymptotically converges to $\mathcal{A}_q$ if it is complete. If ξ is not complete, following the discussion in the proof of Lemma 3.3.2, ξ is bounded. Since all complete solutions to (3.51) converge to $\mathcal{A}_q$, and all solutions are bounded, we have that $\mathcal{A}_q$ is globally pre-attractive. Completeness of all maximal solutions can be proven by applying Theorem 2.2.5. Robust uniform global asymptotic stability of $\mathcal{A}_q$ follows then from Theorem 2.3.9. □

Remark 15. *For many marine vehicles forward motion is in general more favorable than backward motion. Similarly to what we observed for the unicycle hybrid stabilizer at the end of Section 3.2.3, different control gains can be assigned to the front and rear camera in* (3.50c)*, as long as they satisfy the assumptions of Theorems 3.3.3 and 3.3.4. This may allow for a slower control action corresponding to the backward motion, compatible with the reduced agility of the vehicle.*

3.3.4 EXTENSION TO THE FULL DYNAMIC MODEL

In this section we drop the assumption in (3.35) requiring that the sway speed can be approximated as $v_2 = -\mu\omega v_1$, and leading to the kinematic model. Instead, we focus on the full dynamic model (3.33)-(3.34) and design the inputs F and T by leveraging the kinematic stabilizer presented in Section 3.3.3. Following similar steps to the ones presented in Lemma 3.3.1, we define the extended state $\zeta = [r\ \beta\ \alpha\ q\ v_1\ v_2\ \omega]^\top \in \mathcal{C} \times \mathbb{R}^3$ and input $\rho = [F\ T]^\top \in \mathbb{R}^2$ whose dynamics yield

$$\dot{\zeta} = \bar{f}(\zeta,\rho), \qquad \zeta \in \mathcal{C}^\zeta = \mathcal{C} \times \mathbb{R}^3, \tag{3.55}$$

with right-hand side

$$\bar{f}(\zeta,\rho) = \left[\begin{array}{c} -qv_1\cos(\alpha) - qv_2\sin(\alpha) \\ -\omega \\ q\frac{v_1}{r}\sin(\alpha) - \omega - q\frac{v_2}{r}\cos(\alpha) \\ 0 \\ \hline v_2\omega - \frac{d_\nu}{m}v_1 + \frac{1}{m}F \\ -v_1\omega - \frac{d_\nu}{m}v_2 \\ -\frac{d_r}{J}\omega + \frac{1}{J}T \end{array}\right]. \tag{3.56}$$

Then, (3.55), (3.56) represent an extension of the dynamics (3.50b) where we have separated the components corresponding to (3.33) and (3.34) with a horizontal line, for a better illustration.
To define a controller for (3.56), we first propose a stabilizing controller for the dynamics (3.34).

Lemma 3.3.5. *For $k_F, k_T \in \mathbb{R}_{>0}$, the feedback law*

$$\begin{bmatrix} F \\ T \end{bmatrix} = \begin{bmatrix} d_\nu v_1 - m v_2 \omega - m k_F v_1 \\ d_r \omega - J k_T \omega \end{bmatrix} \tag{3.57}$$

globally asymptotically stabilizes the origin of the dynamical system (3.34).

Proof. In (3.34), the feedback law (3.57) leads to the closed loop dynamics

$$\begin{aligned} \dot{v}_1 &= -k_F v_1, \\ \dot{v}_2 &= -v_1 \omega - \tfrac{d_\nu}{m} v_2, \\ \dot{\omega} &= -k_T \omega. \end{aligned} \tag{3.58}$$

Thus, from the first and the third equation we can conclude exponential convergence of v_1 and ω to zero, which implies that v_2 asymptotically converges to zero according to the second equation. Hence, global asymptotic stability of the origin can be concluded. □

Instead of stabilizing the origin of (3.34), we intend to track the reference signal (3.50c) given by the kinematic stabilizer, i.e.,

$$\kappa^{\text{ref}}(\xi) = \begin{bmatrix} v_1^{\text{ref}} \\ w^{\text{ref}} \end{bmatrix} = \begin{bmatrix} q r k_r \cos(\alpha) \\ k_\alpha \sin(\alpha) \end{bmatrix}, \tag{3.59}$$

(where additionally the coordinate transformation (3.44) has been taken into account). Accordingly, we extend the feedback law (3.57), to $\rho = \sigma(\zeta)$,

$$\sigma(\zeta) = \begin{bmatrix} d_\nu v_1 - m v_2 \omega + m \dot{\kappa}_1^{\text{ref}}(\xi) - m k_F (v_1 - \kappa_1^{\text{ref}}(\xi)) \\ d_r \omega + J \dot{\kappa}_2^{\text{ref}}(\xi) - J k_T (\omega - \kappa_2^{\text{ref}}(\xi)) \end{bmatrix} \tag{3.60}$$

leading to the closed-loop dynamics

$$\begin{aligned} \tfrac{d}{dt}(v_1 - \kappa_1^{\text{ref}}(\xi)) &= -k_F (v_1 - \kappa_1^{\text{ref}}(\xi)), \\ \tfrac{d}{dt} v_2 &= -v_1 \omega - \tfrac{d_\nu}{m} v_2, \\ \tfrac{d}{dt}(\omega - \kappa_2^{\text{ref}}(\xi)) &= -k_T (\omega - \kappa_2^{\text{ref}}(\xi)), \end{aligned} \tag{3.61}$$

instead of (3.58). Thus, if $\kappa^{\text{ref}}(\xi)$ varies sufficiently slowly, good reference tracking can be expected from Lemma 3.3.5.
We continue with the presentation of an extension of the hybrid system (3.50), taking the dynamics (3.34) and the controller (3.60) into account. By

extending the function (3.50f) in a natural way, i.e.,

$$\bar{g}_\beta(\zeta) := \left[\begin{array}{c} r \\ \beta - 2\pi\mathrm{sign}(\beta) \\ \alpha \\ q \\ \hline v_1 \\ v_2 \\ \omega \end{array}\right], \quad \bar{g}_\alpha(\zeta) := \left[\begin{array}{c} r \\ \beta \\ \alpha - \pi\mathrm{sign}(\alpha) \\ -q \\ \hline v_1 \\ v_2 \\ \omega \end{array}\right], \tag{3.62}$$

$\mathcal{D}^\zeta_\beta = \mathcal{D}_\beta \times \mathbb{R}^3$, $\mathcal{D}^\zeta_\alpha = \mathcal{D}_\alpha \times \mathbb{R}^3$, $\mathcal{D}^\zeta = \mathcal{D}^\zeta_\beta \cup \mathcal{D}^\zeta_\alpha$ and

$$\zeta^+ \in \bar{G}(\zeta) = \begin{cases} \{\bar{g}_\beta(\zeta)\}, & \text{if } \zeta \in \mathcal{D}^\zeta_\beta \backslash \mathcal{D}^\zeta_\alpha, \\ \{\bar{g}_\alpha(\zeta)\}, & \text{if } \xi \in \mathcal{D}^\zeta_\alpha \backslash \mathcal{D}^\zeta_\beta, \\ \{g_\alpha(\zeta)\} \cup \{g_\beta(\zeta)\}, & \text{if } \xi \in \mathcal{D}^\zeta_\alpha \cap \mathcal{D}^\zeta_\beta, \end{cases} \tag{3.63}$$

the extended closed-loop hybrid system is obtained as

$$\mathcal{H}^\zeta : \begin{cases} \dot{\zeta} = \bar{f}(\zeta, \sigma(\zeta)), & \zeta \in \mathcal{C}^\zeta, \\ \zeta^+ \in \bar{G}(\zeta), & \zeta \in \mathcal{D}^\zeta. \end{cases} \tag{3.64}$$

3.3.5 NUMERICAL SIMULATIONS

In this section we numerically investigate and compare the closed-loop properties of the control laws discussed in Section 3.3.3. For the simulations, the parameters $m = 5.15\ kg, J = 0.047\ kg\ m^2, d_\nu = 4.5\ kg/s, d_r = 0.41\ kg\ m/s$ reported in [28] are used. The feedback gains are selected as $k_\alpha = 2, k_r = \frac{1}{2}\frac{k_\alpha}{1+\mu k_\alpha}, k_F = k_T = 5$ and the parameter δ defining the overlap of the field of view of the cameras is set to $\delta = \frac{\pi}{6}$.

Figure 3.7 shows the closed-loop trajectories with the kinematic model (3.51) (left plot) and with the full dynamics (3.64) (right plot) in the $p = (p_1, p_2)$ plane. Here, the closed loop dynamics are initialized through $p(0) = [-10\ 0]^\top$ and different initial orientations $\phi(0)$. The initial position is indicated with a black circle in the figure, while a black cross marks the target position. For (3.64) at the right of Figure 3.7, the additional states v_1, v_2 and ω are initialized at zero, so that some nontrivial transient is visible. Additionally, the blue trajectories indicate that the hovercraft is moving backwards (using the rear camera) with $q = -1$ while the red trajectories indicate that the hovercraft is driving forward (using the front camera) with $q = 1$.

We observe that the controller successfully ensures convergence of $p(t) \to 0$ for $t \to \infty$, as expected. Moreover, we observe that the full dynamic controller (3.60) provides a similar performance in terms of closed-loop trajectories as that obtained with the simplified kinematic controller (3.50c).

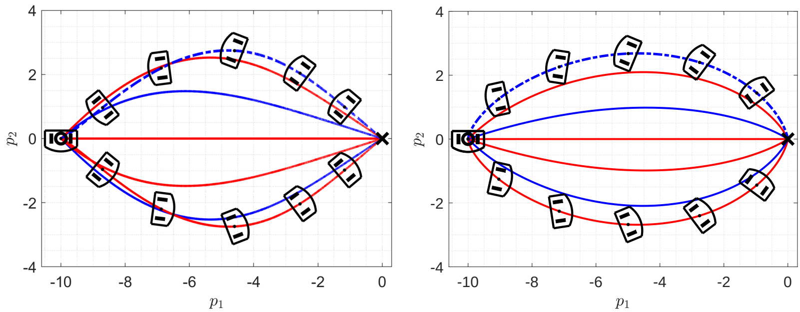

Figure 3.7: Closed-loop trajectories of the dynamics (3.21) (left) and the dynamics (3.64) (right) in the $p = (p_1, p_2)$ plane for $p(0) = [-10\ 0]^\top$ but with different initial orientation. Blue trajectories indicate that the hovercraft is moving backwards (using the rear camera) while red trajectories indicate that the hovercraft is driving forward (using the front camera).

Figure 3.7 additionally shows some snapshots of the hovercraft for selected trajectories, highlighting the hovercraft's position and orientation. From the orientation along the trajectory, different to the unicycle dynamics, we observe that the sway speed is unequal to zero, contributing by a significant component to the overall speed of the hovercraft.
The closed-loop solutions depicted through dashed lines in Figure 3.7 are shown again in Figure 3.8 for comparison. Solid lines in Figure 3.8 indicate quantities associated with the kinematic response from (3.51), while dashed lines represent the response from the full dynamic model (3.64). Again, we observe that both control laws provide a similar performance. As expected from the controller design, the feedback law ensures $r(t) \to 0$ (i.e., $p(t) \to 0$) and $\alpha(t) \to 0$ for $t \to \infty$.
For comparison, the evolution of (3.44), i.e., the input (with respect to (3.51)) and the states (with respect to (3.64)), corresponding to the solutions in Figure 3.8 are shown in Figure 3.9. Additionally, the reference signal κ^{ref} in (3.59) is shown. As expected, the mismatch between $\left[\begin{smallmatrix} v_1 \\ w \end{smallmatrix}\right]$ and $\kappa^{\mathrm{ref}}(\xi)$ is vanishing, thus highlighting the tracking performance of $\sigma(\zeta)$.

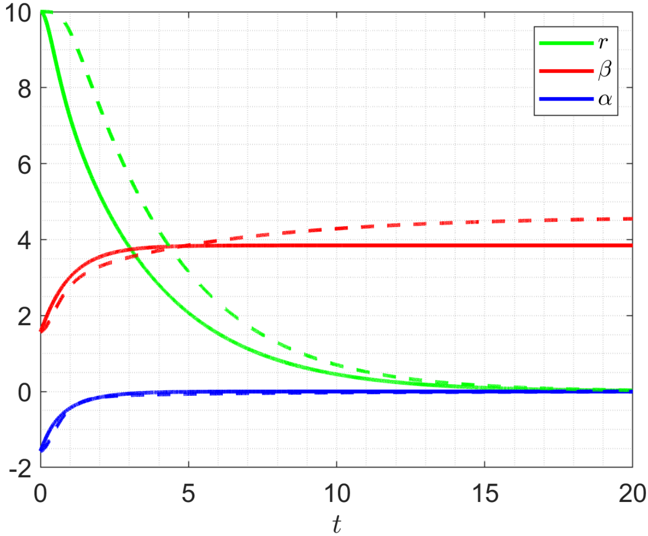

Figure 3.8: Visualization of the closed-loop solutions highlighted through dashed lines in Figure 3.7. Here, the solid lines correspond to (3.51) and the dashed lines correspond to (3.64), respectively.

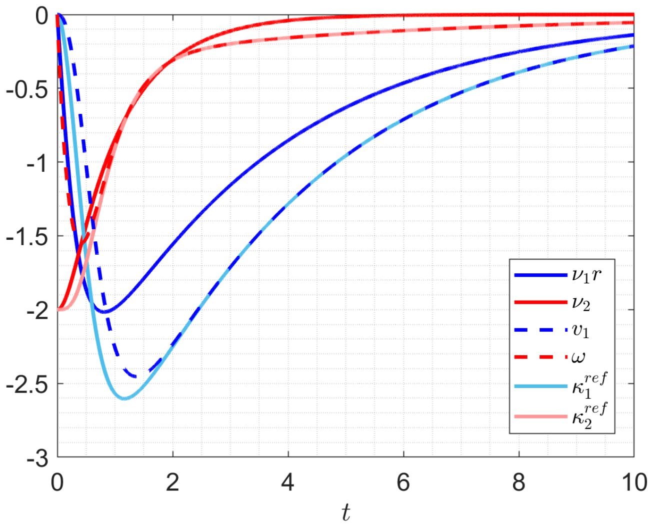

Figure 3.9: Comparison of the input and the state, corresponding to the solutions shown in Figure 3.8 for (3.51) (solid line) and (3.64) (dashed line). The reference signal κ^{ref} is also shown.

CHAPTER 4

AUGMENTING STABILIZATION WITH AVOIDANCE

In this chapter we discuss two control redesign approaches that can be applied to a broad class of systems to endow a given stabilizer with some avoidance properties. The fundamental assumption we make is that a stabilizing feedback and a Lyapunov function, certifying the stability properties of the set of interest for the nominal closed-loop system, are known. Under this assumption, we propose a hybrid control architecture achieving avoidance while preserving decrease of the Lyapunov function along solutions. We highlight that our solution ensures robustness of the stability properties despite the discontinuous action required.

Section 4.1 addresses the problem of simultaneous stabilization and obstacle avoidance for input-affine nonlinear system, where the obstacles are points in the state space. The key idea of preserving the decrease of a Lyapunov function, certifying the stabilization task, while performing the avoidance motion, is introduced in Section 4.1.1. Section 4.1.2 recalls the avoidance shell *construction introduced in [91] and explains its relation with the avoidance input defined in our solution. Section 4.1.3 provides a selection for the avoidance input, and a hybrid control architecture is defined in Section 4.1.4 to orchestrate the switch between the nominal and avoidance controller, when solutions get close to an obstacle. Numerical simulations are used to illustrate the avoidance mechanism in Section 4.1.5. Section 4.2 considers the problem of stabilizing a given plant while ensuring that the control input never takes an unwanted value. We first address the problem in the linear setting, introducing the proposed hybrid control architecture in Section 4.2.1, stating the main* *results in Section 4.2.2, whose proofs are given in Section 4.2.4 not to break the flow of exposition, and analyze a case study in Section 4.2.3. We then extend the proposed solution to the class of input-affine nonlinear systems in Section 4.2.5, with the proofs of the main results being in Section 4.2.7, and finally discuss a nonlinear case study in Section 4.2.6.*

4.1 STATE AVOIDANCE

Let us consider control-affine dynamical systems

$$\dot{x} = f(x) + g(x)u, \qquad x_0 = x(0) \in \mathbb{R}^n \tag{4.1}$$

with state $x \in \mathbb{R}^n$, input $u \in \mathbb{R}^m$, $g : \mathbb{R}^n \to \mathbb{R}^{n\times m}$ and $f : \mathbb{R}^n \to \mathbb{R}^n$ such that the pair (f, g) possesses a non-trivial drift term. We require that f and g be locally Lipschitz. Additionally, we use the notation $g_i : \mathbb{R}^n \to \mathbb{R}^m$, $i \in \mathbb{N}_m$, to refer to the individual columns of g, and write $g = [g_1(x) \cdots g_m(x)]$. By (f, g) possessing a non-trivial drift term we mean that $f(x)$ cannot be cancelled via a feedback transformation $u = -\kappa(x) + v$ such that $f(x) - g(x)\kappa(x) = 0$ for all $x \in \mathbb{R}^n$.

Problem 4.1.1. (Augmenting stabilization with semiglobal $\hat{x}$-avoidance) Given an open set $\mathcal{U} \subset \mathbb{R}^n$, $\{0\} \in \mathcal{U}$, a set of obstacle centroids $\{\hat{x}_1, \dots, \hat{x}_\beta\} \in \mathcal{U} \setminus \{0\}$, $\beta \in \mathbb{N}$, that define spherical obstacles and a Lipschitz continuous stabilizing state feedback $u_{\mathrm{s}}(x) = \kappa_{\mathrm{s}}(x)$, for a sufficiently small $\delta > 0$, design a feedback selection of u that guarantees

(i) (Semiglobal preservation) the feedback $u(x)$ matches the original stabilizer $u(x) = \kappa_{\mathrm{s}}(x)$ for all $x \in \mathcal{U} \setminus \cup_{i=1}^{\beta} \delta\mathbb{B}(\hat{x}_i)$;

(ii) (Semiglobal $\hat{x}$-avoidance) all solutions starting outside the balls $\cup_{i=1}^{\beta} \delta\mathbb{B}(\hat{x}_i)$ never enter a suitable avoidance neighborhood $\chi_i\mathbb{B}(\hat{x}_i)$, having measure greater than zero, around the centroids $\hat{x}_i$, $i \in \mathbb{N}_\beta$;

(iii) (RUAS) robust uniform asymptotic stability of the origin $\mathcal{A} = \{0\} \in \mathbb{R}^n$ with $\mathcal{U} \subset \mathcal{B}_{\mathcal{A}}$.

To simplify the notation in the following, we use

$$f_{\mathrm{s}}(x) = f(x) + g(x)\kappa_{\mathrm{s}}(x) \tag{4.2}$$

to denote the right-hand side of the closed-loop system resulting from a prescribed stabilizing controller, whose existence is assumed in Problem 4.1.1. To solve Problem 4.1.1 we make the following standing assumption.

Assumption 4.1.2. *Consider the dynamics* (4.1) *and obstacle centroids* $\hat{x}_1, \dots, \hat{x}_\beta \in \mathcal{U} \setminus \{0\}$, $\beta \in \mathbb{N}$, *with* $\mathcal{U}$ *defined as in Problem 4.1.1.*

(a) *The feedback* $\kappa_{\mathrm{s}} : \mathcal{U} \to \mathbb{R}^m$ *renders the origin of the closed-loop system* (4.2) *asymptotically stable, the function* $V : \operatorname{dom} V \to \mathbb{R}_{\geq 0}$, $\operatorname{dom} V \subset \mathbb{R}^n$, *is a Lyapunov function candidate on* $\mathcal{U}$ *with respect to the origin for* (4.2), *with* $\mathcal{U} \subset \operatorname{dom} V$ *being an open sublevel set of* V, *such that*

$$\langle \nabla V(x), f(x) + g(x)\kappa_{\mathrm{s}}(x) \rangle \leq -\rho(x), \ \forall\ x \in \mathcal{U}, \tag{4.3}$$

for some $\rho \in \mathcal{P}$.

(b) *For every* $i \in \mathbb{N}_\beta$, *there exists* $v \in \mathbb{R}^m$ *such that*

$$\langle \nabla V(\hat{x}_i), g(\hat{x}_i)v(\hat{x}_i) \rangle = 0 \text{ and } g(\hat{x}_i)v(\hat{x}_i) \neq 0 \tag{4.4}$$

are satisfied.

Assumption 4.1.2(a) states that the feedback law $u_{\mathrm{s}} = \kappa_{\mathrm{s}}(x)$ stabilizes the origin for system (4.1), without obstacles, and that an estimate of the basin of attraction of the origin, for the nominal closed-loop system, is given by the sublevel set $\mathcal{U}$ of V. Item (*iii*) of Problem 4.1.1 then asks that, under the new selection of u, the basin of attraction of the modified closed-loop systems still contains $\mathcal{U}$. Assumption 4.1.2(b) states that in a neighborhood around each $\hat{x}_i$ it is possible to select an input perpendicular to the gradient of the Lyapunov function. This degree of freedom will be used to design an avoidance controller. Assumption 4.1.2(b) holds if, for each $\hat{x}_i, i \in \mathbb{N}_\beta$, there exist $k, j \in \mathbb{N}_m$ such that $g_k(\hat{x}_i)$ and $g_j(\hat{x}_i)$ are linearly independent. This is for example satisfied if $m \geq 2$ and $g(\cdot)$ is constant.

4.1.1 LYAPUNOV DECREASE PROPERTY

Consider a Lyapunov function candidate $V : \operatorname{dom} V \to \mathbb{R}_{\geq 0}$ and the stabilizing feedback law $\kappa_s : \mathcal{U} \to \mathbb{R}^m$ according to Assumption 4.1.2(a). To guarantee obstacle avoidance, we will locally modify the nominal control law $u(x) = \kappa_s(x)$ near each obstacle centroid $\hat{x}_i, i \in \mathbb{N}_\beta$ in the following way

$$u(x) = \kappa_s(x) + \alpha_p(x)\Lambda(\hat{x}_i), \quad p \in \{-1, 1\} \tag{4.5}$$

where $\Lambda(\hat{x}_i) \in \mathbb{R}^m$ defines an avoidance direction depending on the obstacle and $\alpha_1, \alpha_{-1} : r\mathbb{B}(\hat{x}_i) \to \mathbb{R}$ are continuous scaling functions defined in a ball centered at $\hat{x}_i$ having radius $r > 0$. The scaling can be positive as well as negative, which is determined by the parameter $p \in \{-1, 1\}$. The functions α_1, α_{-1}, as well as the direction $\Lambda(\hat{x}_i)$, are determined in the following sections to guarantee specific avoidance properties. In the following we use the notation

$$v_p^i(x) = \alpha_p(x)\Lambda(\hat{x}_i), \tag{4.6}$$

to capture the avoidance component of the feedback law (4.5), based on the centroid $i \in \mathbb{N}_\beta$ and the scaling $p \in \{-1, 1\}$.

The directions $\Lambda(\hat{x}_i)$ in (4.6) will be defined in Section 4.1.2 so that the conditions (4.4) hold for all $i \in \mathbb{N}_\beta$. Then, along solutions of (4.1), (4.5), for all $i \in \mathbb{N}_\beta$ one has

$$\begin{aligned}&\langle \nabla V(\hat{x}_i), f(\hat{x}_i) + g(\hat{x}_i)(\kappa_s(\hat{x}_i) + v_p^i(\hat{x}_i))\rangle \\ &\quad = \langle \nabla V(\hat{x}_i), f(\hat{x}_i) + g(\hat{x}_i)\kappa_s(\hat{x}_i)\rangle \leq -\rho(\hat{x}_i),\end{aligned} \tag{4.7}$$

with ρ defined in Assumption 4.1.2(a). Since ∇V, f, g and κ_s are continuous by assumption, there exist $\eta_i \in \mathbb{R}_{>0}$ such that

$$\begin{aligned}&\langle \nabla V(x), f(x) + g(x)(\kappa_s(x) + v_p^i(\hat{x}_i))\rangle \\ &= \langle \nabla V(x), f(x) + g(x)\kappa_s(x)\rangle + \langle \nabla V(x), g(x)v_p^i(x)\rangle \\ &= -\rho(x) + \alpha_p(x)\langle \nabla V(x), g(x)\Lambda(\hat{x}_i)\rangle < 0,\end{aligned} \tag{4.8}$$

is satisfied for all $x \in \eta_i\mathbb{B}(\hat{x}_i)$. While the size of the η_i-neighborhood depends on the selection of the function α_p, for every continuous function α_p, a corresponding $\eta_i > 0$ with the decrease property in (4.8) exists. Therefore, for every continuous selection of the scaling factor α_p, choosing the direction $\Lambda(\hat{x}_i)$ of the avoidance input (4.6) so that condition (4.4) is satisfied preserves negative definiteness of the Lyapunov derivative in a sufficiently small neighborhood of each obstacle. Once α_p has been defined, in a way that guarantees avoidance of the obstacles $\hat{x}_i$, we select the modified control input (4.5), following a switching logic activating when solutions enter some suitably defined set contained in $\eta_i\mathbb{B}(\hat{x}_i)$. Since decrease of the Lyapunov function is preserved under the modified input selection (4.5) in the set $\eta_i\mathbb{B}(\hat{x}_i)$, this redesign logic can achieve avoidance of $\hat{x}_i$ while preserving the stabilization task, thus solving item (iii) of Problem 4.1.1.
For this reason, we choose to carry out the design of the avoidance control input $v_p^i(x)$ without accounting for the size of the avoidance neighborhood. Once $\alpha_p(x)$ and $\Lambda(\hat{x}_i)$ have been determined, the largest admissible value of η_i can be determined, for example, as the solution of the optimization problem

$$\begin{aligned}\eta_i = \min_{x\in\mathbb{R}^n} \; &|x - \hat{x}_i| - \varepsilon, \\ \text{s.t. } &-\rho(x) + \alpha_p(x)\nabla V(x)^\top g(x)\Lambda(\hat{x}_i) \geq 0\end{aligned} \tag{4.9}$$

for each $\hat{x}_i, i \in \mathbb{N}_\beta$ and for an arbitrarily small $\varepsilon > 0$.

4.1.2 AVOIDANCE SHELL AND AVOIDANCE DIRECTION

The avoidance controller (4.6) is activated in a shell-shaped neighborhood around the obstacle. We will see in this section that the use of this specific neighborhood provides a criterion for the selection of the direction $\Lambda(\hat{x}_i)$ of

the avoidance input (4.5). Once the direction $\Lambda(\hat{x}_i)$ has been chosen, the scaling α_p in (4.5) will be defined in Section 4.1.3. While the shell-shaped set follows the same definition as in the linear setting in [121, Section IV], the definition of the avoidance controller deviates from the linear setting. To effectively present the avoidance controller (4.6), we briefly recall the definitions of the shell-shaped avoidance neighborhood introduced in [121].
We recall that an avoidance neighborhood with a non-smooth boundary is necessary to ensure that, despite the smoothness of f, g and u, for each point on the boundary of the avoidance neighborhood, there exists an input $u \in \mathbb{R}^m$ such that $\dot{x} = f(x) + g(x)u$ does not point inside the avoidance neighborhood.

Definition 4.1.3 (Avoidance shell, [121, Section IV])**.** *Consider an obstacle centroid $\hat{x} \in \{\hat{x}_1, \ldots, \hat{x}_\beta\}$ together with parameters:*

1. $\delta \in \mathbb{R}_{>0}$ *(size of the shell);*
2. $\mu \in (0, 2)$ *(aspect ratio of the shell);*
3. $b \in \mathbb{R}^n$ *(orientation of the shell).*

Moreover, let

$$\delta_\mu := \delta\left(\tfrac{1}{\mu} - \tfrac{\mu}{4}\right), \tag{4.10}$$

$$\mathcal{O}_p := \left(\tfrac{\mu\delta}{2} + \delta_\mu\right)\mathbb{B}(\hat{x} - p\delta_\mu b), \quad p \in \{+1, -1\}, \tag{4.11}$$

$$\mathcal{S}(\delta) := \mathcal{O}_{+1} \bigcap \mathcal{O}_{-1}. \tag{4.12}$$

Then, (4.12) *defines an eye-shaped set centered at $\hat{x}$, called* avoidance shell *in the following.*

Note that $\mu \in (0, 2)$ fixes the aspect ratio of the shell, whose height corresponds to $\mu\delta$. The set $\mathcal{S}(\delta)$ is visualized in Figure 4.1, which also shows the role of the shell parameters.
Before we proceed with the construction of the avoidance controller we recall the following result, proven in [122].

Lemma 4.1.4 (Avoidance shell set-inclusion; [122, Lemma 1])**.** *Given an aspect ratio $\mu \in (0, 2)$ and an orientation $b \in \mathbb{R}^n$, $|b| = 1$, for each $\delta > 0$, the following inclusions hold for the shell $\mathcal{S}(\delta)$ defined in* (4.12)*:*

$$\tfrac{\mu\delta}{2}\mathbb{B}(\hat{x}) \subset \mathcal{S}(\delta) \subset \delta\mathbb{B}(\hat{x}). \tag{4.13}$$

Selecting the size parameter $\delta \leq \eta_i$ (where η_i is defined in (4.9)) of the avoidance shell $\mathcal{S}(\hat{x}_i)$ corresponding to the i-th obstacle centroid, allows us to design the avoidance controller focusing solely on solving item (ii) of Problem 4.1.1. Indeed, from the inclusion (4.13), we have $\mathcal{S}(\hat{x}_i) \subset \eta_i\mathbb{B}(\hat{x}_i)$, and, following the discussion in Section 4.1.1, the modified input selection

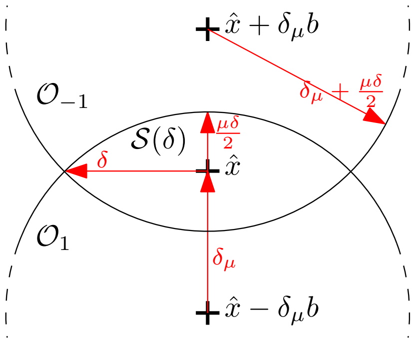

Figure 4.1: Visualization of the avoidance shell defined in Definition 4.1.3.

(4.5) preserves the decrease of the Lyapunov function in $\eta_i \mathbb{B}(\hat{x}_i)$, and therefore also in $\mathcal{S}(\hat{x}_i)$, as long as the direction $\Lambda(\hat{x}_i)$ is defined so that condition (4.4) holds.

In the avoidance controller design, we first choose the orientation $b_i = b(\hat{x}_i)$ of the avoidance shell based on the obstacle centroid of interest. First, we define the directions

$$D(\hat{x}_i) := \frac{\nabla V(\hat{x}_i)}{|\nabla V(\hat{x}_i)|}, \quad i \in \mathbb{N}_\beta. \tag{4.14}$$

Then, for each obstacle centroid $\hat{x}_i, i \in \mathbb{N}_\beta$, it is desirable to select $b(\hat{x}_i)$ and $\Lambda(\hat{x}_i)$ so that $\Lambda(\hat{x}_i)$ is perpendicular to $D(\hat{x}_i)$ in (4.14), thus satisfying (4.4) for the avoidance input (4.6), and the inner product $b(\hat{x}_i)^\top g(\hat{x}_i)\Lambda(\hat{x}_i)$ is maximized, i.e., $b(\hat{x}_i)$ is the vector maximally aligned with the subspace spanned by the columns of $g(\hat{x}_i)$.

As we will see in Section 4.1.3, this heuristic design choice is aimed at reducing the magnitude of the scaling α_p in (4.5) needed to perform the avoidance maneuver, thus requiring a reduced effort from the actuators.

To guarantee that the avoidance control input defined in (4.6) satisfies (4.4) for each $\hat{x}_i$, $i \in \mathbb{N}_\beta$, we restrict the choice of $\Lambda(\hat{x}_i)$ to non-zero vectors satisfying $D(\hat{x}_i)^\top g(\hat{x}_i)\Lambda(\hat{x}_i) = 0$. For each $\hat{x}_i, i \in \mathbb{N}_\beta$, we define the kernel of $D(\hat{x}_i)^\top g(\hat{x}_i)$, i.e., we define

$$V_\perp(\hat{x}_i) = [v_1 \ \cdots \ v_p] \in \mathbb{R}^{m \times p}, \tag{4.15}$$

such that $D(\hat{x}_i)^\top g(\hat{x}_i) V_\perp(\hat{x}_i) = 0$ and where $v_1, .., v_p$, $p \in \mathbb{N}$, denote orthonormal basis vectors of the kernel. Assumption 4.1.2(b) guarantees that $p \geq 1$. Then we select

$$\Lambda(\hat{x}_i) = V_\perp(\hat{x}_i)\overline{\Lambda}(\hat{x}_i), \tag{4.16}$$

where the vector $\overline{\Lambda}(\hat{x}_i) \in \mathbb{R}^p$ defines a linear combination of the columns of $V_\perp(\hat{x}_i)$. Based on these definitions, we are interested in solving the following optimization problem

$$(b(\hat{x}_i), \overline{\Lambda}(\hat{x}_i)) \in \begin{array}{l} \underset{\mathfrak{b}\in\mathbb{R}^n, \Lambda\in\mathbb{R}^p}{\operatorname{argmax}} \ \mathfrak{b}^\top g(\hat{x}_i)V_\perp(\hat{x}_i)\Lambda, \\ \text{s.t.} |\mathfrak{b}| = 1, |\Lambda| = 1, \end{array} \tag{4.17}$$

for each $\hat{x}_i, i \in \mathbb{N}_\beta$. It follows from the definition of the optimization problem that $(b(\hat{x}_i), \overline{\Lambda}(\hat{x}_i))$ is optimal if and only if $(-b(\hat{x}_i), -\overline{\Lambda}(\hat{x}_i))$ is optimal. Even though the optimization problem (4.17) is non-convex and solutions are not unique, it can be solved explicitly.

Lemma 4.1.5. *Consider the dynamics* (4.1)*, let Assumption 4.1.2 be satisfied and $D(\hat{x}_i)$, $V_\perp(\hat{x}_i)$ be defined as in* (4.14), (4.15) *respectively. Let $\lambda_M(\hat{x}_i)$ be a normalized eigenvector of the symmetric matrix $(g(\hat{x}_i)V_\perp(\hat{x}_i))^\top g(\hat{x}_i)V_\perp(\hat{x}_i)$ corresponding to the largest eigenvalue, denoted by $\sigma_M(\hat{x}_i)$. Then it holds that $\sigma_M(\hat{x}_i) > 0$, a solution to* (4.17) *is given by*

$$(b(\hat{x}_i), \overline{\Lambda}(\hat{x}_i)) = \left(\frac{g(\hat{x}_i)V_\perp(\hat{x}_i)\lambda_M(\hat{x}_i)}{\sqrt{\sigma_M(\hat{x}_i)}}, \lambda_M(\hat{x}_i) \right) \tag{4.18}$$

and $D(\hat{x}_i)^\top g(\hat{x}_i)V_\perp(\hat{x}_i)\overline{\Lambda}(\hat{x}_i) = 0$ for each $\hat{x}_i, i \in \mathbb{N}_\beta$.

Proof. For ease of notation, we drop the dependence on $\hat{x}_i$ in the proof. Since in (4.17) $gV_\perp\overline{\Lambda}$ belongs to the hyperplane orthogonal to D (due to the definition of $V_\perp$ in (4.15)) and b is a unit vector, the maximum of the inner product $b^\top gV_\perp\overline{\Lambda}$ is attained when b is aligned with $gV_\perp\overline{\Lambda}$, and thus $b = \frac{gV_\perp\overline{\Lambda}}{|gV_\perp\overline{\Lambda}|}$. Substituting this selection of b into the objective function of (4.17) gives

$$\frac{(gV_\perp\overline{\Lambda})^\top gV_\perp\overline{\Lambda}}{|gV_\perp\overline{\Lambda}|} = |gV_\perp\overline{\Lambda}|. \tag{4.19}$$

Since $\overline{\Lambda}$, with $|\overline{\Lambda}| = 1$, maximizes (4.19) if and only if it maximizes $|gV_\perp\overline{\Lambda}|^2$, we now focus on the maximization of the function

$$|gV_\perp\overline{\Lambda}|^2 = \overline{\Lambda}^\top V_\perp^\top g^\top gV_\perp\overline{\Lambda}. \tag{4.20}$$

Let us consider the matrix $M := V_\perp^\top g^\top gV_\perp$. Since M is a symmetric positive semi-definite matrix, substituting the definition of M into (4.20) one has the following upper bound $|gV_\perp\overline{\Lambda}|^2 = \overline{\Lambda}^\top M\overline{\Lambda} \le \sigma_M|\overline{\Lambda}|^2 = \sigma_M$ for all $\overline{\Lambda} \in \mathbb{R}^m$, where $|\overline{\Lambda}| = 1$ and σ_M denotes the largest eigenvalue of M, i.e.,

$M\lambda_M = V_\perp^\top g^\top g V_\perp \lambda_M = \sigma_M \lambda_M$. Due to Assumption 4.1.2(b), $gV_\perp \neq 0$ and thus $\mathrm{rank}(gV_\perp) > 0$. Using the properties of the $\mathrm{rank}(\cdot)$ operator, one has $\mathrm{rank}(M) = \mathrm{rank}(V_\perp^\top g^\top g V_\perp) = \mathrm{rank}((gV_\perp)^\top g V_\perp) = \mathrm{rank}(gV_\perp)$, which implies that $\mathrm{rank}(M) = \mathrm{rank}(gV_\perp) > 0$ for all $\hat{x}_i, i \in \mathbb{N}_\beta$. Then, $\sigma_M > 0$ and substituting $\overline{\Lambda} = \lambda_M$ into (4.20) gives $|gV_\perp \lambda_M|^2 = \lambda_M^\top V_\perp^\top g^\top g V_\perp \lambda_M = \sigma_M$, implying that the maximum of (4.19), which coincides with the maximum of (4.17), is $|gV_\perp \lambda_M| = \sqrt{\sigma_M}$. Vector b can therefore be written as $b = \frac{gV_\perp \lambda_M}{|gV_\perp \lambda_M|} = \frac{gV_\perp \lambda_M}{\sqrt{\sigma_M}}$ (giving (4.18)) and $D^\top g V_\perp \overline{\Lambda} = 0$ follows from the definition of $V_\perp$ in (4.15). □

4.1.3 AVOIDANCE CONTROLLER

For each obstacle centroid $\hat{x}_i, i \in \mathbb{N}_\beta$, Lemma 4.1.5 provides vectors $b(\hat{x}_i)$ and $\overline{\Lambda}(\hat{x}_i)$ defining the orientation of the avoidance shell in (4.12) and the direction of the avoidance controller in (4.6), (4.16), respectively. With $\overline{\Lambda}(\hat{x}_i)$ defined as in Lemma 4.1.5, $v_p^i(\hat{x}_i)$ defined in (4.6), (4.16) satisfies (4.4).
In this section we focus on the derivation of $\alpha_p(x)$ for $p \in \{-1, 1\}$, which is the missing component in the definition of $v_p^i(x)$. Given an arbitrary obstacle centroid $\hat{x}_i$ and a selection of parameters δ_i, μ_i, defining the size and shape of the avoidance shell $\mathcal{S}(\hat{x}_i)$ centered at $\hat{x}_i$ as in Definition 4.1.3, the role of the scaling factor α_p is to guarantee that solutions do not enter inside $\mathcal{S}(\delta_i)$ when the modified input (4.5) is selected. Via inclusion (4.13), this implies that solutions never enter the set $\frac{\mu_i \delta_i}{2}\mathbb{B}(\hat{x}_i)$ and so item (ii) is solved with $\chi_i \leq \frac{\mu_i \delta_i}{2}$. Let

$$c_p := \hat{x} - p\delta_\mu b, \qquad p \in \{-1, +1\} \tag{4.21}$$

denote the centers of the balls $\mathcal{O}_p$, $p \in \{-1, +1\}$ in (4.11) for a generic obstacle centroid $\hat{x} \in \{\hat{x}_1, \dots, \hat{x}_\beta\}$ and corresponding $b(\hat{x})$ defined in (4.18). The avoidance controller is defined so that

$$\tfrac{d}{dt}|x(t) - c_p|^2 = 0, \qquad p \in \{-1, 1\}, \tag{4.22}$$

holds for any $x \in \mathcal{S}(\delta)$. This condition, in particular, ensures that if the modified input (4.5) is selected when a solution reaches the boundary of the avoidance shell $\partial\mathcal{S}(\delta)$, and the value of p is selected in accordance with the side of the shell that the solution has reached, then the solution will "slide" on the boundary of the shell, as its distance to the point c_p will remain constant, while its distance to the other shifted point, c_{-p}, may increase or decrease. Enforcing condition (4.22) to hold in the whole avoidance shell $\mathcal{S}(\delta)$, rather than just on its boundary $\partial\mathcal{S}(\delta)$, ensures that, in the event of a delay in the selection of the modified input (4.5), solutions will "slide" on the boundary of a smaller avoidance shell. In such case, the property of obstacle avoidance still holds for a smaller value of χ_i in item (ii) of Problem 4.1.1, rather than

being lost. This guarantees a margin of robustness of the avoidance to delays in the input switch.
Imposing (4.22) will give us the definition of $\alpha_p(\hat{x}_i)$ in (4.6). We now show that by selecting $\overline{\Lambda}(\hat{x}_i)$ and $b(\hat{x}_i)$ according to Lemma 4.1.5 there always exists a sufficiently small neighborhood for each obstacle centroid, and thus, via inclusion (4.32), a sufficiently small avoidance shell, inside which condition (4.22) holds.

Lemma 4.1.6. *Consider the dynamics* (4.1), (4.5)*. Let Assumption 4.1.2 be satisfied, $\hat{x}_i, i \in \mathbb{N}_\beta$ be an obstacle centroid, $b(\hat{x}_i), \sigma_M(\hat{x}_i)$, $\overline{\Lambda}(\hat{x}_i)$ be defined as in Lemma 4.1.5, $V_\perp(\hat{x}_i)$ and $\Lambda(\hat{x}_i)$ be defined as in* (4.15) *and* (4.16)*. Then, for all $\overline{\mu}_i \in (0,2)$ there exists $\overline{\delta}_i \in \mathbb{R}_{>0}$ defining the shell $\mathcal{S}(\overline{\delta}_i)$ such that the avoidance control input* (4.6) *with*

$$\alpha_p(x) = \frac{-f_s(x)^\top (x - \hat{x}_i + p\delta_\mu b(\hat{x}_i))}{(g(x)\Lambda(\hat{x}_i))^\top (x - \hat{x}_i + p\delta_\mu b(\hat{x}_i))}, \tag{4.23}$$

is well-defined and satisfies (4.22) *for all $x \in \mathcal{S}(\overline{\delta}_i)$.*

Proof. We start by rewriting (4.22), substituting (4.1), the closed-loop dynamics (4.2), and the control input selection $u_a(x) = \kappa_s(x) + \alpha_p(x)\Lambda(\hat{x}_i)$, with $\Lambda(\hat{x}_i)$ defined as in (4.16),

$$\begin{aligned} &\tfrac{d}{dt}|x(t) - c_p|^2 = \dot{x}^\top (x - c_p) = (f(x) + g(x)u_a)^\top (x - c_p) \\ &= f_s(x)^\top (x - \hat{x}_i + p\delta_\mu b(\hat{x}_i)) \\ &\quad + \alpha_p(x)(g(x)\Lambda(\hat{x}_i))^\top (x - \hat{x}_i + p\delta_\mu b(\hat{x}_i)). \end{aligned} \tag{4.24}$$

Imposing (4.24) to be zero results in the condition on α_p (4.23). We now show that for each $\overline{\mu}_i \in (0,2)$ there exists $\overline{\delta}_i > 0$ such that the denominator of (4.23) is non-zero for all $x \in \mathcal{S}(\overline{\delta}_i)$. Observe that for $x = \hat{x}_i$ the denominator of (4.23) simplifies to

$$(g(\hat{x}_i)\Lambda(\hat{x}_i))^\top p\delta_\mu b(\hat{x}_i) = p\delta_\mu \sqrt{\sigma_M(\hat{x}_i)},$$

which is greater than zero for all $\delta > 0, \mu \in (0,2)$. Moreover, for each $\delta > 0$, Lipschitz continuity of g implies the existence of $L_g > 0$ such that

$$|g(x)\Lambda(\hat{x}_i) - g(\hat{x}_i)\Lambda(\hat{x}_i)| \leq L_g|x - \hat{x}_i|$$

for all $x \in \delta\mathbb{B}(\hat{x}_i)$, which in turn implies

$$g(x)\Lambda(\hat{x}_i) \in g(\hat{x}_i)\Lambda(\hat{x}_i) + L_g\delta\mathbb{B} \tag{4.25}$$

for all $x \in \delta\mathbb{B}(\hat{x}_i)$. We now prove that there always exist $\hat{\delta}, \hat{\mu} > 0$ sufficiently small such that the denominator of (4.23) is non-zero for all $x \in \mathcal{S}(\hat{\delta})$, where

$\mathcal{S}(\hat{\delta})$ is the avoidance shell defined by $\hat{\delta}, \hat{\mu}$ according to (4.12). Using inclusion (4.25) and the fact that $|b(\hat{x}_i)| = 1$ and $|g(\hat{x}_i)\Lambda(\hat{x}_i)| = \sqrt{\sigma_M(\hat{x}_i)}$, one obtains that the lower bound on the denominator of (4.23)

$$\begin{aligned}
&|(g(x)\Lambda(\hat{x}_i))^\top (x - \hat{x}_i + pb(\hat{x}_i)\delta_\mu)| \\
&\geq -|(g(\hat{x}_i)\Lambda(\hat{x}_i))^\top (x - \hat{x}_i)| - L_g\delta^2 \\
&+ |(g(\hat{x}_i)\Lambda(\hat{x}_i))^\top p\delta_\mu b(\hat{x}_i)| - L_g\delta\delta_\mu \\
&\geq \sqrt{\sigma_M(x)}(\delta_\mu - \delta) - L_g\delta^2 - L_g\delta\delta_\mu
\end{aligned} \tag{4.26}$$

holds for all $x \in \delta\mathbb{B}(\hat{x}_i)$. One can verify that, for every $\mu \in (0, 2(\sqrt{2}-1))$, $\delta_\mu - \delta$ is positive for all $\delta > 0$. Then, given $\hat{\mu} \in (0, 2(\sqrt{2}-1))$, it is possible to show that there always exists a sufficiently small $\hat{\delta} > 0$ such that (4.26) is positive. Define $\overline{\delta}_i := \frac{\hat{\mu}\hat{\delta}}{2}$. From (4.13) one has $\overline{\delta}_i\mathbb{B}(\hat{x}_i) \subset \mathcal{S}(\hat{\delta})$ and $\mathcal{S}(\overline{\delta}_i) \subset \overline{\delta}_i\mathbb{B}(\hat{x}_i)$, which show that for every $\overline{\mu}_i \in (0, 2)$ there exists a sufficiently small $\overline{\delta}_i > 0$ such that the denominator of (4.23) is non-zero for all $x \in \mathcal{S}(\overline{\delta}_i)$. □

Remark 16. *The argument used in the proof of Lemma 4.1.6, to show that* (4.23) *is well-defined inside a sufficiently small avoidance shell* $\mathcal{S}(\overline{\delta}_i)$*, exploits the contribution of the inner product* $(g(\hat{x}_i)\Lambda(\hat{x}_i))^\top b(\hat{x}_i)$ *to the denominator of* (4.23) *via inequality* (4.26)*. The selection of* $(\Lambda(\hat{x}_i), b(\hat{x}_i))$ *in Lemma 4.1.5, maximizing the inner product* $(g(\hat{x}_i)\Lambda(\hat{x}_i))^\top b(\hat{x}_i)$*, results in a larger term in the denominator of* (4.23)*, and therefore a larger admissible size* $\overline{\delta}_i$ *and, possibly, depending on* f_s*, a smaller* α_p*.*

Lemma 4.1.6 guarantees the existence of $\overline{\delta}_i > 0$ such that $\alpha_p(x)$ is well-defined for all $x \in \mathcal{S}(\overline{\delta}_i)$. To be able to use $\alpha_p(x)$ in the avoidance controller design, we want to ensure that the size of the avoidance shell satisfies $\overline{\delta}_i \leq \eta_i$, where η_i is defined through (4.9), so that the decrease of the Lyapunov function is preserved during the avoidance maneuver, as discussed in Section 4.1.2. However, (4.9) depends on the selection of $\overline{\delta}_i$ and $\overline{\mu}_i$ via α_p defined as in (4.23). To avoid the need to compute η_i, we consider the optimization problem

$$\overline{\delta}_{i,p} = \min_{x \in \mathbb{R}^n \, \delta \geq 0} \delta, \tag{4.27}$$

$$\text{s.t.} \; -\rho(x) + \alpha_p(x)\nabla V(x)^\top g(x)\Lambda(\hat{x}_i) \geq 0 \tag{4.28}$$

$$|x - c_p| \leq \delta_\mu + \tfrac{\mu\delta}{2}, \; p(x - \hat{x}_i)^\top b_i(\hat{x}_i) \geq 0 \tag{4.29}$$

for $p \in \{-1, 1\}$ and a fixed aspect ratio $\mu \in (0, 2)$. Here, $\overline{\delta}_{i,p}$ defines the largest δ such that the decrease condition (4.8) is not satisfied for all x in the half shell $x \in \mathcal{S}(\delta) \cap \{x \in \mathbb{R}^n : \ pb_i(\hat{x})^\top (x - \hat{x}_i) \geq 0\}$. Accordingly, the decrease condition (4.8) and the properties of Lemma 4.1.6 are satisfied for

$$\overline{\delta}_i \in (0, \min\{\overline{\delta}_{i,1}, \overline{\delta}_{i,-1}\}). \tag{4.30}$$

Remark 17. *Since the half shell in* (4.29) *is bounded, an approximate solution of the optimization problem* (4.27) *can be computed numerically, by discretizing the half shell for different values of* δ *and by evaluating* (4.28) *over the set of discretized states.*

Remark 18. *As in [122] condition* (4.22) *can be changed to* $\frac{d}{dt}|x(t)-c_p|^2 > 0$, $p \in \{-1, 1\}$, *to obtain robust avoidance properties. Here, we restrict our attention to the nominal setting covered through Lemma 4.1.6.*

4.1.4 HYBRID CONTROLLER DESIGN

In this section we follow the construction presented in [122, Section IV] to orchestrate the switching between the nominal control law and the modified control law (4.5). We briefly recall the definitions given in [122, Section IV] of the inner avoidance shell and upper/lower parts of the avoidance shell.

Definition 4.1.7 ([121, Section IV])**.** *Consider an obstacle centroid* $\hat{x} \in \{\hat{x}_1, \ldots, \hat{x}_\beta\}$ *together with the parameter* $h \in (0,1)$, *called hysteresis factor, and let*

$$\mathcal{O}_{h,p} := (h\tfrac{\mu\delta}{2} + \delta_\mu)\mathbb{B}(c_p), \quad p \in \{-1, 1\}, \tag{4.31}$$

$$\mathcal{S}_h(\delta) := \mathcal{O}_{h,+1} \cap \mathcal{O}_{h,-1}. \tag{4.32}$$

Then, (4.32) *defines a smaller eye-shaped set centered around* $\hat{x}_i$ *called* inner avoidance shell *in the following, and*

$$\mathcal{\$}_p := \mathcal{S}(\delta) \cap \{x \in \mathbb{R}^n : pb^\top (x - \hat{x}) \geq 0\}, \ p \in \{-1, 1\} \tag{4.33}$$

defines the lower and upper halves of the avoidance shell with respect to the orientation b.

To account for multiple obstacles, we substitute $p \in \{-1, 1\}$ used in the previous section with the logic variable $q \in \mathbb{Z}_\beta$ and write

$$c_q := \hat{x}_{|q|} - \frac{q}{|q|}\delta_{\mu_{|q|}} b_{|q|}, \quad q \in \mathbb{Z}_\beta \setminus \{0\}. \tag{4.34}$$

Moreover, when referring to an obstacle centroid $\hat{x}_i, i \in \mathbb{N}_\beta$, we will use the notation $\cdot^i, i \in \mathbb{N}_\beta$, to refer to quantities corresponding to the i-th obstacle centroid $\hat{x}_i, i \in \mathbb{N}_\beta$. Using q we define the overall hybrid state as $\xi := [x^\top \; q]^\top \in \Xi := \mathbb{R}^n \times \mathbb{Z}_\beta$, and write the new feedback law as

$$u(\xi) := \begin{cases} \kappa_s(x), & \text{if } q = 0, \\ \kappa_s(x) + v_a^{|q|}(x), & \text{if } q \in \mathbb{Z}_\beta \setminus \{0\}. \end{cases} \tag{4.35}$$

The jump dynamics, modeling the switching between nominal and modified control law, can be written as

$$\begin{aligned} \mathcal{D}_{+i} &:= \left(\mathcal{S}_h^i(\delta_i) \cap \mathcal{F}_{+1}^i\right) \times \{0\}, \quad i \in \mathbb{N}_\beta \\ \mathcal{D}_{-i} &:= \left(\mathcal{S}_h^i(\delta_i) \cap \mathcal{F}_{-1}^i\right) \times \{0\}, \quad i \in \mathbb{N}_\beta \\ \mathcal{D}_0 &:= \overline{\mathbb{R}^n \setminus \cup_{i\in\mathbb{N}_\beta} \mathcal{S}^i(\delta_i)} \times (\mathbb{Z}_\beta \setminus \{0\}) \\ q^+ \in G_q(x,q) &:= \begin{cases} i, & \text{if } (x,q) \in \mathcal{D}_{+i} \setminus \mathcal{D}_{-i},\ i \in \mathbb{N}_\beta \\ -i, & \text{if } (x,q) \in \mathcal{D}_{-i} \setminus \mathcal{D}_{+i},\ i \in \mathbb{N}_\beta \\ \{i, -i\}, & \text{if } (x,q) \in \mathcal{D}_{+i} \cap \mathcal{D}_{-i},\ i \in \mathbb{N}_\beta \\ 0, & \text{if } (x,q) \in \mathcal{D}_0, \end{cases} \end{aligned} \tag{4.36}$$

where the flow and jump sets are compactly written as

$$\mathcal{C} := \overline{\Xi \setminus (\cup_{q\in\mathbb{Z}_\beta} \mathcal{D}_q)}, \quad \mathcal{D} := \cup_{q\in\mathbb{Z}_\beta} \mathcal{D}_q, \tag{4.37}$$

and the overall hybrid dynamical system can be written as

$$\dot{\xi} = \begin{bmatrix} \dot{x} \\ \dot{q} \end{bmatrix} = \begin{bmatrix} f(x) + g(x)u(\xi) \\ 0 \end{bmatrix}, \qquad \xi \in \mathcal{C}, \tag{4.38}$$

$$\xi^+ = \begin{bmatrix} x^+ \\ q^+ \end{bmatrix} \in \begin{bmatrix} x \\ G_q(x,q) \end{bmatrix}, \qquad \xi \in \mathcal{D}. \tag{4.39}$$

When the state $\xi = [x^\top \; q]^\top$ enters the jump set $\mathcal{D}$, the jump map (4.36) updates q while keeping x constant. The variable q is responsible for the selection of the nominal or modified control law, as it can be seen from (4.35). When the x component of the state ξ enters the inner avoidance shell $\mathcal{S}_h^i(\delta)$, q is set to either i or $-i$. When x leaves the avoidance shell $\mathcal{S}^i(\delta)$, q is reset to 0. Since the avoidance controller is activated once trajectories reach the inner avoidance shell $\mathcal{S}_h^i(\delta_i)$, the avoidance requirement in item (ii) of Problem 4.1.1 is satisfied for the set $\frac{h\mu_i\delta_i}{2}\mathbb{B}(\hat{x}_i) \subset \mathcal{S}_h^i(\delta_i)$, and thus for $\chi_i = \frac{h\mu_i\delta_i}{2}$.
We are now ready to state the main result of this section.

Theorem 4.1.8. *Let Assumption 4.1.2 be satisfied and $h \in (0,1)$, $\mu_i \in (0,2)$, $i \in \mathbb{N}_\beta$, be arbitrary. Then, there exist $\delta_i > 0$, $i \in \mathbb{N}_\beta$, such that the hybrid system* (4.37), (4.38), (4.39), *solves Problem 4.1.1 for $\chi_i = \frac{h\mu_i\delta_i}{2}$.*

Proof. For each obstacle centroid $\hat{x}_i, i \in \mathbb{N}_\beta$, consider δ_i defined from (4.27)-(4.30). From the inclusion (4.13) we have $\mathcal{S}^i(\delta_i) \subset \delta_i\mathbb{B}(\hat{x}_i)$, and since the modified control law is only used inside the avoidance shell $\mathcal{S}^i(\delta_i)$ of an obstacle, this proves that the hybrid system satisfies item (i) of Problem 4.1.1 by taking $\delta = \max_{i\in\mathbb{N}_\beta} \delta_i$.
Let us now focus on item (ii) of Problem 4.1.1. Consider an arbitrary obstacle centroid $\hat{x}_i, i \in \mathbb{N}_\beta$, and let $(t, j) \mapsto \xi(t, j)$ be a solution of (4.37)-(4.39) such that $\xi(0, 0) \notin \mathcal{D}$, which implies $x(0, 0) \notin \cup_{i=1}^{\beta}\delta\mathbb{B}(\hat{x}_i)$, with δ defined as above. Assume that there exists a time $(t_0, j_0) \in \operatorname{dom} \xi$ at which the solution reaches the inner avoidance shell of the obstacle $\hat{x}_i$, $\xi(t_0, j_0) \in \mathcal{D}_i \cup \mathcal{D}_{-i}$. Then, the solution will jump according to the jump map (4.36), with q^+ set to either $-i$ or i, and, according to (4.35), the control law $u(\xi) = \kappa_s(x) + v_a^i(x)$ will be selected to perform the avoidance maneuver.
Lemma 4.1.6 ensures that the x component of the state ξ never enters the interior of the avoidance shell $\mathcal{S}^i_{h_i}(\delta_i)$ during the avoidance maneuver, thus implying, using the inclusion (4.13), that x never enters the set $\frac{h\mu_i\delta_i}{2}\mathbb{B}(\hat{x}_i)$, proving (ii) of Problem 4.1.1.
We now focus on item (iii) of Problem 4.1.1. First, we observe that the hybrid system (4.37)–(4.39) satisfies the Hybrid Basic Conditions in Definition 2.2.1. Consider the Lyapunov function defined in Assumption 4.1.2(a). Since $\hat{x}_i \neq 0$ and $\hat{x}_i \in \mathcal{U}$ for all $i \in \mathbb{N}_\beta$, it is always possible to scale the parameters δ_i to ensure that $0 \notin \mathcal{D}$ and $\cup_{i=1}^{\beta}\mathcal{S}^i(\delta_i) \subset \mathcal{U}$.
Then, the set $\cup_{i=1}^{\beta}\mathcal{S}^i(\delta_i)$ is bounded away from the origin, and there exists a neighborhood of the origin inside which the solutions evolve continuously according to (4.2). Then, Lyapunov stability of the origin for (4.2) implies Lyapunov stability of the origin for (4.37)–(4.39).
We proceed by proving pre-attractivity of the origin for (4.37)-(4.39).
Since V does not depend on q, we write $V(\xi) = V(x)$. When the solution jumps, one has $V(\xi^+) - V(\xi) = 0$ for all $\xi \in \mathcal{D}$.
By choosing δ_i small enough for all $i \in \mathbb{N}_\beta$ so that $\delta_i \leq \overline{\delta}_i$, with $\overline{\delta}_i$ defined as in (4.30), and $\cup_{i=1}^{\beta}\mathcal{S}^i(\delta_i) \subset \mathcal{U}$, we have that the decrease property in (4.8) holds for all $x \in \mathcal{S}^i(\delta_i)$, and, together with the decrease (4.3) guaranteed by the nominal control law $u(\xi) = \kappa_s(\xi)$, this shows that $\dot{V} < 0$ for every $\xi \in \mathcal{C} \cap (\mathcal{U} \times \mathbb{Z}_\beta)$ with $x \neq \{0\}$.
Thus, we have that the Lyapunov function V does not increase when solutions to (4.37)-(4.39) jump or flow for all $\xi \in \mathcal{U} \times \mathcal{Z}_q$. Recalling that $\mathcal{U}$ is defined in Assumption 4.1.2 as an open sublevel set of V, for any solution $(t, j) \mapsto \xi(t, j)$ to (4.37)-(4.39) starting in $\mathcal{U} \times \mathbb{Z}_\beta$ there exists a finite $\mu \in \mathbb{R}_{\geq}0$ such that $\xi(0, 0) \in \Gamma \times \mathbb{Z}_\beta$, with $\Gamma := \{x \in \mathcal{U} : V(x) \leq \mu\}$ being a sublevel set of V contained in $\mathcal{U}$.
Since V is non-increasing along all solutions to (4.37)-(4.39), we have that ξ remains inside this set for all $(t, j) \in \operatorname{dom} \xi$. Boundedness of $\Gamma \times \mathbb{Z}_\beta$, coming

from the fifth requirement on V in Definition 2.4.1, implies that ξ is bounded. Since the above argument applies to all solutions starting in $\mathcal{U} \times \mathbb{Z}_\beta$, we can conclude that all solutions starting in $\mathcal{U} \times \mathbb{Z}_\beta$ are bounded. Due to the definition of the jump sets (4.37) one has $G(\mathcal{D}) \cap \mathcal{D} = \emptyset$, and therefore Theorem 2.2.6 implies that all solutions starting in $\mathcal{U} \times \mathbb{Z}_\beta$ have a non-zero dwell-time.
Since V is always decreasing when solutions flow with $x \neq \{0\}$, and after a jump solutions must flow, we can conclude that the only complete solutions $\xi(t,j)$ along which V remains constant must satisfy $V(\xi(t,j)) = 0$ for all $(t,j) \in \operatorname{dom} \xi$, and thus $x(t,j) = \{0\}$ for all $(t,j) \in \operatorname{dom} \xi$. The invariance principle for hybrid systems stated in Corollary 2.4.6 allow us to conclude convergence of all complete solutions starting in $\mathcal{U} \times \mathbb{Z}_\beta$ to the origin. This proves that the origin is pre-attractive with basin of pre-attraction $\mathcal{B}^p_{\mathcal{A}} \supseteq \mathcal{U} \times \mathbb{Z}_\beta$. From Lyapunov stability and pre-attractivity of the origin, we can conclude pAS of the origin with $\mathcal{B}^p_{\mathcal{A}} \supseteq \mathcal{U} \times \mathbb{Z}_\beta$.
Robustness and uniformity follow from Theorem 2.3.9, thus proving item (iii) of Problem 4.1.1.
Completeness of all maximal solutions starting in $\mathcal{U}\times\mathbb{Z}_\beta$ follows from Theorem 2.2.5 by observing that, (i) as a consequence of uniform stability of the origin, all solutions starting in $\mathcal{U} \times \mathbb{Z}_\beta$ are bounded, that (ii) $G(\mathcal{D}) \subset \mathcal{C} \cup \mathcal{D}$, and that (iii) all points $\xi \in \mathcal{C} \setminus \mathcal{D}$ are also in the interior of $\mathcal{C}$, therefore $T_{\mathcal{C}}(\xi) = \mathbb{R}^n$.
□

4.1.5 NUMERICAL SIMULATIONS

To illustrate the effectiveness of the proposed avoidance architecture, we consider the input-affine nonlinear system

$$\begin{bmatrix} \dot{x}_1 \\ \dot{x}_2 \\ \dot{x}_3 \end{bmatrix} = f(x) + g(x)u = \begin{bmatrix} x_2 + x_1^2 \\ x_1^2 + x_3 \\ 0 \end{bmatrix} + \begin{bmatrix} 0 & 0 \\ 1 & 0 \\ 0 & 1 \end{bmatrix} \begin{bmatrix} u_1 \\ u_2 \end{bmatrix},$$

which is a modified version of the nonlinear system presented in [123, Sec. 3.3]. We assume that the stabilization task has to be performed by u_2, while u_1 is an additional input that can be used during avoidance. Through backstepping, the stabilizing controller $u_s = [0 \; u_n]^\top$,with

$$u_n = -3x_1 - 5x_2 - 3x_3 - 8x_1x_2 - 2x_1x_3 - 8x_1^2x_2 - 8x_1^2 - 10x_1^3 - 2x_2^2 - 6x_1^4,$$

and the Lyapunov function

$$V(x) = \tfrac{1}{2}x_1^2 + \tfrac{1}{2}(x_2 + x_1 + x_1^2)^2 + \tfrac{1}{2}(2x_1 + 2x_2 + x_3 + 2x_1(x_1^2 + x_2) + 3x_1^2)^2$$

are obtained. To illustrate the properties of our hybrid redesign, in Figure 4.2 and 4.3 we show numerical simulations obtained by considering three obstacle centroids, $\hat{x}_1 = [0.54, -0.42, -0.6]^\top$, $\hat{x}_2 = [0.5, 0.3, -0.8]^\top$, $\hat{x}_3 = [0.54, -0.22, -1.2]^\top$. The parameters used for the construction of the shells are $h_i = 0.75$, $\mu_i = 1$, for $i \in \mathbb{N}_3$, and $\delta_1 = 0.3, \delta_2 = 0.5, \delta_3 = 0.15$. In Figure 4.2 one can see three trajectories, two encountering more than one obstacle along their path. The dashed line is used to indicate when the avoidance controller is active. In Figure 4.3 one can see the time evolution of V, confirming that stability of the origin is preserved, and $u = [u_1\ u_2]^\top$ along one of the trajectories shown in the right plot (comparable plots can be obtained for the other two trajectories).

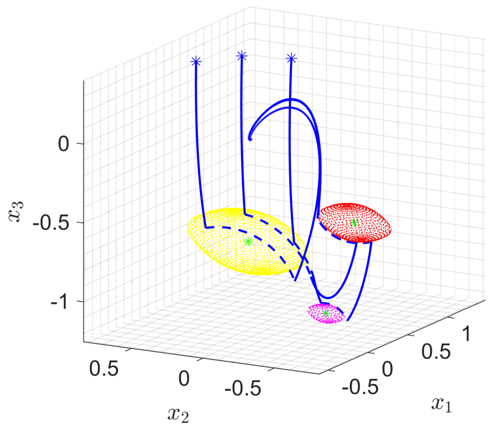

Figure 4.2: State trajectories (blue) avoiding the interior of avoidance shells $\mathcal{S}_h(\delta_i)$.

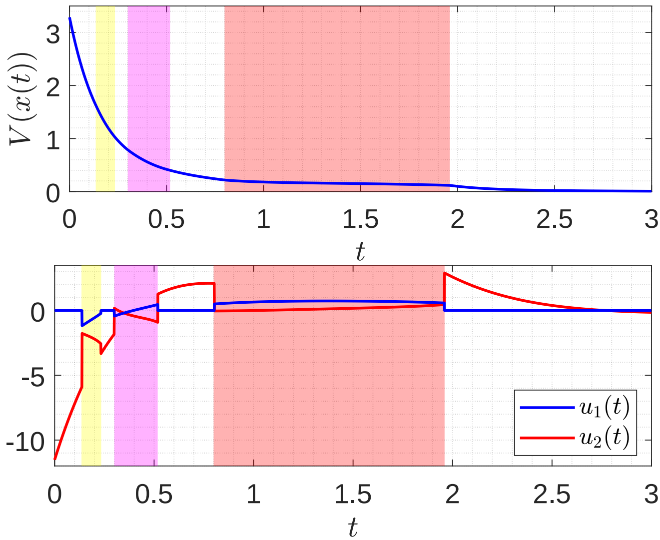

Figure 4.3: Time evolution of the input u and Lyapunov function V along one trajectory. The colored patches indicate when the avoidance controller is active.

4.2 INPUT AVOIDANCE

We now address the problem of stabilizing a given plant while ensuring that the control input never takes an unwanted value. We formulate our redesign solution first for single-input linear system, and then extend it to the class of input-affine nonlinear systems. Let us start by considering the strictly proper linear plant

$$\begin{cases} \dot{x}_p = A_p x_p + B_p u_n \\ y = C_p x_p, \end{cases} \tag{4.40}$$

with $x_p \in \mathbb{R}^{n_p}$, $u_n \in \mathbb{R}$, $y \in \mathbb{R}^{m_p}$, in feedback interconnection with a linear dynamic controller

$$\begin{cases} \dot{x}_c = A_c x_c + B_c y \\ u_n = C_c x_c + D_c y, \end{cases} \tag{4.41}$$

with $x_c \in \mathbb{R}^{n_c}$. Defining the full state $x := [x_p^\top \; x_c^\top]^\top \in \mathbb{R}^n$, with $n = n_p + n_c$, the output u_n can be written as

$$u_n = D_c C_p x_p + C_c x_c = K \begin{bmatrix} x_p \\ x_c \end{bmatrix} \tag{4.42}$$

and the linear feedback interconnection becomes

$$\dot{x} = Ax + Bu_n = (A + BK)x, \tag{4.43}$$

with $A = \begin{bmatrix} A_p & 0 \\ B_c C_p & A_c \end{bmatrix}, B = \begin{bmatrix} B_p \\ 0 \end{bmatrix}, K = \begin{bmatrix} D_c C_p & C_c \end{bmatrix}$.

Any linear stabilizing control design (such as H_∞ or linear quadratic control) yields a controller of the form (4.41), thus making our redesign technique broadly applicable.

Problem 4.2.1. Under the assumption that $A + BK$ is Hurwitz, define a hybrid controller modifying the closed-loop (4.40)-(4.41) such that the following properties hold:

(i) RUGAS: the origin is robustly uniformly globally asymptotically stable.

(ii) Unit input avoidance: the redesigned input u never takes the value 1 along solutions.

(iii) Local preservation: the redesigned controller preserves the nominal linear closed-loop dynamics (4.43) in a neighborhood of the origin.

(iv) Output feedback: the redesigned controller only uses the knowledge of x_c and y, namely, only quantities available to the linear controller.

Remark 19. *Item (ii) of Problem 4.2.1 can be generalized to any nonzero value by properly rescaling u_n and B_p.*

4.2.1 LINEAR REDESIGNED CONTROLLER ARCHITECTURE

A logic variable $q \in \{-1, 1\}$ is introduced to model a switch between the nominal feedback interconnection (4.40)-(4.41) ($q = 1$), and a modified feedback interconnection obtained by rescaling the output of the control system ($q = -1$). The redesigned output selection induced by q is given by

$$u = \frac{1-2q\overline{\varepsilon}}{1-2\overline{\varepsilon}} u_n = \begin{cases} u_n, & \text{if } \ q = 1, \\ \dfrac{1+2\overline{\varepsilon}}{1-2\overline{\varepsilon}} u_n, & \text{if } \ q = -1, \end{cases} \tag{4.44}$$

where $\overline{\varepsilon} \in (0, \frac{1}{2})$ is a tuning parameter determining the trade-off between robustness to measurement noise and preservation of the nominal closed-loop performance. The resulting feedback interconnection is shown in Figure 4.4. The logic defining the value of q is implemented using the function

$$\phi(u, q) = (q + 2\overline{\varepsilon})u - q - \overline{\varepsilon}, \tag{4.45}$$

which induces the flow and jump sets

$$\begin{aligned} \mathcal{C} :=& \{(x, q) \in \mathbb{R}^n \times \{-1, 1\} \mid \phi(u, q) \leq 0\} \\ \mathcal{D} :=& \{(x, q) \in \mathbb{R}^n \times \{-1, 1\} \mid \phi(u, q) \geq 0\}. \end{aligned} \tag{4.46}$$

The jump set $\mathcal{D}$ generated by the inequality $\phi(u, q) \geq 0$, shown in Figure 4.5, can be expressed as

$$\phi(u, q) \geq 0 \Leftrightarrow \begin{cases} u \geq 1 - \dfrac{\overline{\varepsilon}}{1+2\overline{\varepsilon}} & \text{for } \ q = 1, \\ u \leq 1 + \dfrac{\overline{\varepsilon}}{1-2\overline{\varepsilon}} & \text{for } \ q = -1. \end{cases} \tag{4.47}$$

Defining the augmented state $z = (x, q) \in \mathbb{R}^n \times \{-1, 1\}$ and the jump map toggling the value of q and leaving x unchanged, the hybrid system describing

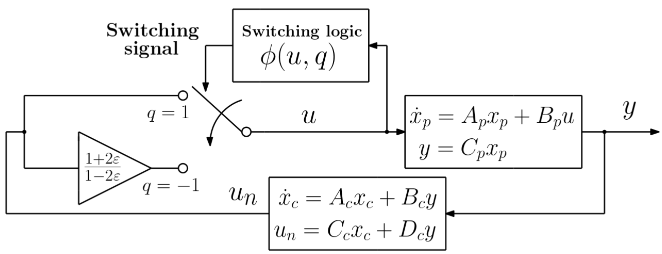

Figure 4.4: Redesigned plant/controller feedback interconnection.

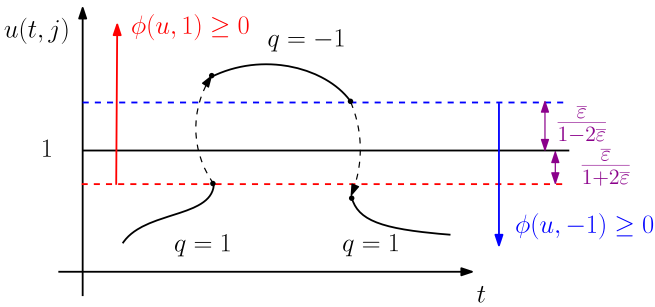

Figure 4.5: Example of input evolution generated by the hybrid architecture with jump sets generated by the function $\phi(u, q)$.

the dynamics of z can be written as

$$\begin{cases} \dot{z} = \begin{bmatrix} \dot{x} \\ \dot{q} \end{bmatrix} = \begin{bmatrix} Ax + Bu \\ 0 \end{bmatrix}, & z \in \mathcal{C} \\ z^+ = \begin{bmatrix} x^+ \\ q^+ \end{bmatrix} = \begin{bmatrix} x \\ -q \end{bmatrix}, & z \in \mathcal{D}. \end{cases} \tag{4.48}$$

The closed-loop hybrid dynamical system is then given by (4.44), (4.45), (4.46), (4.48). Exploiting expression (4.47), Figure 4.5 illustrates a possible trajectory of the input and how the switching logic ensures that it never crosses the line $u = 1$.

4.2.2 MAIN RESULTS AND TUNING METHOD

In accordance with Figure 4.5, to ensure $\frac{\overline{\varepsilon}}{1-2\overline{\varepsilon}} > 0$ and $\frac{\overline{\varepsilon}}{1+2\overline{\varepsilon}} > 0$, we constrain $\overline{\varepsilon} \in (0, \frac{1}{2})$, which also guarantees that $u = 0, q = 1$ is not in the jump set and that the scaling factor in equation (4.44) is not unbounded. More specifically, we show next that there exists $\varepsilon^* \in (0, \frac{1}{2})$ such that, for any $\overline{\varepsilon} \in (0, \varepsilon^*)$, hybrid system (4.44), (4.45), (4.46), (4.48) solves Problem 4.2.1. We also provide a computationally attractive way to estimate ε^*.
First note that $A + BK$ being Hurwitz implies that there exists $\alpha > 0$ and $P = P^\top > 0$ such that

$$\mathrm{He}(P(A + BK)) \leq -2\alpha P, \tag{4.49}$$

where α is any value less than or equal to the spectral abscissa of $A+BK$. To simplify the notation in the following equations, we introduce the additional variable $\eta = \frac{1-2\overline{\varepsilon}}{2\overline{\varepsilon}} > 0$, which maps $(0, \frac{1}{2})$ to $(0, \infty)$ with $\overline{\varepsilon} = (2(1 + \eta))^{-1}$.

It is then possible to select $\varepsilon^* = (2(1+\eta^*))^{-1}$, where $\eta^* \in [0, +\infty)$ is any number satisfying

$$\mathrm{He}(PBK) \leq \eta^* \alpha P. \tag{4.50}$$

We emphasize that a large enough η^* solving (4.50) always exists, which will lead to a small enough $\varepsilon^* = (2(1+\eta^*))^{-1}$. We observe that the smaller the value of ε^*, the closer the nominal controller will get to the unit value before jumping (see Figure 4.5), which reduces the margin around the value $u = 1$. For this reason, it is of interest to solve the following quasi-convex generalized eigenvalue problem:

$$\eta^* = \min_{\eta, P} \quad \eta \quad \text{subject to } (4.49), (4.50). \tag{4.51}$$

Remark 20. *Given the relations* $\eta = \frac{1-2\overline{\varepsilon}}{2\overline{\varepsilon}} \in (0, +\infty)$*, since* $\overline{\varepsilon} \in (0, \frac{1}{2})$*, and* $\overline{\varepsilon} = \frac{1}{2(1+\eta)}$*, we have that maximizing* $\overline{\varepsilon}$ *is equivalent to minimizing* η*. Thus, the best selection for* η *is the solution of the optimization problem in* (4.51)*.*

Theorem 4.2.2. *For any plant-controller interconnection* (4.40)-(4.41) *such that* $A + BK$ *is Hurwitz, pick any* α *in* (4.49) *smaller than or equal to the spectral abscissa of* $A+BK$*, and select* η^* *as in* (4.51) *and* $\varepsilon^* = (2(1+\eta^*))^{-1}$*. For any* $\overline{\varepsilon} \in (0, \varepsilon^*)$*, hybrid system* (4.44), (4.45), (4.46), (4.48) *solves Problem 4.2.1.*

Remark 21. *Following the steps of [110, Theorem 2] it is possible to prove uniform global exponential stability in the t-direction for* (4.44), (4.45), (4.46), (4.48)*, thus showing a guaranteed t-exponential decrease induced by the redesign law.*

Remark 22. *As illustrated in Figure 4.5, the proposed hybrid redesign* (4.44), (4.45), (4.46), (4.48) *ensures that the input u never enters the interval* $(1 - \frac{\overline{\varepsilon}}{1+2\overline{\varepsilon}}, 1 + \frac{\overline{\varepsilon}}{1-2\overline{\varepsilon}})$*. Therefore, item (ii) of Problem 4.2.1 can be generalized to the avoidance of a sufficiently small bounded interval around the value* 1*.*

The following corollary gives an alternative way to compute a suitable matrix P for the tuning of $\overline{\varepsilon}$, which is more conservative than the solution of (4.51) but can be used when the minimization problem is too computationally expensive.

Corollary 4.2.3. *Consider an arbitrary plant-controller interconnection* (4.40)-(4.41) *such that* $A + BK$ *is Hurwitz. Given the matrix* $P = P^\top > 0$ *resulting from solving the Lyapunov equation* $He(P(A+BK)) = -I$*, select* $\eta^* = 2\lambda_M(PBK + (PBK)^\top)$ *and* $\varepsilon^* = (2(1+\eta^*))^{-1}$*. Then, the hybrid system* (4.44), (4.45), (4.46), (4.48) *solves Problem 4.2.1 for any* $\overline{\varepsilon} \in (0, \varepsilon^*)$*.*

Under mild controllability conditions, the next corollary shows that using linear quadratic control to tune the gain matrix K guarantees that the hybrid system (4.44), (4.45), (4.46), (4.48) solves Problem 4.2.1 for any $\overline{\varepsilon}$ in the admissible range.

Corollary 4.2.4. *Given any* $R = R^\top > 0$ *and* $Q = Q^\top \geq 0$ *and assuming* (A, B) *stabilizable and* $(A, Q^{1/2})$ *detectable, when selecting* $K = -R^{-1}B^\top P$ *with* $P = P^\top > 0$ *being the unique solution to the algebraic Riccati equation* $He(PA) + Q - PBR^{-1}B^\top P = 0$*, then the hybrid system* (4.44), (4.45), (4.46), (4.48) *solves Problem 4.2.1 for any* $\overline{\varepsilon} \in (0, \frac{1}{2})$.

The proof follows immediately by noting that linear quadratic control guarantees a gain margin in the range $[-6\text{dB}, +\infty)$, which implies that the corresponding closed-loop system is uniformly robustly GAS for any $\overline{\varepsilon} \in (0, \frac{1}{2})$ such that $\frac{1+2\overline{\varepsilon}}{1-2\overline{\varepsilon}} \geq \frac{1}{2}$, which holds $\forall \overline{\varepsilon} \in (0, \frac{1}{2})$.

Remark 23. *The control scheme in Figure 4.4 can be interpreted as a feedback interconnection of an open loop plant with input* u *and output* u_n *connected to a memoryless time-varying gain in the sector* $[1, \frac{1+2\overline{\varepsilon}}{1-2\overline{\varepsilon}}]$*. Input-Output stability arguments based on the circle criterion can then be exploited to develop generalized dynamical output feedback schemes.*

To rule out rapid repeated jumps, we also prove *uniform semiglobal dwell-time*, namely for each $r > 0$ there exists $\tau > 0$ such that, for any solution z satisfying $|z(0,0)| \leq r$, $t_{j+1} - t_j \geq \tau$ for all consecutive jump times t_j, t_{j+1} with $j \geq 1$, and $(t, j) \in \text{dom } z$.

Proposition 4.2.5. *System* (4.44), (4.45), (4.46), (4.48) *enjoys a uniform semiglobal dwell-time property.*

4.2.3 LINEAR EXAMPLE STUDY

Consider the linearized vertical dynamics of a quadrotor UAV with mass m

$$\dot{z} = v, \quad m\dot{v} = mg - T_c + d \tag{4.52}$$

for which we consider the goal of asymptotically stabilizing a desired altitude setpoint z_d in the presence of an unknown constant disturbance d and with the input constraint $T_c \neq 0$, which is needed in hierarchical control strategies to avoid singularity conditions [103]. Hierarchical control strategies for quadcopters achieve asymptotic tracking of a reference position trajectory by ensuring that the total thrust vector generated by the propellers converges to a desired thrust vector. This is implemented by matching the norm of the desired thrust vector with the thrust force generated by the propellers, and by steering the orientation of the quadcopter so that the thrust axes of the propellers are aligned to the direction of the desired thrust vector. Since

propellers can usually spin in one direction only, the control architecture should guarantee that the thrust force required from the propellers never crosses the zero value (so that it is always either positive, as is the case in [103, Equation (5)], or negative, depending on the convention used for the z direction). In this simplified example, $|T_c|$ can be interpreted as the thrust generated by the propellers, while the sign of T_c can be interpreted as the direction of the desired thrust vector. A jump of T_c from a positive to negative value, or vice versa, can therefore be interpreted as an instantaneous change in the direction of the desired thrust vector, from pointing upwards to downwards, or vice versa. Since the jump logic ensures $|T_c| > 0$ along all solutions, the thrust generated by the propellers is guaranteed to remain positive. The transient needed to steer the quadcopter attitude, so that the thrust axes of the propellers are aligned to the direction of the desired thrust vector after a jump, is not accounted for in this simplified example.
To solve this task, select $T_c = mg(1-u)$, where u is the output of the following PID control law with feedforward gravity compensation

$$\begin{aligned} \dot{x}_i &= e, \quad \dot{x}_d = -\tfrac{1}{\tau_d}(x_d + e) \\ u &= -\overline{k}_p e - \overline{k}_d x_d - k_i x_i \end{aligned} \tag{4.53}$$

In (4.53) $e := z - z_d$ represents the stabilization error and $\overline{k}_p = k_p + \overline{k}_d$ and $\overline{k}_d = \frac{k_d}{\tau_d}$. Defining $x_p := [e\ v]^\top$, $x_c := [x_i - \frac{d}{mgk_i}\ x_d]^\top$, the closed-loop error system associated with (4.52)-(4.53) has the same form as (4.43) with $A_p = \left[\begin{smallmatrix} 0 & 1 \\ 0 & 0 \end{smallmatrix}\right]$, $B_p = [0\ g]^\top$, $C_p = [1\ 0]$ and $D_c = -\overline{k}_p$, with the constraint $u \neq 1$. We consider a quadcopter with mass $m = 0.5$ kg that has to reach a desired altitude of $z_d = -0.1$ m and is subject to a constant disturbance force $d = -2.8$ N (which pushes the drone upwards against the gravity). Assigning the gains $k_p = 1.05$, $k_d = 0.75$ and $k_i = 0.45$ and the time constant as $\tau_d = \frac{k_d}{10k_p}$, we get the successful simulation results in Figure 4.6. To tune the value of $\overline{\varepsilon}$ we used the approach of Theorem 4.2.2, which results in $\overline{\varepsilon} = 0.0439$.

4.2.4 PROOFS

We begin with some preliminary results. The following Lemma, which will be used in the proofs of Theorem 4.2.2 and Proposition 4.2.5, ensures that after a jump from $\mathcal{D}$ solutions can not immediately jump again but must first flow.

Lemma 4.2.6. *Across jumps of* (4.45)-(4.48) *we have* $\phi(u^+, q^+) - \phi(u, q) \leq -2\overline{\varepsilon}$.

Proof. Assume $z \in \mathcal{D}$, which implies $\phi(u, q) \geq 0$. From (4.46) we have $\phi(u, q) = (q + 2\overline{\varepsilon})u - q - \overline{\varepsilon} \geq 0$, namely

$$q + \overline{\varepsilon} \leq (q + 2\overline{\varepsilon})u. \tag{4.54}$$

Substituting (4.54) in the expression of $\phi(u^+, q^+)$ gives

$$\begin{aligned}\phi(u^+, q^+) &= (-q + 2\bar{\varepsilon})u^+ + q - \bar{\varepsilon} = (-q + 2\bar{\varepsilon})u^+ + q - 2\bar{\varepsilon} + \bar{\varepsilon} \\ &\leq (-q + 2\bar{\varepsilon})u^+ + (q + 2\bar{\varepsilon})u - 2\bar{\varepsilon} \\ &= (-q + 2\bar{\varepsilon})\frac{1 + 2q\bar{\varepsilon}}{1 - 2\bar{\varepsilon}}u_n + (q + 2\bar{\varepsilon})\frac{1 - 2q\bar{\varepsilon}}{1 - 2\bar{\varepsilon}}u_n - 2\bar{\varepsilon} \\ &= -2\bar{\varepsilon},\end{aligned}$$

which concludes the proof. □

Let us now proceed with the proof of Theorem 4.2.2.
Proof of Theorem 4.2.2. To show RUGAS in item (i) of Problem 4.2.1, accounting for the new logical state q, we prove global asymptotic stability of the compact set $\mathcal{A}_0 = \{0\} \times \{1\}$ for the hybrid system (4.44), (4.45), (4.46), (4.48), and invoke Theorem 2.3.9 to conclude uniformity and robustness.
Consider the output signal defined in (4.44). For $q = 1$, the control law returns the nominal state feedback $u = Kx$. Since η^* is selected according to (4.51), then the closed-loop flow dynamics $\dot{x} = (A + BK)x$ satisfies (4.49), (4.50) for a suitable $\alpha > 0$ and $P = P^\top > 0$. Consider now $q = -1$. The

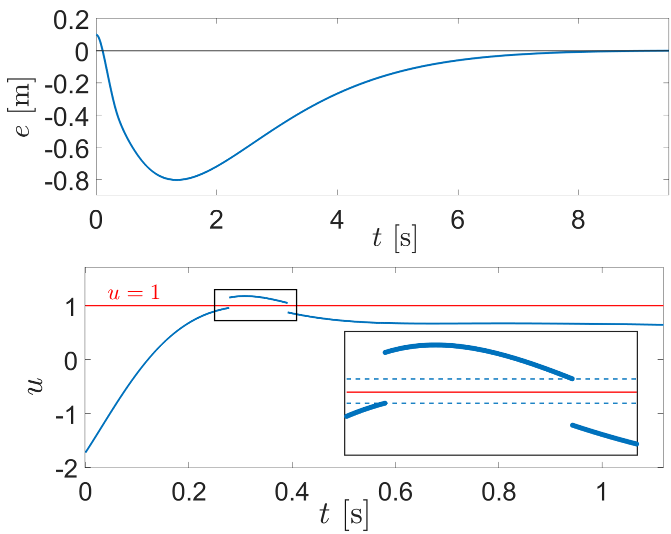

Figure 4.6: Closed-loop solution of (4.52)-(4.53). Altitude error time evolution (Top). PID output with zoom around $u = 1$, showing the boundary of $\mathcal{D}$ with dashed lines (Bottom).

control law (4.44) reads

$$u = \frac{1+2\overline{\varepsilon}}{1-2\overline{\varepsilon}}Kx = \frac{1-2\overline{\varepsilon}+4\overline{\varepsilon}}{1-2\overline{\varepsilon}}Kx = Kx + \frac{4\overline{\varepsilon}}{1-2\overline{\varepsilon}}Kx, \tag{4.55}$$

and the resulting closed-loop flow dynamics reads

$$\dot{x} = \Big(A + BK + \frac{4\overline{\varepsilon}}{1-2\overline{\varepsilon}}BK\Big)x. \tag{4.56}$$

Given $P = P^\top > 0$ and η^* solving (4.51), consider an arbitrary $\overline{\varepsilon} \in (0, \varepsilon^*)$ and define $\eta = \frac{1-2\overline{\varepsilon}}{2\overline{\varepsilon}}$. For dynamics (4.56) we obtain, using the bounds (4.49), (4.50)

$$\begin{aligned}
&\mathrm{He}(P(A + BK + \frac{4\overline{\varepsilon}}{1-2\overline{\varepsilon}}BK)) \\
&= \mathrm{He}(P(A+BK)) + \frac{2}{\eta}\mathrm{He}(PBK) \\
&\leq \mathrm{He}(P(A+BK)) + \frac{2}{\eta}\eta^*\alpha P \\
&\leq -2\alpha P + 2\frac{\eta^*}{\eta}\alpha P = 2\alpha P(\frac{\eta^*}{\eta} - 1) < 0
\end{aligned} \tag{4.57}$$

where we use the fact that, for $\overline{\varepsilon} \in (0, \varepsilon^*)$, we have $\eta^* = \frac{1-2\varepsilon^*}{2\varepsilon^*} < \frac{1-2\overline{\varepsilon}}{2\overline{\varepsilon}} = \eta$, which implies $\frac{\eta^*}{\eta} < 1$. Thus, we have that P defines a common quadratic Lyapunov function for the nominal and modified closed-loop dynamics.
Consider now the candidate Lyapunov function $V = \frac{1}{2}x^\top Px$, which is positive definite with respect to $\mathcal{A} = \mathcal{A}_0 \cup \mathcal{A}_1 = \{x = 0, q = 1\} \cup \{x = 0, q = -1\}$. Due to (4.49) and (4.57), via (4.56) we have that the Lyapunov function decreases when the solution flows, i.e., $\dot{V}(z) < 0,\ \forall z \in \mathcal{C} \setminus \mathcal{A}$. It is immediate to see from (4.48) that V is also constant across jumps, since $x^+ = x$. This implies uniform global stability of $\mathcal{A}$ according to Theorem 2.4.3, and, in particular, that all solutions are bounded. Lemma 4.2.6 shows that $G(\mathcal{D}) \cap \mathcal{D} = \emptyset$, since after a jump from $\mathcal{D}$ solutions must flow. Then, since (4.44), (4.45), (4.46), (4.48) satisfies the Hybrid Basic Conditions in Definition 2.2.1, by applying Theorem 2.2.6 we can conclude that all solutions have a non-zero dwell-time. The Invariance Principle for hybrid dynamical systems, stated in Corollary 2.4.6, let us then conclude convergence of all complete solutions to $\mathcal{A}$. Uniform global pre-asymptotic stability of $\mathcal{A}$ then follows from stability, boundedness of all solutions, and convergence of all complete solutions to $\mathcal{A}$, according to Definition 2.3.3 and Theorem 2.3.9. Completeness of solutions follows from Theorem 2.2.5, since $G(\mathcal{D}) \subset \mathcal{C}$ and all points $x \in \mathcal{C} \setminus \mathcal{D}$ are in the interior of $\mathcal{C}$, and therefore condition (2.2) holds trivially.
Since $\mathcal{A}$ is the union of the two points $\mathcal{A}_0, \mathcal{A}_1$, then solutions either converge to $\mathcal{A}_0$ or to $\mathcal{A}_1$. Assume now that there exists a solution $z(t, j)$ that asymptotically converges to $\mathcal{A}_1$. Uniform global attractivity of $\mathcal{A}$ implies that for any

$\delta > 0$ there exist $T > 0$ such that $|z(t,j)|_{\mathcal{A}_1} \leq \delta$, $\forall (t,j) \in \operatorname{dom} z$ s.t. $t+j \geq T$. Pick a small enough δ such that $|z|_{\mathcal{A}_1} \leq \delta$ implies $|u| \leq \left|\frac{1+2\bar{\varepsilon}}{1-2\bar{\varepsilon}} Kx\right| < 1 - \frac{\bar{\varepsilon}}{1+2\bar{\varepsilon}}$. Such a δ always exists since $u = \frac{1-2q\bar{\varepsilon}}{1-2\bar{\varepsilon}} Kx = 0$ for $x = 0$ and $|x| \leq |z|_{\mathcal{A}_1}$. Then, $|u| < 1 - \frac{\bar{\varepsilon}}{1+2\bar{\varepsilon}}$ $\forall (t,j) \in \operatorname{dom} z$ such that $t+j \geq T$. From the expression of $\mathcal{D}$ in (4.47) it follows that the solution must, at some point, jump to $q^+ = 1$ and can never jump again, which means that no solution can asymptotically converge to $\{x = 0, q = -1\}$. This, together with the fact that solutions from $\mathcal{A}_1 = \{x = 0, q = -1\} \in \mathcal{D}$ jump to $\mathcal{A}_0$, proves global attractivity of $\mathcal{A}_0$. Lyapunov stability of $\mathcal{A}_0$ follows from Lyapunov stability of $\mathcal{A}$ and the fact that $\mathcal{A}_0, \mathcal{A}_1$ are two disjoint points. Finally, robust uniform global asymptotic stability of $\mathcal{A}_0$ follows from global attractivity and Lyapunov stability of $\mathcal{A}_0$ and the fact that system (4.48) satisfies the Hybrid Basic Conditions in Definition 2.2.1, which allows using Theorem 2.3.9.

Let us now continue with the proof that item (ii) of Problem 4.2.1 is also satisfied. Consider a generic solution $(t,j) \to z(t,j)$ to system (4.48) and assume that $z(0,0)$ is such that $u(0,0) \neq 1$. Observe from the definition of $\mathcal{C}$ that the solution can only flow for $\phi(u,q) \leq 0$. This implies that $z(t,j)$ can not flow with the value $u = 1$ while $z \in \mathcal{C}$, due to the definition of $\mathcal{D}$ in (4.47). What is left to check is that, after a jump of z, u is guaranteed to be not unitary. With a slight abuse of notation, we will express the jump in the control law generated by the jump map as $u^+ = \frac{1+2q^+\bar{\varepsilon}}{1-2q^+\bar{\varepsilon}} u$. For $q = 1$ we have $u^+ = \frac{1+2\bar{\varepsilon}}{1-2\bar{\varepsilon}} u \geq \frac{1+2\bar{\varepsilon}}{1-2\bar{\varepsilon}}(1 - \frac{\bar{\varepsilon}}{1+2\bar{\varepsilon}}) = \frac{1+\bar{\varepsilon}}{1-2\bar{\varepsilon}} > 1$. For $q = -1$ instead we have $u^+ = \frac{1-2\bar{\varepsilon}}{1+2\bar{\varepsilon}} u \leq \frac{1-2\bar{\varepsilon}}{1+2\bar{\varepsilon}}(1 + \frac{\bar{\varepsilon}}{1-2\bar{\varepsilon}}) = \frac{1-\bar{\varepsilon}}{1+2\bar{\varepsilon}} < 1$. Thus, u is guaranteed not to land on the value $u = 1$ after a jump from $\mathcal{D}$.

To prove item (iii) of Problem 4.2.1, it is enough to show that the controller never switches to $q = -1$ when $u = 0$. Substituting $u = 0, q = 1$ in (4.47) and recalling that $\bar{\varepsilon} > 0$ gives $0 \geq 1 - \frac{\bar{\varepsilon}}{1+2\bar{\varepsilon}} \Leftrightarrow \bar{\varepsilon} \geq 1 + 2\bar{\varepsilon}$, which is never true for $\bar{\varepsilon} \in (0, \frac{1}{2})$, thus leading to a contradiction. Then, the hybrid controller never switches to the modified control law in a neighborhood of the origin. Additionally, the jump dynamics only depends on the knowledge of u and q, and does not require knowledge of the plant state, which proves item (iv) of Problem 4.2.1. □

Proof of Corollary 4.2.3. Select $P = P^\top > 0$ satisfying the Lyapunov equation $\operatorname{He}(P(A+BK)) = -I$ and $\eta > 2\lambda_M(PBK + (PBK)^\top)$. The same steps as those in the proof of Theorem 4.2.2 can be followed, with (4.57) replaced by

$$\begin{aligned}
&\operatorname{He}(P(A+BK)) + \frac{4\bar{\varepsilon}}{1-2\bar{\varepsilon}} \operatorname{He}(PBK) \\
&= -I + \frac{2}{\eta} \operatorname{He}(PBK) < -I + \frac{1}{\lambda_M(\operatorname{He}(PBK))} \operatorname{He}(PBK),
\end{aligned}$$

where the last term is negative semi-definite. Following the proof of Theorem 4.2.2, the four items of Problem 4.2.1 follow. $\square$

We now prove a uniform dwell-time result, which is of independent interest and is only based on a *Uniform Global Boundedness* (UGB) assumption (also known as *Lagrange stability*), namely for each $r > 0$, $\exists M_r > 0$ such that all solutions z with $|z(0,0)| \leq r$ satisfy $|z(t,j)| \leq M_r$ for all $(t,j) \in \mathrm{d}omz$. Its proof is inspired by [124, §2].

Lemma 4.2.7. *For a well-posed hybrid system with hybrid data $(F, G, \mathcal{C}, \mathcal{D})$, if $\mathcal{D} \cap G(\mathcal{D}) = \emptyset$ and solutions are uniformly globally bounded, then solutions enjoy a uniform semiglobal dwell-time property.*

Proof. Due to UBG, all solutions satisfying $|\phi(0,0)| \leq r$ are uniformly bounded. Then, applying Theorem 2.2.6, we obtain that each solution enjoys a non-zero dwell-time. From the stated assumptions, to prove uniformity we proceed by contradiction. Suppose that for some $r > 0$ there exist solutions ϕ_k, $k \in \mathbb{N}$ and indices $i_k \geq 1$ with jump times t_{i_k} and t_{i_k+1} satisfying $t_{i_k+1} - t_{i_k} = \tau_k$ and $\tau_k \to 0$ as $k \to \infty$. Similar to [124, Lemma 1], define shifted solutions $\overline{\phi}_k$ as $\overline{\phi}_k(t,j) = \phi_k(t_{i_k-1} + t, i_k + j - 1)$ (namely, $\overline{\phi}_k$ is the tail of ϕ_k with the shrinking dwell-time between its jump times t_1 and t_2). Due to well-posedness [48, Def. 6.2] there exists a converging subsequence of $\overline{\phi}_k$ whose limit is a solution $\overline{\phi}_\infty$. By construction, the domain of $\overline{\phi}_\infty$ satisfies $t_2 - t_1 = \lim_{k\to\infty} \tau_k = 0$. However, this solution contradicts the dwell-time property established by Theorem 2.2.6. $\square$

Proof of Proposition 4.2.5. First observe that system (4.44), (4.45), (4.46), (4.48) satisfies the Hybrid Basic Conditions in Definition 2.2.1 and due to [48, Theorem 6.8] it is well-posed. Moreover, the UGS property proven in Theorem 4.2.2 implies uniform global boundedness, and $\mathcal{D} \cap G(\mathcal{D}) = \emptyset$ follows from Lemma 4.2.6. Then the result follows from Lemma 4.2.7. $\square$

4.2.5 NONLINEAR REDESIGNED CONTROLLER ARCHITECTURE

We now extend the proposed hybrid architecture to a class of input-affine nonlinear systems

$$\dot{x} = f(x) + g(x)u, \tag{4.58}$$

where $x \in \mathbb{R}^n$ is the state and $u \in \mathbb{R}$ is the control input. For a compact set $\mathcal{A} \subset \mathbb{R}^n$, assume that f and g are continuous functions of x and that there exists a continuous selection $u = u_n(x)$ and a Lyapunov function candidate

V on $\mathbb{R}^n$ with respect to $\mathcal{A}$ for the closed-loop system, such that, for the closed-loop system $\dot{x} = f(x) + g(x)u_n(x)$, it holds that

$$\begin{aligned} \dot{V}(x) &= \nabla V(x)^\top f(x) + \nabla V(x)^\top g(x)u_n(x) \\ &=: -\psi(x) < 0, \quad \forall x \in \mathbb{R}^n \setminus \mathcal{A}. \end{aligned} \tag{4.59}$$

Paralleling the reasoning in Figure 4.5, assume the following.

Assumption 4.2.8. *There exists $\overline{\varepsilon} \in (0, \frac{1}{2}]$ such that $u_n(x) < 1 - \frac{\overline{\varepsilon}}{1+2\overline{\varepsilon}}$ for all $x \in \mathcal{A}$.*

Following the redesign presented for the linear case, we introduce a logic state $q \in \{-1, 1\}$ and define the full state $z = (x, q) \in \mathbb{R}^n \times \{-1, 1\}$ and a modified control law

$$u = \frac{1 - 2q\varepsilon(x)}{1 - 2\varepsilon(x)} u_n(x), \tag{4.60}$$

where the constant $\overline{\varepsilon}$ used for the linear case in (4.44) is replaced by a globally bounded function $x \mapsto \varepsilon(x) : \mathbb{R}^n \to [0, \overline{\varepsilon})$, to be defined, satisfying $|\varepsilon(x)| < \overline{\varepsilon}$ for all $x \in \mathbb{R}^n$, where $\overline{\varepsilon}$ comes from Assumption 4.2.8. Mimicking the linear redesign, the flow set $\mathcal{C}$ and jump set $\mathcal{D}$ are induced by the function

$$\phi(x, q) = (q + 2\varepsilon(x))u - q - \varepsilon(x), \tag{4.61}$$

as in (4.45), (4.46). The redesigned system is given by (4.60) with

$$\begin{aligned} \dot{z} = & \begin{bmatrix} \dot{x} \\ \dot{q} \end{bmatrix} = \begin{bmatrix} f(x) + g(x)u \\ 0 \end{bmatrix}, \quad && z \in \mathcal{C} \\ z^+ = & \begin{bmatrix} x^+ \\ q^+ \end{bmatrix} = \begin{bmatrix} x \\ -q \end{bmatrix}, && z \in \mathcal{D}, \end{aligned} \tag{4.62}$$

where the function $x \mapsto \varepsilon(x)$ is selected as

$$\varepsilon(x) = \mu\overline{\varepsilon} \frac{\psi(x)}{2|\nabla V(x)^\top g(x)u_n(x)| + \psi(x)}, \tag{4.63}$$

and $\mu \in (0, 1)$ is a parameter determining the trade-off between avoidance robustness and preservation of the nominal controller. Observe that (4.63) implies $0 \leq \varepsilon(x) < \overline{\varepsilon} \leq \frac{1}{2}$, and that continuous differentiability of V and continuity of f and g imply that ε is a continuous function of x.
The following theorem is a nonlinear extension of the linear results in Theorem 4.2.2 and Proposition 4.2.5.

Theorem 4.2.9. *Under Assumption 4.2.8, the set $\mathcal{A} \times \{1\}$ is robustly uniformly globally asymptotically stable for* (4.46), (4.60)–(4.63). *Additionally, system* (4.46), (4.60)–(4.63) *satisfies items (ii) and (iii) of Problem 4.2.1 and enjoys uniform semiglobal dwell-time.*

4.2.6 NONLINEAR EXAMPLE STUDY

Consider the plant from [123, Section 3.3]

$$\begin{bmatrix} \dot{x}_1 \\ \dot{x}_2 \end{bmatrix} = f(x) + g(x)u = \begin{bmatrix} x_2 + x_1^2 \\ x_1^2 \end{bmatrix} + \begin{bmatrix} 0 \\ 1 \end{bmatrix} u, \tag{4.64}$$

where $x = [x_1 \; x_2]^\top \in \mathbb{R}^2$ is the state and $u \in \mathbb{R}$ is the control input. For the selection

$$u = u_n = -2x_1 - 2x_2 - 3x_1^2 - 2x_1(x_2 + x_1^2), \tag{4.65}$$

it is shown in [123] that $V(x) = \frac{1}{2}x_1^2 + \frac{1}{2}(x_2 + x_1 + x_1^2)^2$ is a strong Lyapunov function with respect to the origin, as its negative definite time derivative is

$$\dot{V}(x) = -x_1^4 - 2x_1^3 - 2x_1^2 x_2 - 2x_1^2 - 2x_1 x_2 - x_2^2 =: -\psi(x).$$

Since (4.65) is zero at the origin, we may select $\overline{\varepsilon} = \frac{1}{2}$ for (4.64). Additionally, it is immediate to verify that $\nabla V(x)^\top g(x) = x_2 + x_1 + x_1^2$.
Applying the redesign to (4.64), Theorem 4.2.9 holds. Choosing $\mu = 0.1$ and initial conditions $x_1(0) = -0.5$, $x_2(0) = -3$ leads to the desirable simulations shown in Figure 4.7.

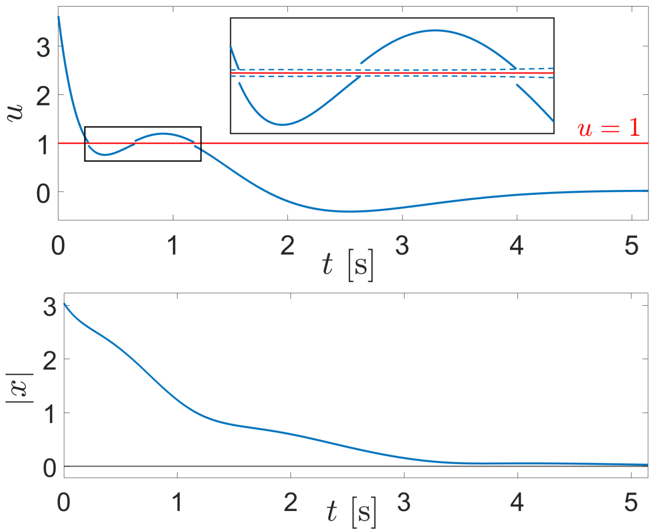

Figure 4.7: Closed-loop solution of the hybrid redesigned feedback (4.46), (4.60), (4.61), (4.62), (4.63) applied to (4.64),(4.65).

4.2.7 PROOF OF THEOREM 4.2.9

We first show that the modified input (4.60), (4.63) ensures Lyapunov decrease along solutions when they flow.

Lemma 4.2.10. *Given plant* (4.58)*, a stabilizer u_n and a function V satisfying* (4.59)*, along the solutions of the hybrid system* (4.46), (4.60), (4.61), (4.62), (4.63) *it holds that $\dot{V}(z) < 0$, $\forall z \in \mathcal{C} \setminus (\mathcal{A} \times \{-1, 1\})$.*

Proof. For $q = 1$, and any $z = (x, q)$ with $x \notin \mathcal{A}$, we have $u = u_n(x)$ and (4.59) implies $\dot{V}(z) = -\psi(x) < 0$. For the non-trivial case $q = -1$, and $z = (x, q)$ with $x \notin \mathcal{A}$, first note that $\mu < 1$ and $\overline{\varepsilon} \leq \frac{1}{2}$, together with (4.63) and the fact that $\mu\overline{\varepsilon} < \frac{1}{2}$, imply that $4\varepsilon(x)|V(x)^\top g(x)u_n(x)| < \psi(x) - 2\varepsilon(x)\psi(x)$, which can be rearranged to get

$$\frac{4\varepsilon(x)}{1 - 2\varepsilon(x)}|\nabla V(x)^\top g(x)u_n(x)| < \psi(x).$$

Then, proceeding as in (4.55), we obtain

$$\begin{aligned}\dot{V}(z) &= \nabla V(x)^\top f(x) + \nabla V(x)^\top g(x)u = \nabla V(x)^\top f(x)\\ &+ \nabla V(x)^\top g(x)u_n(x) + \frac{4\varepsilon(x)}{1 - 2\varepsilon(x)}\nabla V(x)^\top g(x)u_n(x)\\ &= -\psi(x) + \frac{4\varepsilon(x)}{1 - 2\varepsilon(x)}\nabla V(x)^\top g(x)u_n(x) < 0,\end{aligned}$$

as to be proven. □

The following Lemma ensures that after a jump the solution must flow, unless it jumps from $\mathcal{A} \times \{-1\}$. Its proof is the same as the one presented for Lemma 4.2.6, therefore it is omitted.

Lemma 4.2.11. *Let z be a solution of* (4.46), (4.60), (4.61), (4.62), (4.63)*. Then, $\phi(x^+, q^+) - \phi(x, q) \leq -2\varepsilon(x) < 0$ for all $z \in \mathcal{D}$.*

Proof of Theorem 4.2.9. Mimicking the proof of Theorem 4.2.2, we start by showing that $\mathcal{A} \times \{-1, 1\}$ is uniformly globally asymptotically stable for (4.46), (4.60), (4.61), (4.62), (4.63). For $z \in \mathcal{C}$, Lemma 4.2.10 guarantees the decrease of V.
Consider now $z \in \mathcal{D}$. Since the jump map in (4.62) toggles the value of q and V only depends on x, we have that the Lyapunov function remains constant across jumps. Then, uniform global stability of the set $\mathcal{A}$ follows from Theorem 2.4.3, so that all solutions are bounded. Additionally, Lemma 4.2.11 ensures that after a jump the solution must flow, so that, by applying Theorem 2.2.6, we have that all solutions have a non-zero dwell-time. Since the Hybrid Basic Conditions hold, then uniform global asymptotic stability

of $\mathcal{A} \times \{-1, 1\}$ follows from the Invariance Principle for hybrid dynamical systems stated in Corollary 2.4.6 and Theorem 2.3.9. Following the remaining steps of the proof of Theorem 4.2.2 we may prove robust uniform global asymptotic stability of $\mathcal{A} \times \{1\}$ and completeness of all maximal solutions.
Items (ii) and (iii) of Problem 4.2.1 can be proven exploiting at the structure of $\mathcal{C}$ and $\mathcal{D}$. Substituting $\varepsilon = \varepsilon(x)$ into (4.47) and using the fact that $\varepsilon(x)$ is a continuous function of x, only zero for $x \in \mathcal{A}$, we conclude that there exists a neighborhood of $\mathcal{A} \times \{1\}$ where the nominal controller is preserved. Furthermore, $u = 1$ being in the interior of $\mathcal{D}$ implies that solutions never flow with $u = 1$. Finally, $u^+ \neq 1$ can be proven by following the bounds on u^+ derived at the end of Theorem 4.2.2 with $\overline{\varepsilon}$ replaced by $\varepsilon(x)$.
The semiglobal dwell-time property can be proven by following exactly the same steps as those in the proof of Proposition 4.2.5, by exploiting Lemma 4.2.7. $\square$

CHAPTER 5

CONCLUSIONS AND FUTURE WORK

5.1 CONCLUSIONS

This thesis focused on two main problems: achieving stabilization of planar unmanned vehicles using only relative measurements of position and pose, coming from on-board sensors, and endowing it with specific avoidance properties, either in the state-space, in terms of point-obstacles avoidance, or in the input-space, in terms of avoidance of an unwanted input value.
Chapter 2 presented the framework of hybrid dynamical systems, which proved to be an effective tool for addressing the problems outlined above. Within this framework, we proposed hybrid control architectures capable of overcoming known topological obstructions, thanks to their ability to generate discontinuous control actions, while ensuring robustness of the resulting stability properties.
In Chapter 3 we discussed how measurements from on-board sensors can be modelled using a properly defined set of polar coordinates. We emphasized that, due to the limited sensing capabilities of low-cost devices, multiple sensors are generally required to achieve global stabilization for an unmanned vehicle. In particular, we considered robots equipped with two cameras, one facing forward and one facing backward, providing relative measurements of the robot pose as long as the target is inside their respective fields of view. Focusing on ground wheeled robots whose dynamics can be approximated by the unicycle kinematic model, Section 3.2 proposed two Lyapunov-based stabilizers for the front and rear camera, stabilizing the robot's position and pose in the polar coordinates, which we then hybridly combined to achieve global results and completeness of solutions. We characterized robustness,

as seen in the polar coordinates, in terms of measurement errors, external perturbations, and uncertainties affecting the camera switch and the reset of the robot orientation. Furthermore, we clarified how properties in the polar coordinates translate to the Cartesian coordinates: although convergence of the robot pose to the origin is preserved when moving from one set of coordinates to the other, no stability-like bound holds in the Cartesian coordinates. Moreover, convergence in the Cartesian coordinates is robust to small external perturbations. In Section 3.3 we introduced a kinematic model approximating the dynamics equations of a hovercraft model, for which the control inputs are defined as the forward and angular velocities. Under the assumption of slow-varying velocities, the control architecture developed for the unicycle model naturally extends to this new setting. We proposed a control law stabilizing the hovercraft position using the measurements coming from two cameras, and discussed an extension to the full dynamic model, where the overall force and torque generated by the actuators are used to exponentially track a reference profile for the forward and angular velocities, defined as the stabilizing input of the kinematic model. While no formal guarantees are provided for the full dynamic model, numerical simulations suggest that the kinematic model can be used as a valid approximation.
Chapter 4 addressed the problem of augmenting a given stabilizer with avoidance properties. The key idea underlying the proposed approach is to preserve the decrease of a given Lyapunov function, ensured by a nominal feedback selection, while performing avoidance, thus preserving the stabilization task. Section 4.1 focused on the avoidance of point-obstacles in the state space for input-affine nonlinear systems. Our solution exploited a degree of freedom in the selection of the control input that, under a mild controllability assumption, allows reshaping trajectories without affecting the decrease of the Lyapunov function. This is achieved by adding an avoidance term to the nominal input, generating a velocity component orthogonal to the gradient of the Lyapunov function, and hence not affecting the decrease of the Lyapunov function. In this sense, stabilization and avoidance can be viewed as independent tasks in our approach. We made use of a hybrid architecture, previously proposed for continuous-time linear systems, which uses a suitably defined avoidance shell to orchestrate the switch between nominal feedback and modified input. Following this approach we proved that an arbitrary number of point-obstacles, arbitrarily placed in the state space, can be avoided. Section 4.2, instead, focused on the problem of achieving stabilization while avoiding an unwanted value of the input. For the class of single-input linear continuous-time systems, we showed that it is always possible to rescale a nominal input, stabilizing the origin, while preserving decrease of a given Lyapunov function. We then proposed a simple hybrid architecture to switch between the nominal input and its rescaled version, achieving avoidance of an unwanted value of the input. A characterization of the admissible rescaling factor was given via a LMI-based

optimization problem. A more conservative, but computationally cheaper, estimate can be achieved by solving a Lyapunov matrix equation. Finally, we extended the proposed control architecture to the class of single-input control-affine nonlinear systems.

5.2 FUTURE WORK

The extension of the hybrid control architecture developed for mobile ground robots in Section 3.2 to the kinematic model of the hovercraft, as presented in Section 3.3, suggests that this control design can likely be generalized to other unmanned vehicles. However, several aspects specific to the hovercraft were not addressed in Section 3.3. First, the proposed control law stabilizes only the position, but not the orientation. Deriving a stabilizer for the full pose is then the next natural step. Secondly, unlike the study carried out in Section 3.2 for mobile ground robots, we have not yet provided a detailed analysis of the behavior of the hovercraft, driven by the camera-based stabilizers, in the Cartesian coordinates. In particular, it remains to be seen whether robustness results similar to those obtained for the unicycle model also hold for the hovercraft model. Third, while the heuristic extension of the control strategy to the full dynamic model, based on the idea of tracking the reference inputs of the kinematic model, seems to perform reasonably well in numerical simulations, establishing theoretical guarantees for the full model should be the focus of future works. Lastly, it would be valuable to quantitatively characterize the conditions under which the proposed kinematic model is a good approximation of the full dynamic model, and to what degree. To properly extend the control architecture proposed in Section 3.2 to other types of unmanned vehicles, constraints on the direction of motion should also be accounted. Such constraints are relevant for some marine and air vehicles, for which only forward motion is possible. While this is not immediately compatible with the proposed control architecture, which relies on switching between forward and backward motion, via the use of front and rear cameras, an extension in this direction may be the subject of future works.

While the redesign we propose to achieve simultaneous stabilization and obstacle avoidance is quite general, in that it applies to input-affine nonlinear systems and arbitrarily placed obstacles, it also presents some noteworthy limitations. The first main limitation is that the size of the avoidance neighborhood is not a design parameter. This is a consequence of the fact that the orthogonality condition, involving the gradient of the Lyapunov function and the velocity component generated by the avoidance input, is enforced only at the center of the obstacle. Negative definiteness of the Lyapunov derivative is then preserved in a sufficiently small neighborhood of the center thanks to continuity of the dynamics and smoothness of the Lyapunov function.

Moreover, estimating the size of the admissible avoidance shell, for which the avoidance controller is well-defined and the decrease of the Lyapunov function is preserved during the avoidance maneuver, requires solving the nonlinear, non-convex, optimization problems defined in Sections 4.1.1 & 4.1.3. In particular, on-line estimation of the size of the avoidance shell, for possibly moving obstacles, would come at significant computational cost. In the proposed construction the direction of the avoidance input remains constant during the avoidance maneuver and depends only on the obstacle position. Allowing the direction of the avoidance input to change along solutions, as a function of the state, so that the orthogonality condition is always satisfied during the avoidance maneuver, could potentially allow to arbitrarily enlarge the avoidance shell, since the nominal decrease of the Lyapunov function would be preserved, removing the need to estimate the admissible size of the avoidance shell. However, this would also lead to a non-fixed avoidance shell, as its orientation would change with the direction of the avoidance input, therefore increasing the complexity of all the related computations and making it more difficult to ensure that the avoidance input is always well-defined. The second main limitation is that the proposed redesign is directly applicable only when obstacles are modeled as bounded neighborhoods of some points in the state space. One possible generalization would be to introduce an output in the system model and define obstacles as points in the output space. This approach could be suited, for example, to achieve position-only obstacle avoidance in autonomous navigation. Indeed, in the case of planar robots, obstacles are usually defined in terms of positions to be avoided, regardless of the orientation. Thus, obstacles are not points in the state space (position and orientation), but rather in the position space. Given a model of the robot dynamics, the avoidance condition can be formulated by introducing an output, similar to the Cartesian output introduced in Section 3.2.5, representing the position of the robot along trajectories, and requiring that such output never takes undesired values. An avoidance shell can then be defined in the output space, where the obstacle is a point, and the proposed avoidance construction may then be applied. What role the output map would play in this modified construction is to be determined. As a final observation, we point out that, while we made use of the hybrid architecture introduced in [91] to implement obstacle avoidance, the idea of generating velocities orthogonal to the gradient of a Lyapunov function to reshape trajectories is not inherently tied to this control architecture, nor to the obstacle avoidance problem, and could potentially be exploited in different applications.

When it comes to the input avoidance problem, the motivating examples, such as the control of a quadcopter UAV, involve multidimensional control inputs. Thus, extending the proposed redesign from single-input to multi-input systems is the next natural step. Depending on the specific application, particular attention may be required in defining the switching logic. For instance, in the case of quadcopter UAVs, hierarchical control strategies often use the force input to define a reference attitude to be tracked, so that the overall force generated by the propellers aligns with the desired force asked by the control law. This coupling between translational and rotational dynamics makes it nontrivial to characterize the effect that a discontinuity in the force input selection has on the overall dynamics of the system, and thus a careful analysis is required. In the context of single-input avoidance, it may be possible to extend the hybrid redesign architecture (4.44), (4.45), (4.46), (4.48) to the avoidance of a finite number of values for the inputs. The result stated in Theorem 4.2.2 provides an upper bound for the selection of the parameter ε, which, in turns, defines an upper bound to the scaling factor in (4.44), such that global asymptotic stability is preserved under the modified input for any value of the scaling factor smaller than this upper bound. Given a set of unwanted values, one way to achieve avoidance may be to use different scaling factors, such that their products is smaller than the admissible upper bound. Once the input reaches a suitably defined neighborhood of one unwanted value, avoidance may be achieved by rescaling the input by one of these scaling factors, in the same way as it is done in the current redesign architecture for the unit value. Multiple consecutive rescalings of the input, to avoid multiple unwanted values, would then be allowed, as the product of the scaling factors would be smaller than its admissible upper bound, and global asymptotic stability would be preserved under the resulting modified input.

BIBLIOGRAPHY

[1] F. Rubio, F. Valero, and C. Llopis-Albert. “A review of mobile robots: Concepts, methods, theoretical framework, and applications”. In: *International Journal of Advanced Robotic Systems* 16.2 (2019), p. 1729881419839596.

[2] J.-P. Laumond. “Feasible trajectories for mobile robots with kinematic and environment constraints”. In: *Intelligent Autonomous Systems, An International Conference*. 1986, pp. 346–354.

[3] J. Borenstein and Y. Koren. “The vector field histogram-fast obstacle avoidance for mobile robots”. In: *IEEE transactions on robotics and automation* 7.3 (1991), pp. 278–288.

[4] D. Fox, W. Burgard, and S. Thrun. “The dynamic window approach to collision avoidance”. In: *IEEE robotics & automation magazine* 4.1 (2002), pp. 23–33.

[5] M.-D. Hua, T. Hamel, P. Morin, and C. Samson. “Introduction to feedback control of underactuated VTOLvehicles: A review of basic control design ideas and principles”. In: *IEEE Control systems magazine* 33.1 (2013), pp. 61–75.

[6] P. Lasota, T. Fong, and J. Shah. “A survey of methods for safe human-robot interaction”. In: *Foundations and Trends® in Robotics* 5.4 (2017), pp. 261–349.

[7] L. Sentis and O. Khatib. “A whole-body control framework for humanoids operating in human environments”. In: *Proceedings 2006 IEEE International Conference on Robotics and Automation, 2006. ICRA 2006.* IEEE. 2006, pp. 2641–2648.

[8] M. Krstic, P. Kokotovic, and I. Kanellakopoulos. *Nonlinear and adaptive control design*. John Wiley & Sons, Inc., 1995.

[9] I. Alberto. *Nonlinear Control Systems*. Berlin, Heidelberg: Springer-Verlag, 1997. ISBN: 0387199160.

[10] S. Sastry. *Nonlinear systems: analysis, stability, and control.* Vol. 10. Springer Science & Business Media, 2013.
[11] S.G. Tzafestas. *Introduction to Mobile Robot Control.* Elsevier, 2013.
[12] R.W. Brockett. "Asymptotic stability and feedback stabilization". In: *Differential Geometric Control Theory* 27.1 (1983), pp. 181–191.
[13] E.P. Ryan. "On Brockett's condition for smooth stabilizability and its necessity in a context of nonsmooth feedback". In: *SIAM Journal on Control and Optimization* 32.6 (1994), pp. 1597–1604.
[14] K. Pathak and S.K. Agrawal. "An integrated path-planning and control approach for nonholonomic unicycles using switched local potentials". In: *IEEE Transactions on Robotics* 21.6 (2005), pp. 1201–1208.
[15] A. De Luca, G. Oriolo, and M. Vendittelli. "Stabilization of the unicycle via dynamic feedback linearization". In: *IFAC Proceedings Volumes* 33.27 (2000), pp. 687–692.
[16] W. Oelen, H. Berghuis, H. Nijmeijer, and C.C. de Wit. "Implementation of a hybrid stabilizing controller on a mobile robot with two degrees of freedom". In: *Proceedings of the 1994 IEEE International Conference on Robotics and Automation* (1994), pp. 1196–1201.
[17] A. Astolfi. "Discontinuous control of nonholonomic systems". In: *Systems & Control Letters* 27 (1996), pp. 37–45.
[18] A. Astolfi. "Discontinuous Control of the Brockett Integrator". In: *European Journal of Control* 4 (1998), pp. 49–63.
[19] A. Astolfi. "Exponential Stabilization of a Wheeled Mobile Robot Via Discontinuous Control". In: *Journal of Dynamic Systems, Measurement, and Control* 121.1 (1999), pp. 121–126.
[20] P. Braun, L. Grüne, and C.M. Kellett. "Feedback design using nonsmooth control Lyapunov functions: A numerical case study for the nonholonomic integrator". In: *56th IEEE Conference on Decision and Control.* 2017, pp. 4890–4895.
[21] J.B. Pomet, B. Thuilot, G. Bastin, and G. Campion. "A hybrid strategy for the feedback stabilization of nonholonomic mobile robots". In: *Proceedings 1992 IEEE International Conference on Robotics and Automation* (1992), pp. 129–134.
[22] V. I. Arnold. *Geometrical Methods in the Theory of Ordinary Differential Equations.* Springer, Berlin, 1987.
[23] C. Prieur. "Asymptotic controllability and robust asymptotic stabilizability". In: *IFAC Proceedings Volumes* 34.6 (2001), pp. 435–440.
[24] C. Prieur and A. Astolfi. "Robust stabilization of chained systems via hybrid control". In: *IEEE Transactions on Automatic Control* 48.10 (2003), pp. 1768–1772.
[25] T. I. Fossen. *Guidance and control of ocean vehicles.* 1999.
[26] I. Fanton, R. Lozano, F. Mazenc, and K.Y. Pettersen. "Stabilization of a nonlinear underactuated hovercraft". In: *Proceedings of the 38th*

IEEE Conference on Decision and Control (Cat. No.99CH36304). Vol. 3. 1999, 2533–2538 vol.3.

[27] J. Ghommam, F. Mnif, A. Benali, and N. Derbel. "Asymptotic backstepping stabilization of an underactuated surface vessel". In: *IEEE Transactions on Control Systems Technology* 14.6 (2006), pp. 1150–1157.

[28] A.P. Aguiar, L. Cremean, and J.P. Hespanha. "Position tracking for a nonlinear underactuated hovercraft: Controller design and experimental results". In: 4 (2003), pp. 3858–3863.

[29] K.Y. Pettersen and H. Nijmeijer. "Tracking control of an underactuated surface vessel". In: *Proceedings of the 37th IEEE Conference on Decision and Control (Cat. No.98CH36171)*. Vol. 4. 1998, 4561–4566 vol.4.

[30] T.I. Fossen, M. Breivik, and R. Skjetne. "Line-of-sight path following of underactuated marine craft". In: *IFAC proceedings volumes* 36.21 (2003), pp. 211–216.

[31] T.I. Fossen, K.Y. Pettersen, and R. Galeazzi. "Line-of-Sight Path Following for Dubins Paths With Adaptive Sideslip Compensation of Drift Forces". In: *IEEE Transactions on Control Systems Technology* 23.2 (2015), pp. 820–827.

[32] A.P. Aguiar and A.M. Pascoal. "Dynamic positioning and way-point tracking of underactuated AUVs in the presence of ocean currents". In: *Proceedings of the 41st IEEE Conference on Decision and Control, 2002.* Vol. 2. 2002, 2105–2110 vol.2. Doi: 10.1109/CDC.2002.1184840.

[33] P. Murrieri, D. Fontanelli, and A. Bicchi. "A Hybrid-Control Approach to the Parking Problem of a Wheeled Vehicle Using Limited View-Angle Visual Feedback". In: *The International Journal of Robotics Research* (2004), pp. 437–448.

[34] F. Conticelli, D. Prattichizzo, F. Guidi, and A. Bicchi. "Vision-based dynamic estimation and set-point stabilization of nonholonomic vehicles". In: *Proceedings 2000 ICRA. Millennium Conference. IEEE International Conference on Robotics and Automation. Symposia Proceedings (Cat. No. 00CH37065)*. Vol. 3. IEEE. 2000, pp. 2771–2776.

[35] J.P. Hespanha. "Single-camera visual servoing". In: *Proceedings of the 39th IEEE Conference on Decision and Control (Cat. No.00CH37187)*. Vol. 3. 2000, 2533–2538 vol.3.

[36] M. Maghenem, A. Loría, and E. Panteley. "Lyapunov-based formation-tracking control of nonholonomic systems under persistency of excitation". In: *IFAC-PapersOnLine* 49.18 (2016). 10th IFAC Symposium on Nonlinear Control Systems NOLCOS 2016, pp. 404–409.

[37] E. Restrepo, A. Loría, I. Sarras, and J. Marzat. "Leader-Follower Consensus of Unicycles With Communication Range Constraints via

Smooth Time-Invariant Feedback”. In: *IEEE Control Systems Letters* 5.2 (2021), pp. 737–742.

[38] M. Aicardi, G. Casalino, A. Bicchi, and A. Balestrino. “Closed loop steering of unicycle like vehicles via Lyapunov techniques”. In: *IEEE Robotics Automation Magazine* 2.1 (1995), pp. 27–35.

[39] E. Badreddin and M. Mansour. “Fuzzy-tuned State-Feedback Control of a Non-Holonomic Mobile Robot”. In: *IFAC Proceedings Volumes* 26.2, Part 3 (1993), pp. 769–772. ISSN: 1474-6670.

[40] H. Durrant-Whyte and T. Bailey. “Simultaneous localization and mapping: part I”. In: *IEEE Robotics & Automation Magazine* 13.2 (2006), pp. 99–110.

[41] C. Cadena, L. Carlone, H. Carrillo, Y. Latif, D. Scaramuzza, J. Neira, I. Reid, and J.J. Leonard. “Past, Present, and Future of Simultaneous Localization and Mapping: Toward the Robust-Perception Age”. In: *IEEE Transactions on Robotics* 32.6 (2016), pp. 1309–1332.

[42] D. Scaramuzza and F. Fraundorfer. “Visual Odometry [Tutorial]”. In: *IEEE Robotics & Automation Magazine* 18.4 (2011), pp. 80–92.

[43] B. Kitt, A. Geiger, and H. Lategahn. “Visual odometry based on stereo image sequences with RANSAC-based outlier rejection scheme”. In: *2010 IEEE Intelligent Vehicles Symposium*. 2010, pp. 486–492.

[44] E. Olson. “AprilTag: A robust and flexible visual fiducial system”. In: *2011 IEEE International Conference on Robotics and Automation*. 2011, pp. 3400–3407.

[45] V. Lepetit, F. Moreno-Noguer, and P. Fua. “EPnP: An accurate O(n) solution to the PnP problem”. In: *International Journal of Computer Vision* 81.2 (2009), pp. 155–166.

[46] R. Ballaben, A. Astolfi, P. Braun, and L. Zaccarian. “Orchestrating on-board sensors for global hybrid robust stabilization of unicycles”. To appear in Automatica. 2025. URL: `https://hal.science/hal-05004452`.

[47] R. Ballaben, A. Astolfi, P. Braun, and L. Zaccarian. “Towards global stabilization of a hovercraft model using hybrid systems and discontinuous feedback laws”. To appear in Proceedings of the IEEE Conference on Decision and Control (CDC), 2025.

[48] R. Goebel, R.G. Sanfelice, and A.R. Teel. *Hybrid Dynamical Systems: Modeling, Stability, and Robustness*. Princeton University Press, 2012.

[49] R.G. Sanfelice. *Hybrid Feedback Control*. Princeton University Press, 2019.

[50] R. Goebel, R.G. Sanfelice, and A.R. Teel. “Hybrid dynamical systems”. In: *IEEE Control Systems* 29 (2009), pp. 28–93.

[51] P.A. Ioannou and C.C. Chien. “Autonomous intelligent cruise control”. In: *IEEE Transactions on Vehicular Technology* 42.4 (1993), pp. 657–672.

[52] E.J. Rossetter and J.C. Gerdes. “Lyapunov Based Performance Guarantees for the Potential Field Lane-keeping Assistance System”. In: *J. Dyn. Sys., Meas., Control* 128.3 (2005), pp. 510–522.

[53] J. Borenstein and Y. Koren. “Real-time obstacle avoidance for fast mobile robots”. In: *IEEE Transactions on Systems, Man, and Cybernetics* 19.5 (1989), pp. 1179–1187.

[54] D.V. Dimarogonas, S.G. Loizou, K.J. Kyriakopoulos, and M.M. Zavlanos. “A feedback stabilization and collision avoidance scheme for multiple independent non-point agents”. In: *Automatica* 42.2 (2006), pp. 229–243.

[55] Y. Gao and C. Huang. “Evaluation of Socially-Aware Robot Navigation”. In: *Frontiers in Robotics and AI* 8 (2022).

[56] C.W. Warren. “Global path planning using artificial potential fields”. In: *1989 IEEE International Conference on Robotics and Automation*. 1989, pp. 316–321.

[57] O. Khatib. “Real-time obstacle avoidance for manipulators and mobile robots”. In: *Proceedings. 1985 IEEE International Conference on Robotics and Automation*. Vol. 2. 1985, pp. 500–505.

[58] E. Rimon and D.E. Koditschek. “Exact robot navigation using artificial potential functions”. In: *IEEE Transactions on Robotics and Automation* 8.5 (1992), pp. 501–518.

[59] E.G. Hernandez-Martinez and E. Aranda-Bricaire. “Convergence and Collision Avoidance in Formation Control: A Survey of the Artificial Potential Functions Approach”. In: *Multi-Agent Systems*. Ed. by Faisal Alkhateeb, Eslam Al Maghayreh, and Iyad Abu Doush. Rijeka: IntechOpen, 2011. Chap. 6.

[60] S. Prajna and A. Jadbabaie. “Safety Verification of Hybrid Systems Using Barrier Certificates”. In: *Hybrid Systems: Computation and Control*. Ed. by R. Alur and G.J. Pappas. Springer Berlin Heidelberg, 2004, pp. 477–492.

[61] P. Wieland and F. Allgöwer. “Constructive safety using control barrier funtions”. In: *IFAC Proceedings Volumes* 40.12 (2007). 7th IFAC Symposium on Nonlinear Control Systems, pp. 462–467.

[62] M.Z. Muhammad and J. Bayu. “Stabilization with guaranteed safety using Control Lyapunov–Barrier Function”. In: *Automatica* 66 (2016), pp. 39–47.

[63] E. D. Sontag. “Control-Lyapunov functions”. In: *Open Problems in Mathematical Systems and Control Theory*. Ed. by V. Blondel, E.D. Sontag, M. Vidyasagar, and J.C. Willems. Springer London, 1999, pp. 211–216.

[64] V. Andrieu and C. Prieur. “Uniting Two Control Lyapunov Functions for Affine Systems”. In: *IEEE Transactions on Automatic Control* 55.8 (2010), pp. 1923–1927.

[65] S. Grammatico, F. Blanchini, and A. Caiti. “Control-Sharing and Merging Control Lyapunov Functions”. In: *IEEE Transactions on Automatic Control* 59.1 (2014), pp. 107–119.

[66] E.D. Sontag. “A "universal" construction of Artstein’s theorem on nonlinear stabilization”. In: *Systems & Control Letters* 13.2 (1989), pp. 117–123.

[67] A.D. Ames, X. Xu, J.W. Grizzle, and P. Tabuada. “Control Barrier Function Based Quadratic Programs for Safety Critical Systems”. In: *IEEE Transactions on Automatic Control* 62.8 (2017), pp. 3861–3876.

[68] J.M. Maciejowski. *Predictive Control: With Constraints.* London, U.K.:Pearson Educ., 2002.

[69] J. Rawlings, D.Q. Mayne, and M. Diehl. *Model Predictive Control: Theory, Computation, and Design.* Madison, WI, USA: Nob Hill Publishing, 2017.

[70] A. Bemporad, F. Borrelli, and M. Morari. “Model predictive control based on linear programming - the explicit solution”. In: *IEEE Transactions on Automatic Control* 47 (2002), pp. 1974–1985.

[71] F. Borrelli, M. Baotic, A. Bemporad, and M. Morari. “Efficient On-Line Computation of Constrained Optimal Control”. In: *IEEE Conference on Decision and Control.* Orlando, Florida, 2001, pp. 1187–1192.

[72] T. A. Johansen, I: Petersen, and O. Slupphaug. “Explicit sub-optimal linear quadratic regulation with state and input constraints”. In: *Automatica* 38.7 (2002), pp. 1099–1111.

[73] F. Allgower, R. Findeisen, and Z.K. Nagy. “Nonlinear model predictive control: From theory to application”. In: *Journal-Chinese Institute Of Chemical Engineers* 35.3 (2004), pp. 299–316.

[74] B. Lindqvist, S.S. Mansouri, A. Agha-mohammadi, and G. Nikolakopoulos. “Nonlinear MPC for Collision Avoidance and Control of UAVs With Dynamic Obstacles”. In: *IEEE Robotics and Automation Letters* 5.4 (2020), pp. 6001–6008.

[75] M. Gaertner, M. Bjelonic, F. Farshidian, and M. Hutter. “Collision-Free MPC for Legged Robots in Static and Dynamic Scenes”. In: *2021 IEEE International Conference on Robotics and Automation (ICRA).* 2021, pp. 8266–8272.

[76] J.-R. Chiu, J.-P. Sleiman, M. Mittal, F. Farshidian, and M. Hutter. “A Collision-Free MPC for Whole-Body Dynamic Locomotion and Manipulation”. In: *2022 International Conference on Robotics and Automation (ICRA).* 2022, pp. 4686–4693.

[77] S.H. Nair, E.H. Tseng, and F. Borrelli. “Collision Avoidance for Dynamic Obstacles with Uncertain Predictions using Model Predictive Control”. In: *2022 IEEE 61st Conference on Decision and Control (CDC).* 2022, pp. 5267–5272.

[78] D.E. Koditschek and E. Rimon. “Robot navigation functions on manifolds with boundary”. In: *Advances in Applied Mathematics* 11.4 (1990), pp. 412–442.

[79] E. Rimon and D.E. Koditschek. “Exact robot navigation using artificial potential functions”. In: *IEEE Transactions on Robotics and Automation* 8.5 (1992), pp. 501–518.

[80] P. Braun and C.M. Kellett. “Comment on “Stabilization with guaranteed safety using Control Lyapunov-Barrier Function””. In: *Automatica* 122 (2020), p. 109225.

[81] F.M. Reis, A.P. Aguiar, and P. Tabuada. “Control Barrier Function-Based Quadratic Programs Introduce Undesirable Asymptotically Stable Equilibria”. In: *IEEE Control Systems Letters* 5.2 (2021), pp. 731–736.

[82] P. Braun and C.M. Kellet. “On (the existence of) control Lyapunov barrier functions”. In: *[Online]* (2017). URL: `https://eref.uni-bayreuth.de/40899/`.

[83] E.D. Sontag. “Nonlinear Feedback Stabilization Revisited”. In: ed. by G. Picci and D.S. Gilliam. Birkhäuser Basel, 1999, pp. 223–262.

[84] H. Lee and V.I. Utkin. “Chattering suppression methods in sliding mode control systems”. In: *Annual Reviews in Control* 31.2 (2007), pp. 179–188.

[85] D. Liberzon. *Switching in Systems and Control*. Systems & Control: Foundations & Applications. Birkhäuser Boston, 2012.

[86] E.D. Sontag. “Clocks and Insensitivity to Small Measurement Errors”. In: *ESAIM: Control, Optimisation and Calculus of Variations* 4 (1999), pp. 537–557.

[87] J. Cortes. “Discontinuous dynamical systems”. In: *IEEE Control Systems Magazine* 28.3 (2008), pp. 36–73.

[88] C. Prieur and A.R. Teel. “Uniting local and global output feedback controllers”. In: *IFAC Proceedings Volumes* 40.12 (2007). 7th IFAC Symposium on Nonlinear Control Systems, pp. 492–497.

[89] C. Prieur and L. Praly. “Uniting local and global controllers”. In: *Proceedings of the 38th IEEE Conference on Decision and Control (Cat. No.99CH36304)*. Vol. 2. 1999, 1214–1219 vol.2.

[90] D.V. Efimov. “Uniting global and local controllers under acting disturbances”. In: *Automatica* 42.3 (2006), pp. 489–495.

[91] P. Braun, C.M. Kellett, and L. Zaccarian. “Unsafe Point Avoidance in Linear State Feedback”. In: *2018 IEEE Conference on Decision and Control (CDC)*. 2018, pp. 2372–2377.

[92] P. Braun, C.M. Kellett, and L. Zaccarian. “Explicit Construction of Stabilizing Robust Avoidance Controllers for Linear Systems With Drift”. In: *IEEE Transactions on Automatic Control* 66.2 (2021), pp. 595–610.

[93] R. Ballaben, P. Braun, and L. Zaccarian. “Lyapunov-Based Avoidance Controllers With Stabilizing Feedback”. In: *IEEE Control Systems Letters* 8 (2024), pp. 862–867.

[94] S.P. Karason and A.M. Annaswamy. “Adaptive Control in the Presence of Input Constraints”. In: *1993 American Control Conference*. 1993.

[95] A. Saberi, A.A. Stoorvogel, and P. Sannuti. *Control of linear systems with regulation and input constraints*. Springer Science & Business Media, 2012.

[96] M. Chen, S. Ge Sam, and B. Ren. “Adaptive tracking control of uncertain MIMO nonlinear systems with input constraints”. In: *Automatica* 47.3 (2011), pp. 452–465.

[97] A.H. Glattfelder and W. Schaufelberger. *Control systems with input and output constraints*. Vol. 1. Springer, 2003.

[98] G. Grimm, J. Hatfield, I. Postlethwaite, A.R. Teel, M.C. Turner, and L. Zaccarian. “Antiwindup for stable linear systems with input saturation: an LMI-based synthesis”. In: *IEEE Transactions on Automatic Control* 48.9 (2003), pp. 1509–1525.

[99] S. Galeani, S. Tarbouriech, M. Turner, and L. Zaccarian. “A Tutorial on Modern Anti-windup Design”. In: *European Journal of Control* 15.3 (2009), pp. 418–440.

[100] T. Hu, A.R. Teel, and L. Zaccarian. “Stability and Performance for Saturated Systems via Quadratic and Nonquadratic Lyapunov Functions”. In: *IEEE Transactions on Automatic Control* 51.11 (2006), pp. 1770–1786.

[101] L. Zaccarian and A.R. Teel. *Modern Anti-windup Synthesis: Control Augmentation for Actuator Saturation*. 2011.

[102] M.-D. Hua, T. Hamel, P. Morin, and C. Samson. “Introduction to feedback control of underactuated VTOLvehicles: A review of basic control design ideas and principles”. In: *IEEE Control systems magazine* 33.1 (2013), pp. 61–75.

[103] D. Invernizzi, M. Lovera, and L. Zaccarian. “Dynamic Attitude Planning for Trajectory Tracking in Thrust-Vectoring UAVs”. In: *IEEE Transactions on Automatic Control* 65.1 (2020), pp. 453–460.

[104] R. Naldi, M. Furci, R.G. Sanfelice, and L. Marconi. “Robust Global Trajectory Tracking for Underactuated VTOL Aerial Vehicles Using Inner-Outer Loop Control Paradigms”. In: *IEEE Transactions on Automatic Control* 62.1 (2017), pp. 97–112.

[105] D. Pucci, T. Hamel, P. Morin, and C. Samson. “Nonlinear feedback control of axisymmetric aerial vehicles”. In: *Automatica* 53 (2015), pp. 72–78.

[106] H. Kurokawa. “Survey of theory and steering laws of single-gimbal control moment gyros”. In: *Journal of Guidance, Control, and Dynamics* 30.5 (2007), pp. 1331–1340.

[107] B. Wie. “Singularity escape/avoidance steering logic for control moment gyro systems”. In: *Journal of guidance, control, and dynamics* 28.5 (2005), pp. 948–956.

[108] P. Casau, R.G. Sanfelice, and C. Silvestre. “A hybrid controller for global uniform exponential stabilization of linear systems with singular input constraints”. In: *53rd IEEE Conference on Decision and Control*. IEEE. 2014, pp. 741–746.

[109] X. Zhang, X. Lou, and Z. Jiang. “Stabilization of a class of hybrid systems by switching controllers with input constraints”. In: *Circuits, Systems, and Signal Processing* 39 (2020), pp. 1649–1664.

[110] P. Casau, R.G. Sanfelice, and C. Silvestre. “Hybrid Stabilization of Linear Systems With Reverse Polytopic Input Constraints”. In: *IEEE Transactions on Automatic Control* 62.12 (2017), pp. 6473–6480.

[111] R. Ballaben, U. Sutulovic, D. Invernizzi, and L. Zaccarian. “A Hybrid Redesign for Robust Stabilization Without Unit Input”. In: *IEEE Control Systems Letters* 7 (2023), pp. 2575–2580.

[112] R.K. Goebel. *Set-valued, Convex, and Nonsmooth Analysis in Dynamics and Control: An Introduction*. Society for Industrial and Applied Mathematics, 2024.

[113] R.G. Sanfelice, R. Goebel, and A.R. Teel. “Invariance Principles for Hybrid Systems With Connections to Detectability and Asymptotic Stability”. In: *IEEE Transactions on Automatic Control* 52.12 (2007), pp. 2282–2297.

[114] C.M. Kellett. “A compendium of comparison function results”. In: *Mathematics of Control Signals and Systems* 26 (Mar. 2014).

[115] H.K. Khalil. *Nonlinear Systems*. 3rd ed. Prentice Hall, 2002.

[116] M. Vidyasagar. *Nonlinear Systems Analysis*. Prentice-Hall, 1993.

[117] R.K. Goebel, R.G. Sanfelice, and A.R. Teel. “Hybrid dynamical systems”. In: *IEEE Control Systems Magazine* 29.2 (2009), pp. 28–93.

[118] D. Nešić, A.R. Teel, and L. Zaccarian. “Stability and performance of SISO control systems with First Order Reset Elements”. In: *IEEE Transactions on Automatic Control* 56.11 (2011), pp. 2567–2582.

[119] K. Zimenko, D. Efimov, A. Polyakov, and A. Kremlev. “On necessary and sufficient conditions for output finite-time stability”. In: *Automatica* 125 (2021).

[120] E.D. Sontag and Y. Wang. “Lyapunov Characterizations of Input to Output Stability”. In: *SIAM Journal on Control and Optimization* 39 (1 2000).

[121] P. Braun, C.M. Kellett, and L. Zaccarian. “Unsafe Point Avoidance in Linear State Feedback”. In: *Proc. of the 57th IEEE Conference on Decision and Control*. 2018, pp. 2372–2377.

[122] P. Braun, C.M. Kellett, and L. Zaccarian. “Explicit Construction of Stabilizing Robust Avoidance Controllers for Linear Systems With

Drift”. In: *IEEE Transactions on Automatic Control* 66.2 (2021), pp. 595–610.

[123] C. Prieur, I. Queinnec, S. Tarbouriech, and L. Zaccarian. “Analysis and Synthesis of Reset Control Systems”. In: *Found. Trends Syst. Control.* 6 (2018), pp. 29–93.

[124] P. Casau, R.G. Sanfelice, and C. Silvestre. “On the Robustness of Nominally Well-Posed Event-Triggered Controllers”. In: *IEEE Control Systems Letters* 6 (2022), pp. 415–420.

ACKNOWLEDGMENTS (RINGRAZIAMENTI)

ENGLISH VERSION

I would like to begin by expressing my heartfelt gratitude and affection to all my friends and family who have supported me throughout my life. Without them, the wonderful journey that this PhD has been would not have been possible. Among the many people I hold dear, I wish to thank my mother Giovanna, my brother Leonardo, my sister Aurora, and my close friends Federico, Alberto, and Luca.

While I am deeply grateful to all of them, I believe that a special acknowledgment is due to those with whom I have shared these past three years. Wherever life may take me, I will always carry with me the memories I have made during this PhD.

First, I would like to thank my PhD supervisors, Professor Luca Zaccarian and Professor Philipp Braun, for their continuous guidance over these three years. Through this PhD I discovered my passion for control theory, a passion I hope will turn into a future career path.

I am also deeply thankful to Professor Rafal Goebel from the Loyola University Chicago, USA, who hosted me during my abroad research period from September 2024 to February 2025. I am grateful for the many insightful discussions and frequent exchanges, and for introducing me to bouldering, which has since become a passion of mine.

On that note, a special thanks goes to my climbing buddies, Giovanni, Vittorio, and Federico C., for sharing this passion with me and showing me what a real climber looks like.

While the research activity of a PhD can, at times, be frustrating and exhausting, I was always happy to come to the office and work alongside my PhD colleagues of the Open Space in Povo. You made every day a little brighter, and I am very grateful to have shared the office with you. An

honorable mention goes to my canteen crew; meals do taste better when they are shared with friends (even the university canteen's).
A significant portion of my free time over these past three years has been happily spent thinking about and playing Dungeons and Dragons. I was lucky enough to find (with very little effort, I must add) two amazing groups of friends who share my love for the game, one in Trento and one in my hometown, and to be a part of not one but two three-year-long (and still ongoing) campaigns. A colossal thank you goes to Matteo, Giampaolo, Federico, Carla, Silvio, and Daniele, and Federico L., Federico C., Francesco, and Filippo.
A special acknowledgment also goes to my friend Francesco, for sparing me the ordeal of weekly train commutes between my hometown and Trento by offering me countless car rides, and for all the conversations (and naps) that we shared along the way.
I also want to thank all the members and doctors of the therapy group at the Centro Salute Mentale in Trento, for accompanying me through the difficult moments of this journey with their warmth, compassion, and kindness. I will be forever grateful for the incredible support they gave me, which I consider one of the great strokes of luck life has given me.
Last but not least, a heartfelt thank you to my girlfriend Francesca, for her encouragement and support, as well as for her invaluable help in organizing the celebrations for my PhD.

VERSIONE ITALIANA

Vorrei iniziare esprimendo la mia più sincera gratitudine e il mio affetto a tutti i miei amici e familiari che mi hanno sostenuto lungo il percorso della mia vita. Senza di loro, il meraviglioso viaggio che questo dottorato ha rappresentato non sarebbe stato possibile. Tra le molte persone a me care, desidero ringraziare mia madre Giovanna, mio fratello Leonardo, mia sorella Aurora e i miei cari amici Federico, Alberto e Luca.
Pur essendo profondamente grato a tutti loro, credo che un ringraziamento speciale sia dovuto a coloro con cui ho condiviso questi ultimi tre anni. Ovunque la vita mi condurrà, porterò sempre con me i ricordi di questo dottorato.
Per prima cosa, desidero ringraziare i miei supervisori di dottorato, il Professor Luca Zaccarian e il Professor Philipp Braun, per la loro costante guida in questi tre anni. Grazie a questo dottorato ho scoperto la mia passione per la teoria del controllo, una passione che spero possa trasformarsi in un futuro percorso professionale.
Sono inoltre profondamente grato al Professor Rafal Goebel della Loyola University Chicago, Stati Uniti, che mi ha ospitato durante il mio periodo di

ricerca all'estero, da settembre 2024 a febbraio 2025. Gli sono riconoscente per le numerose discussioni stimolanti, per i frequenti scambi di idee e per avermi fatto scoprire il bouldering, che da allora è diventata una mia grande passione.
A questo proposito, un ringraziamento speciale va ai miei compagni di arrampicata, Giovanni, Vittorio e Federico C., per aver condiviso con me questa passione e per avermi mostrato cosa significa saper arrampicare per davvero.
Sebbene l'attività di ricerca di un dottorato possa talvolta risultare frustrante e estenuante, sono sempre stato felice di venire in ufficio e lavorare accanto ai miei colleghi dell'Open Space di Povo. Avete reso ogni giornata un po' più luminosa, e sono molto grato di aver condiviso l'ufficio con voi. Una menzione d'onore va anche alla mia compagnia della mensa; i pasti sono più buoni quando sono condivisi con amici (persino quelli della mensa universitaria).
Una parte significativa del mio tempo libero negli ultimi tre anni è stata felicemente dedicata a pensare e giocare a Dungeons and Dragons. Ho avuto la fortuna di trovare (con davvero pochissimo sforzo, devo ammettere) due fantastici gruppi di amici che condividono il mio amore per il gioco, uno a Trento e uno nella mia città natale, e di far parte non di una, ma di due campagne che durano da tre anni (e sono ancora in corso). Un colossale grazie va a Matteo, Giampaolo, Federico, Carla, Silvio e Daniele, e a Federico L., Federico C., Francesco e Filippo.
Un ringraziamento speciale va anche al mio amico Francesco, per avermi risparmiato la fatica dei viaggi settimanali in treno tra Conegliano e Trento offrendomi innumerevoli passaggi in auto, e per tutte le conversazioni (e i sonnellini) condivisi lungo la strada.
Desidero inoltre ringraziare tutti i membri e i dottori del gruppo di terapia del Centro Salute Mentale di Trento, per avermi accompagnato nei momenti difficili di questo percorso con calore, compassione e gentilezza. Sarò per sempre grato per l'incredibile sostegno che mi hanno dato, che considero una delle grandi fortune che la vita mi abbia concesso.
Infine, ma non per importanza, un sentito ringraziamento alla mia ragazza Francesca, per il suo incoraggiamento e supporto, oltre che per il suo fondamentale aiuto nell'organizzazione dei festeggiamenti per il mio dottorato.